Universidade de Lisboa

Faculdade de Medicina

New Potential Therapy for Multiple Sclerosis: a role for Adenosine A_{2A} Receptors

Cláudia Filipa Martins Afonso

Orientadores:

Sara Alves Xapelli, PhD

Cláudia Valente de Castro, PhD

Dissertação especialmente elaborada para obtenção do grau de mestre em Neurociências

Lisboa, 2017

A impressão desta dissertação foi aprovada pelo Conselho Científico da Faculdade de Medicina de Lisboa em reunião de 23 de Maio de 2017.

The experimental work described in the present thesis was conducted at the Institute of Pharmacology and Neuroscience, Faculty of Medicine and Unit of Neurosciences, Institute of Molecular Medicine, under the supervision of Sara Alves Xapelli, PhD and Cláudia Valente de Castro, PhD.

O trabalho experimental descrito nesta tese foi realizado no Instituto de Farmacologia e Neurociências, Faculdade de Medicina e Unidade de Neurociências, Instituto de Medicina Molecular, sob a orientação da Doutora Sara Alves Xapelli e Doutora Cláudia Valente de Castro.

Agradecimentos

Gostaria de agradecer à Professora Ana Sebastião pela oportunidade que me concedeu em realizar a dissertação de mestrado no seu grupo e também pelo apoio prestado como coordenadora durante o mestrado em Neurociências.

Queria igualmente agradecer às minhas orientadoras, a Doutora Sara Xapelli e a Doutora Cláudia Valente. À Doutora Sara por me ter aceite como aluna, pela disponibilidade que teve em esclarecer as minhas dúvidas e por todas as sugestões que fez durante a fase de correção da dissertação. À Doutora Cláudia pela ajuda e contribuição durante as experiências *ex vivo*.

Gostaria de agradecer também à Filipa Ribeiro pelo contributo que teve nas experiências *in vivo* e disponibilidade em esclarecer as minhas dúvidas.

Um agradecimento especial a toda a unidade de Bioimagem do Instituto de Medicina Molecular, em particular ao António Temudo, pela ajuda que me prestou durante o processo de aquisição de imagens.

Queria agradecer também a todas as pessoas que me fizeram companhia dentro e fora do laboratório e amizades que fiz neste último ano, em particular à Inês Rosete.

Por fim, tenho de agradecer a toda a minha família, em especial à minha mãe, pelo apoio e amizade incondicionais durante estes anos.

Um sincero obrigado a todos.

Resumo

No Sistema Nervoso Central (SNC) os oligodendrócitos são as células responsáveis pela mielinização dos axónios neuronais. O aparecimento da mielina, uma membrana multilamelar composta maioritariamente por lípidos e proteínas, constituiu um passo evolutivo importante para os vertebrados, uma vez que possibilita a rápida propagação dos potenciais de acção, preservando o diâmetro axonal e reduzindo os custos metabólicos da actividade neuronal. Deste modo, a sua disrupção ou eventual perda modifica a transmissão sináptica entre os neurónios e inicia um processo degenerativo, afectando as capacidades motoras e cognitivas.

A esclerose múltipla (EM) é a doença desmielinizante de maior prevalência mundial. Do ponto de vista fisiopatológico, é caracterizada pela infiltração no SNC de leucócitos sistémicos, que promovem a destruição da mielina em zonas denominadas de placas. Actualmente, não existe cura e as estratégias terapêuticas disponíveis visam exclusivamente a sua componente imunitária, sendo apenas parcialmente eficazes à medida que a doença progride no tempo. Numa proporção considerável de doentes, durante a evolução clínica da EM é possível observar-se remielinização. Assim, a intervenção neste processo de reparação espontâneo, que envolve a proliferação e migração de células precursoras de oligodendrócitos (OPCs) para os locais de dano, poderá constituir uma nova abordagem terapêutica na EM.

A diferenciação de oligodendrócitos é um processo extremamente regulado e dinâmico que ocorre maioritariamente durante o período pós-natal a partir de OPCs do parênquima que expressam o proteoglicano NG2 (*nerve-glial antigen 2*). Uma percentagem significativa destas células permanece num estado proliferativo no SNC adulto, constituindo cerca de 5-8% de toda a população glial. Durante o processo de remielinização observado em doentes com EM, a maioria dos oligodendrócitos que são recrutados para os locais de dano é derivada destes OPCs parenquimatosos. No entanto, uma percentagem pequena advém de células estaminais neurais presentes na zona subventricular (SVZ) situada ao longo dos ventrículos laterais. A SVZ constitui no SNC dos mamíferos adultos o principal nicho de células estaminais, sendo capaz de dar origem a neurónios e células da glia.

A adenosina é um nucleósido endógeno da classe das purinas que se encontra presente em todas as células. É produzida sobretudo a partir do catabolismo da adenosina trifosfato (ATP) e no SNC exibe um papel duplo de regulador homeostático e de neuromodulador da transmissão sináptica através da activação de quatro receptores metabotrópicos: A_1, A_{2A}, A_{2B} e A_3. Enquanto que os receptores A_1 e A_3 estão negativamente acoplados à adenilato ciclase, os receptores A_{2A} e A_{2B} estimulam a actividade desta enzima, aumentando assim a produção de adenosina 3',5'-monofosfato cíclico (cAMP).

Diferentes estudos comprovaram de forma independente o envolvimento do sistema adenosinérgico na patogénese da EM. Em particular, foi demonstrado que os receptores A_{2A} estão sobre-expressos em linfócitos e na substância branca destes doentes. Na encefalomielite auto-imune experimental (EAE), o modelo animal mais usado no estudo da EM, o nível de expressão dos receptores A_{2A} encontra-se também aumentado em linfócitos T e na microglia.

Estes receptores estão igualmente envolvidos no processo de oligodendrogénese, já que se encontra descrito que a sua activação inibe a proliferação *in vitro* de OPCs. Dados prévios do nosso grupo de investigação mostraram que a activação destes receptores com o agonista selectivo CGS21680 (30 nM) promove a diferenciação de OPCs derivados de neuroesferas da SVZ. Assim, a presente dissertação teve por objectivo estudar o possível papel modulador dos receptores A_{2A} na oligodendrogénese derivada da SVZ *in vivo* em condições fisiológicas e *ex vivo* na oligodendrogénese derivada do parênquima e SVZ antes e após insulto desmielinizante com lisofosfatidilcolina usando culturas organotípicas corticais.

Para estudar o efeito da activação dos receptores A_{2A} na oligodendrogénese derivada da SVZ *in vivo*, introduziu-se no ventrículo lateral direito de ratos Wistar com 6 semanas de idade uma cânula ligada a uma mini-bomba osmótica, a partir da qual o agonista CGS21680 (100 nM) ou veículo (líquido cefalorraquidiano artificial) foram continuamente administrados durante 28 dias. A proliferação celular foi avaliada após duas injecções intraperitoneais de 5-bromo-2'-deoxiuridina (BrdU, 100 mg/kg de peso corporal), separadas entre si por intervalos de 2 horas no último dia de tratamento. Para analisar a migração e diferenciação celulares, os animais receberam injecções de BrdU duas vezes ao dia nos primeiros 3 dias de administração farmacológica. Os animais foram sacrificados, os seus cérebros removidos e seccionados em fatias coronais com 30 µm de espessura. Posteriormente, procedeu-se à técnica de imuno-histoquímica por fluorescência contra Olig2, um factor de transcrição cuja expressão é mantida em toda a linhagem oligodendrocítica, e BrdU.

Para investigar o efeito da activação dos receptores A_{2A} na oligodendrogénese *ex vivo* derivada da SVZ e parênquima antes e após um insulto desmielinizante com lisofosfatidilcolina (LPC, 0.5 mg/ml), preparam-se culturas organotípicas corticais contendo a SVZ e o corpo caloso. De forma resumida, os cérebros de ratos Sprague-Dawley foram removidos e cortados em fatias coronais de 400 µm de espessura que foram colocadas em cultura sobre membranas semi-porosas a 37 ^{o}C. Realizaram-se dois protocolos experimentais distintos. No protocolo 1, as fatias foram isoladas de ratos P9 e mantidas em meio MEM até ao dia *in vitro* (DIV) 4, tendo sido então mudadas para meio Neurobasal-A (NB-A). Ao DIV 6, as fatias foram incubadas com LPC ou veículo (etanol) durante 18 horas, tendo-se procedido de seguida ao tratamento farmacológico com o agonista CGS21680 (30 nM) e/ou antagonista ZM241385 (50 nM). Após 36 horas, as fatias foram finalmente fixadas. No protocolo 2, as fatias foram isoladas de ratos P14 e mantidas em meio MEM até ao DIV 1, tendo sido então mudadas para meio NB-A e incubadas com LPC durante 18 horas. Seguiu-se o tratamento farmacológico com o agonista CGS21680 (30 nM) e/ou antagonista ZM241385 (50 nM) e após 36 horas procedeu-se à fixação das fatias. A intensidade de fluorescência da proteína básica de mielina (MBP), um marcador de oligodendrócitos maduros, foi medida no corpo caloso das fatias organotípicas.

De forma inesperada, os resultados do estudo *in vivo* demonstraram que a activação dos receptores A_{2A} provoca uma redução da proliferação de OPCs (células $Olig2^{+}BrdU^{+}$) na SVZ. Além disso, o movimento destas células ao longo da via rostro-migratória (RMS) em direcção ao bolbo olfactivo (OB) encontra-se inibido após activação dos receptores A_{2A}. No entanto, observou-se que não há uma alteração significativa no número de OPCs derivados da SVZ presentes no OB entre animais controlo e tratados com o agonista CGS21680. Por outro lado, os resultados das experiências *ex vivo* mostraram que a activação dos receptores A_{2A} promove a maturação dos

OPCs na ausência de um evento desmielinizante, uma vez que se observou um aumento na intensidade de fluorescência de MBP. A incubação das fatias com LPC a 0.5 mg/ml durante 18 horas não foi suficiente para induzir a desmielinização do corpo caloso. No entanto, o aumento da intensidade de fluorescência de MBP registado com a activação dos receptores A_{2A} não foi replicado quando o tratamento com o agonista se seguiu à incubação com LPC, o que pode indicar que, mesmo a uma concentração insuficiente para provocar desmielinização, este agente tem algum efeito.

Na sua totalidade, os resultados apresentados nesta dissertação indicam que a activação dos receptores A_{2A} modula a oligodendrogénese derivada da SVZ, inibindo a proliferação e migração de OPCs para o OB. Contudo, a activação destes receptores parece desempenhar um papel positivo na oligodendrogénese derivada do parênquima, através do aumento da diferenciação de OPCs. Esta função dupla dos receptores A_{2A} pode revelar-se importante para o desenho de novas estratégias terapêuticas na EM.

PALAVRAS-CHAVE

Oligodendrócitos, Esclerose Múltipla, Zona Subventricular, Adenosina, Receptores A_{2A}

Abstract

Oligodendrocytes are the cells responsible for myelinating neuronal axons in the Central Nervous System (CNS). The emergence of the myelin sheath was an important evolutionary step in vertebrate development, since it allows the rapid propagation of action potentials while preserving axonal diameter and reducing the metabolic costs of neuronal activity. Thus, its disruption constitutes a serious health problem, altering the normal signal transmission between neurons and initiating a degenerative process that affects proper motor and cognitive ability.

Multiple sclerosis (MS) is the most prevalent demyelinating disease worldwide. It is primarily characterized by the presence of inflammatory infiltrates, oligodendrocyte death and destruction of myelin in CNS areas known as plaques. No cure is available and currently the therapeutic strategies target exclusively its immune component, thus being only partially effective as disease continues to progress. During the clinical course of MS, attempts at remyelination occur, with new oligodendrocytes generated mostly from brain parenchymal oligodendrocyte progenitor cells (OPCs). However, a minority of these OPCs are derived from neural stem cells (NSCs) present in the subventricular zone (SVZ) along the lateral ventricles. This spontaneous repair process raises reasonable hopes that recruitment of OPCs towards sites of injury may constitute a novel therapeutic approach in MS.

Numerous studies have independently established the involvement of the adenosinergic system in the pathogenesis of MS, specifically of A_1 and A_{2A} adenosine receptors. Moreover, previous data from our group has demonstrated that activation of A_{2A}Rs promoted the differentiation of oligodendrocytes from neurosphere cultures of postnatal rats. Thus, the present thesis investigated the possible modulatory role of A_{2A}Rs in SVZ oligodendrogenesis *in vivo*, under physiological conditions, and in SVZ and parenchymal oligodendrogenesis *ex vivo*, using forebrain organotypic slice cultures.

Surprisingly, the results concerning the *in vivo* experiments demonstrated that activation of A_{2A}Rs decreases the proliferation of OPCs ($Olig2^+BrdU^+$ cells) in the SVZ. Moreover, the movement of these cells along the rostral migratory stream (RMS) towards the olfactory bulb (OB) was impaired following A_{2A}R activation. However, the number of SVZ-generated OPCs in the OB was not significantly altered in treated animals when compared to controls. In contrast, the data regarding the *ex vivo* experiments suggests that A_{2A}R activation promotes parenchymal OPC maturation in the absence of a demyelinating event, since an increase in the fluorescence intensity of myelin basic protein (MBP) was observed.

In summary, the results presented in this thesis indicate that activation of A_{2A}Rs decreases the proliferation and migration of SVZ-derived OPCs. Moreover, A_{2A}R activation appears to play a positive role in parenchymal oligodendrogenesis through increased OPC differentiation in non-demyelinated organotypic cultures. These biological effects of A_{2A}Rs might prove to be important in the future development of novel therapeutic strategies in MS.

KEYWORDS

Oligodendrogenesis, Multiple Sclerosis, Subventricular Zone, Adenosine, A_{2A} Receptors

Contents

List of Figures

List of Tables

Abbreviations

AC	Adenylyl cyclase
aCSF	Artificial cerebrospinal fluid
AMP	Adenosine monophosphate
ANOVA	Analysis of variance
ARs	Adenosine receptors
ATP	Adenosine triphosphate
BBB	Blood-brain barrier
bHLH	Basic helix-loop-helix
BMP	Bone morphogenic protein
BrdU	5-bromo-2'-deoxyuridine
cAMP	3',5'-cyclic adenosine monophosphate
CC	Corpus callosum
CNS	Central Nervous System
CRE	cAMP response elements
CREB	cAMP-response element-binding protein
CSF	Cerebrospinal fluid
DAG	Diacylglycerol
DAPI	4',6-diamidino-2-phenylindole
DCX	Doublecortin
DG	Dentate gyrus
EAE	Experimental autoimmune encephalomyelitis
EBSS	Earle's balanced salt solution
ENTs	Equilibrative nucleoside transporters
FBS	Fetal bovine serum
GBSS	Gey's balanced salt solution

GCL	Granule cell layer
GL	Glomerular layer
GFAP	Glial fibrillary acidic protein
GLAST	Glutamate aspartate transporter
GPCRs	G-protein coupled receptors
Iba1	Ionized calcium/binding adapter molecule 1
IP_3	Inositol 1,4,5-trisphosphate
ICAM-1	Intercellular adhesion molecule-1
LGE	Lateral ganglionic eminence
LPC	Lysophosphatidylcholine
LPS	Lipopolysaccharide
LTP	Long-term potentiation
MAG	Myelin-associated glycoprotein
MAPK	Mitogen-activated protein kinase
MBP	Myelin basic protein
MEM	Minimal essential medium
MHC	Major histocompatibility complex
MOG	Myelin oligodendrocyte glycoprotein
MS	Multiple sclerosis
NB-A	Neurobasal-A
NE	Neuroepithelial
NG2	Nerve-glial antigen 2
NSCs	Neural stem cells
OB	Olfactory bulb
OPCs	Oligodendrocyte progenitor cells
PB	Phosphate buffer
PBS	Phosphate-buffered saline

PBST	Phosphate-buffered saline with 0.1% Triton x-100
PBT	Phosphate buffer with 0.1% Triton x-100
PDGFRα	Platelet-derived growth factor receptor α
PFA	Paraformaldehyde
PI3K	Phosphoinositide 3-kinase
PIP_3	Phosphatidylinositol 3,4,5-trisphosphate
PKA	Protein kinase A
PKB	Protein kinase B
PLA_2	Phospholipase A_2
PLC	Phospholipase C
PLP	Proteolipid protein
PNS	Peripheral Nervous System
PP_i	Pyrophosphate
PPMS	Primary progressive multiple sclerosis
PRMS	Progressive-relapsing multiple sclerosis
PSA-NCAM	Polysialylated-neural cell adhesion molecule
RMS	Rostral migratory stream
RRMS	Relapsing-remitting multiple sclerosis
SAH	S-adenyl-L-homocysteine
SEM	Standard error of the mean
SGZ	Subgranular zone
Shh	Sonic hedgehog
Sox2	Sex determining region Y-box 2
SPMS	Secondary progressive multiple sclerosis
SVZ	Subventricular zone
TMEV	Theiler's murine encephalomyelitis virus
TTX	Tetrodotoxin

VCAM-1	Vascular cell adhesion molecule-1
VZ	Ventricular zone
WT	Wild type

1. Introduction

1.1 The subventricular zone: a specialized stem cell niche in the adult mammalian brain

Contrary to long-held doctrine, the adult mammalian brain contains two primary regions that continue to generate new progenitor cells: the subventricular zone (SVZ) along the lateral ventricles and the subgranular zone (SGZ) in the hippocampal dentate gyrus (DG).[1] These restricted areas represent specialized microenvironments called neurogenic niches, which regulate the proliferation and differentiation of neural stem cells (NSCs).[2] Although spatially separated, both niches are characterized by the presence of developmental morphogens and signalling pathways, as well as a higher vascular density.[2,3] Whereas NSCs residing in the dentate gyrus only give rise to granule cells, excitatory neurons that later integrate into the hippocampal circuitry,[4] the SVZ represents the largest stem cell niche in the brain and can generate both glial and neuronal lineages.[5]

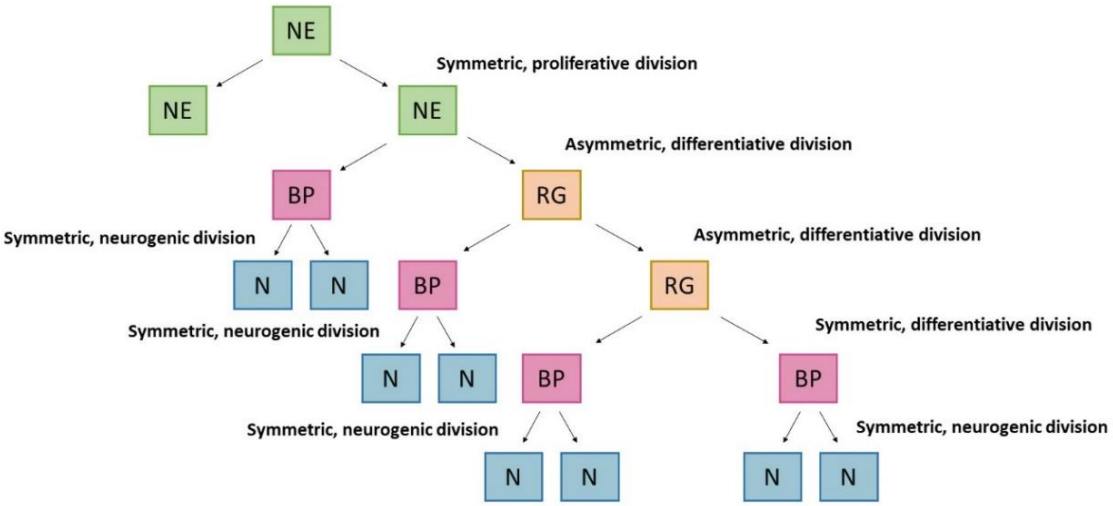

Figure 1.1 – Lineage tree of embryonic neurogenesis. This lineage tree provides an overview of the hierarchical relationship and types of cell division involved between neuroepithelial (NE) cells, radial glial (RG) cells and neurons (N), with basal progenitors (BP) as cellular intermediates in the generation of neurons. Adapted from [6]*Götz et al., 2005*.

In the developing brain, neuroepithelial (NE) cells enclosing the neural tube constitute the ventricular zone (VZ) and at first divide symmetrically on the luminal surface to generate two daughter cells with the same fate.[6,7] With the onset of neurogenesis, these stem cells downregulate epithelial markers and begin to divide asymmetrically, originating another NE cell and either a neuron (with or without basal progenitors as intermediates) or a radial glial cell (Figure 1.1).[6,7] The accumulation of postmitotic neurons and basal progenitors within the developing telencephalon forms a second germinal layer above the VZ, which is called SVZ.[7] Radial glia express molecular and structural phenotypes that are characteristic of the astrocytic lineage and, in addition to serving as a scaffold along which neurons migrate radially to the developing cortex, these cells represent a heterogeneous population already committed to

generating either neuronal or glial progenitor cells.[6,7] The postnatal SVZ is derived from its embryonic counterpart (Figure 1.2) and lineage tracing studies using adenovirus-mediated gene transfer in mice have demonstrated that a fraction of radial glia give rise to the adult NSCs, whereas the remaining acquire an ependymal glial fate.[8,9]

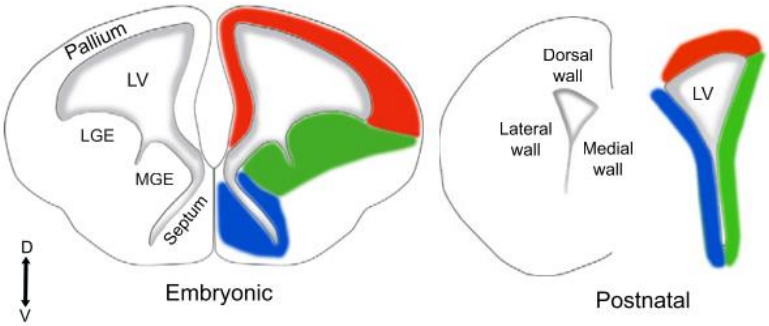

Figure 1.2 – Macroscopic organization of the postnatal SVZ. The lateral, dorsal and medial walls of the adult SVZ (right) are derived from their embryonic counterparts (left): lateral and medial ganglionic eminences (LGE) and (MGE), pallium and septum, respectively.[9]

The adult SVZ is a highly heterogeneous structure and exhibits a three-dimensional organization at two scales. At the macroscopic level, the appearance of this niche changes considerably along the rostro-caudal axis and distinct microdomains generate defined neuronal subtypes, according to fate specification programs conserved from development.[9,10] Coronal sections unveil the SVZ as a narrow fissure in the rostral forebrain, which then widens into its characteristic triangular shape at the mediostriatal level before shrinking again in the temporal horns, as the hippocampus begins to appear (Figure 1.3).[9] In addition, NSCs located in the dorsal, medial and lateral walls of the SVZ are patterned to produce specific subtypes of neurons. At the cellular level, the postnatal SVZ is described as containing five different cell types defined by their morphology (Figure 1.4) and molecular markers (Table 1.1): ependymal cells (E cells), B1 astrocytes, B2 astrocytes, transit amplifying progenitor cells (C cells) and neuroblasts (A cells).[11]

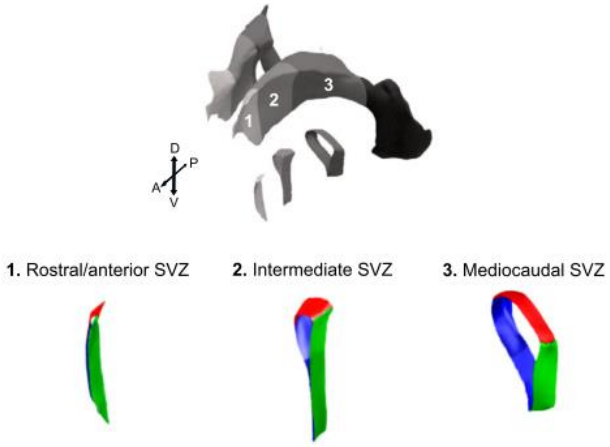

Figure 1.3 – Macroscopic heterogeneity of the postnatal SVZ. A volumetric reconstruction of the lateral ventricles is show at the top. Coronal sections of subdivisions 1, 2 and 3 with color-coded walls (red, dorsal; green, lateral; blue, medial) are shown beneath.[9]

Ependymal cells bearing motile cilia line the lateral ventricles, separating the brain parenchyma from the cerebrospinal fluid (CSF).[12] This array of E cells, however, is non-contiguous and a small fraction of B1 astrocytes sitting atop contacts the ventricular system by extending a single, non-motile cilium.[13] Additionally, type B1 cells also have a basal process with end-feet covering blood vessels.[12] These cells represent the quiescent NSCs of the SVZ and when activated divide asymmetrically to produce type C cells which, in turn, rapidly give rise to type A cells. These migratory neuroblasts travel tangentially from the SVZ through the rostral migratory stream (RMS), differentiating into subpopulations of interneurons in the granule cell layer (GCL) and glomerular layer (GL) of the olfactory bulb (OB).[14] B2 cells, non-neurogenic astrocytes of the SVZ, are organized in glial tubes and support neuroblast chain migration.[11,15] A minority of C cells also originate oligodendrocyte progenitor cells (OPCs), which move radially from the SVZ and RMS to the overlying white matter tracts of the corpus callosum (CC), striatum and fimbria-fornix to differentiate into both non-myelinating and myelinating oligodendrocytes. Under normal conditions, the fraction of oligodendrocytes derived from the SVZ is persistently inferior compared to the number of neurons that migrate to the OB. However, in the presence of a demyelinating injury, the turnover of OPCs in the SVZ is markedly increased and these cells travel to the site of lesion, where they ultimately differentiate into mature oligodendrocytes.[16,17] Microglial cells are also found within the SVZ where they help sustain the niche by excreting soluble factors.[18]

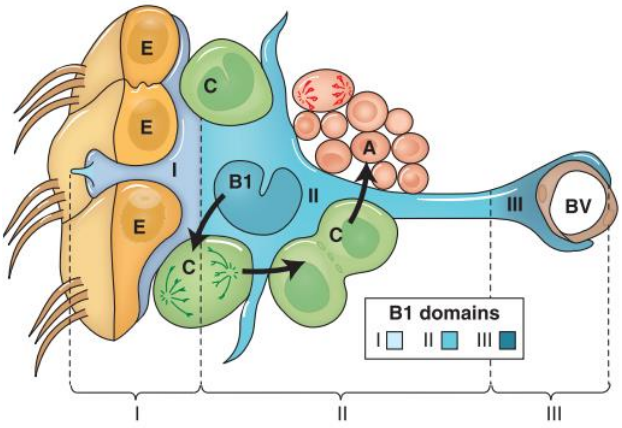

Figure 1.4 – Cellular composition and architecture of the adult SVZ. The quiescent stem cells of the SVZ are type B1 astrocytes (blue). Under the appropriate stimulus, B1 astrocytes can divide to originate type C cells (green). In turn, these transit amplifying cells divide to produce type A cells (red), migratory neuroblasts that travel to the olfactory bulb. The apical surface of B1 cells has a cilium that contacts the ventricular lumen. The SVZ can be divided into three domains depending on the spatial arrangement of type B1 cells. Domain I comprises the apical process of B1 astrocytes and the body of multiciliated ependymal cells. Domain II contains the cell body of most type B1 cells, while domain III encompasses the basal processes of these astrocytes with their end-feet on blood vessels (BV, brown).[12]

Although largely discredited at the time, the first evidence for postnatal neurogenesis in mammals was provided by Joseph Altman in the sixties. By injecting rats with ^{3}H-thymidine, autoradiograms and histological studies revealed the presence of mitotic cells in the subependymal layer of the lateral ventricles and their rostral extension towards the olfactory bulb.[19,20] The constraints involved in the use of a radiolabelled substrate eventually led to the development of 5-bromo-2'-deoxyuridine (BrdU) immunohistochemistry as an alternative strategy for the study of adult neurogenesis.[21] BrdU is a thymidine analogue that becomes

incorporated into nuclei undergoing DNA synthesis in the S-phase of mitosis, but not in proliferating cells at other phases of the cell-division cycle. As a result, multiple pulses of BrdU are required in order to identify the entire proliferating population in the brain and different labelling paradigms have been devised to specifically study proliferation, migration and fate of NSCs.[21,22]

Table 1.1 – Marker expression of the different cell types composing the SVZ. No unique marker exists to distinguish a specific cell type within the adult SVZ, therefore a panel of markers must be employed. This table presents some of the most common markers used and the respective cell types labelled within the SVZ.[11]

Marker	Ependymal Cell	B2 astrocyte	B1 astrocyte	C cell	Neuroblast	Other SVZ cell types
β-III-tubulin	-	-	-	-	+	-
β-catenin	+	-	+	++	-	-
CD11b	-	-	-	-	-	Microglia
Doublecortin (DCX)	-	-	-	-	+	-
Glutamate aspartate transporter (GLAST)	-	+	+	+/-	-	-
Glial fibrillary acidic protein (GFAP)	-	++	++	-	-	-
Ionized calcium-binding adapter molecule 1 (Iba1)	-	-	-	-	-	Microglia
Nestin	-	+/-	+	++	-	-
Nerve-glial antigen 2 (NG2)	-	-	-	-	-	OPCs
Platelet-derived growth factor receptor α (PDGFRα)	-	-	+	-	-	OPCs
Polysialylated-neural cell adhesion molecule (PSA-NCAM)	-	-	-	-	+	OPCs
Sex determining region Y-box 2 (Sox2)	+	++	++	+	+	-

The functional significance of SVZ-derived NSCs in rodents has been well established. A continuous supply of neuroblasts to the OB provides a mechanism for perceptual learning in odour-dependent behaviours, such as those related to reproduction.[23,24] In humans, however, the addition of new neurons in the OB appears to be negligible after birth, with NSCs instead migrating to the striatum.[25,26] While the physiological role of this postnatal cell turnover in the lateral ventricles and striatum remains elusive, it has been demonstrated that a specific depletion of adult-born cells committed to the neuronal and oligodendroglial lineage occurs in Huntington's disease. In addition, the onset of neurodegenerative diseases and necrotic events can activate or inhibit the proliferative capacity of the SVZ, both in humans and rodents.[27,28] Altogether, the SVZ is now recognized as an interesting target for therapeutic strategies and the identification of mechanisms capable of mobilizing and promoting the regenerative potential of these cells in damaged sites is becoming increasingly important.[29]

1.2 Oligodendrogenesis: an embryonic and postnatal process

1.2.1 Oligodendrocyte function and maturation

Oligodendrocytes are the glial cells responsible for the myelination of axons in the Central Nervous System (CNS). The appearance of the myelin sheath was a pivotal event in vertebrate development, allowing the rapid propagation of action potentials while preserving axonal diameter and reducing the metabolic costs of neural activity.[30] It is a specialized multilamellar membrane structure composed mainly of lipids, such as cholesterol, and a small set of proteins.[31] The myelinated segments of axons are interrupted by small gaps of exposed axonal membrane called nodes of Ranvier, which contain a high density of ion channels in order to regenerate action potentials.[32] Oligodendrocytes can myelinate multiple axonal segments unlike Schwann cells, their cellular counterparts in the Peripheral Nervous System (PNS).[33]

The differentiation of oligodendroglial cells is a highly regulated process, which can be classified into four stages according to the differential expression of molecular markers, increasingly complex morphology and ability to proliferate and migrate: oligodendrocyte progenitor cells (OPCs), pre-oligodendrocytes, immature or pre-myelinating oligodendrocytes and mature or myelinating oligodendrocytes (Figure 1.5).[34] OPCs generated during development are proliferative cells and have a remarkable migratory capacity, populating the entire CNS. At this stage, they present a bipolar morphology and are characterized by numerous markers, such as platelet-derived growth factor receptor α (PDGFRα), chondroitin sulfate proteoglycan nerve-glial antigen 2 (NG2) and the transcription factor Olig2. As OPCs begin to develop into pre-oligodendrocytes, short secondary ramifications emerge from the soma and different antigens, such as the marker O4, are expressed. With downregulation of the earlier stage markers, namely NG2 and PDGFRα, expression of O4 persists and immature oligodendrocytes acquire a complex multipolar morphology. Finally, oligodendrocytes reach the mature or myelinating stage and become post-mitotic cells with long ramified branches, extending their membranes around the axons.[34,35] The expression of some molecular markers, in particular Olig2 and Sox10, is retained throughout the entire oligodendroglial lineage. Myelination follows an intrinsic developmental

clock which reflects the sequential expression of myelin basic protein (MBP), proteolipid protein (PLP), myelin-associated glycoprotein (MAG) and lastly myelin oligodendrocyte glycoprotein (MOG).[36]

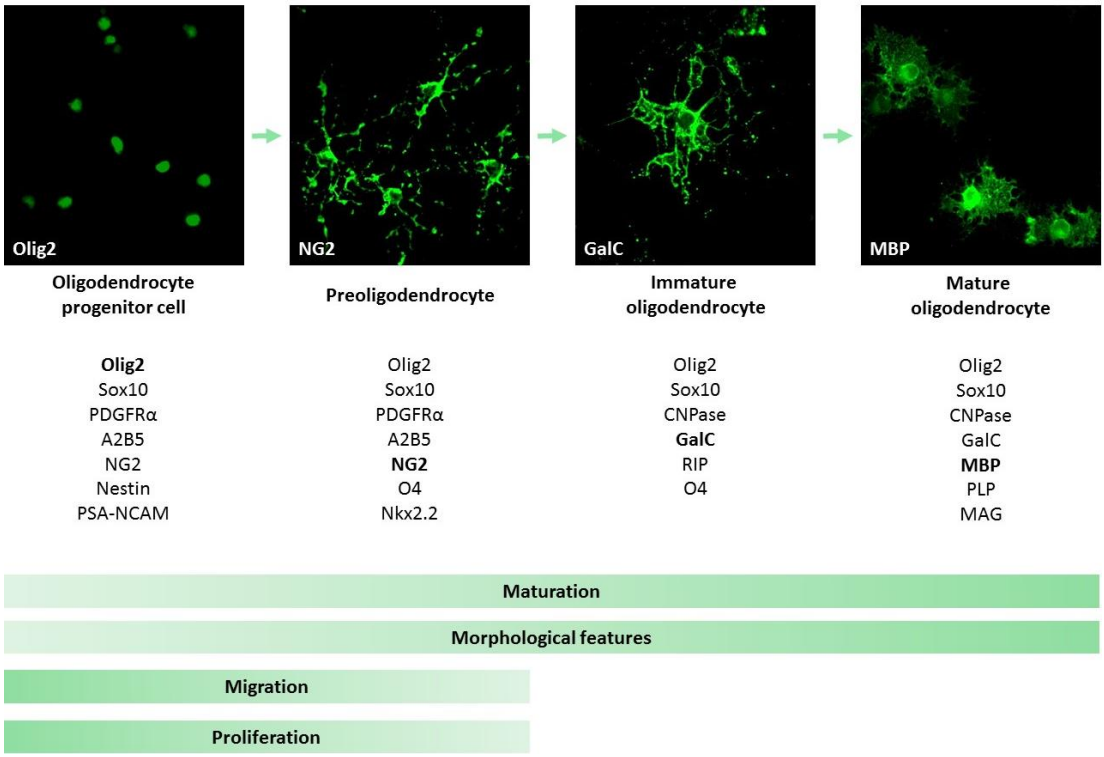

Figure 1.5 – Stages towards oligodendrocyte maturation. These are distinguished by the expression of different molecular markers, their ability to proliferate, migrate and differentiate and their increasingly complex morphology into four stages: oligodendrocyte progenitor cells or OPCs, pre-oligodendrocytes, immature or pre-myelinating oligodendrocytes and mature or myelinating oligodendrocytes. Adapted from *[34]Barateiro et al., 2014, [35]Coppi et al., 2015, and [37]Moreira (MSc thesis), 2015.*

1.2.2 Origin of embryonic oligodendrocyte progenitors

OPCs in the spinal cord and brainstem are mostly derived from a specialized domain of the ventral ventricular zone termed pMN.[38] This germinal zone is induced to express Olig2, a basic helix-loop-helix (bHLH) transcription factor essential for oligodendrocyte specification and development, under the influence of Sonic hedgehog (Shh).[39] These ventrally-generated oligodendrocyte progenitors inhibit the production of most of their dorsal counterparts. In the developing brain, the first oligodendrocyte progenitors are generated in the medial ganglionic eminence (MGE) and anterior entopeduncular area (AEA) in the ventral forebrain at embryonic day 12.5 (E12.5) in mice, migrating laterally and dorsally to populate the entire cortex after E16. As development continues, these progenitors are gradually lost and replaced by two waves of OPCs emerging from the lateral and caudal ganglionic eminences at E15.5 and from the cortex after birth, respectively.[40,41] Thus, in contrast to oligodendrocyte development in the spinal cord, the dorsal-most lineage prevails in the forebrain while the ventral progenitors are eliminated postnatally.[42]

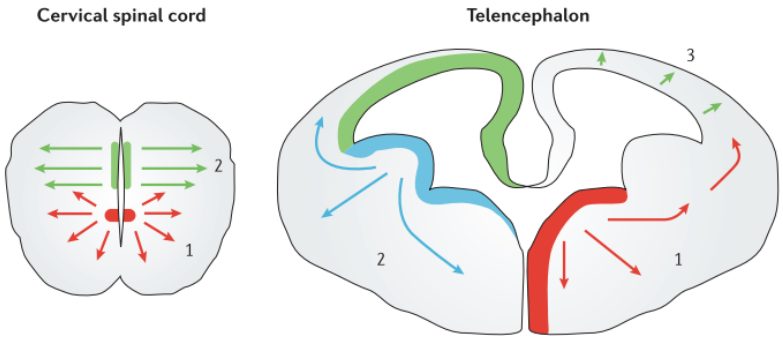

Figure 1.6 – Birth and development of oligodendrocyte precursors in the rodent spinal cord and telencephalon. In the spinal cord, 85% of OPCs are generated from the pMN domain in the ventral ventricular zone (1) at E12.5, while a second wave of dorsal progenitors (2) arises later at E15. In the telencephalon, the first OPCs emerge in the medial ganglionic eminence (1) at E12.5 but are subsequently replaced by two waves of progenitors generated in the lateral and caudal ganglionic eminences (2) at E15.5 and the cortex after birth (3), respectively.[42]

1.2.3 Oligodendrocyte progenitors in the postnatal brain

While neurogenesis in mammals is largely an embryonic event, becoming primarily restricted to the SVZ and DG in the adult, myelination is a postnatal and dynamic process susceptible to modulation.[43] In addition, glial progenitor cells persist in both the grey matter and white matter of the brain.[44] Indeed, $NG2^+$ cells generated during development remain as the main proliferating cell type in the mature CNS, where they constitute 5-8% of the glial population and account for as many as 75% of labelled cells in the cortex, hippocampus and corpus callosum following a 2-hour pulse injection of BrdU.[44,45] These cells are committed to the oligodendroglial lineage and are responsible for the normal turnover of oligodendrocytes during the animal's lifetime, being thus termed adult OPCs.[46,47] Their morphology is remarkably complex, especially in comparison to their embryonic counterparts, with extensive branching processes that make contact with synapses and nodes of Ranvier.[48] $NG2^+$ cells also express glutamine synthetase and the EAAC1 glutamate transporter and are thus thought to monitor neural activity by modulating glutamate neurotransmission.[49] Such observations are consistent with their proposed role in maintaining homeostasis in the CNS and evidence has in fact shown that adult OPCs are recruited to sites of injury, namely following a demyelination event.[50]

The adult SVZ constitutes an additional source of OPCs, albeit a minor one in comparison to the ubiquitous $NG2^+$ cells present in the brain parenchyma. In the SVZ, oligodendrogenesis seems as equally patterned as neurogenesis, with dorsal and lateral aspects considerably giving rise to more OPCs than the ventrolateral SVZ.[51] Furthermore, the proportion of generated OPCs to neuroblasts also varies along the rostrocaudal axis of the SVZ, since a greater number of oligodendrocytes is derived from type B cells in its posterior part (ratio of 1 oligodendrocyte to 3 neurons) compared to the anterior SVZ (ratio of 1 oligodendrocyte to 30 neurons).[16] This mosaic organization of OPCs in the adult SVZ may reflect the regionalization of the forebrain during embryonic oligodendrogenesis.[52] Activation of the canonical Wnt signalling pathway stimulates the selective proliferation within the oligodendroglial lineage, without affecting cell fate of adult NSCs *in vivo*.[51] In contrast, local bone morphogenic protein (BMP) signalling represses the production of OPCs in favour of neurogenesis.[53] Adult NSCs in the SVZ are

consequently fate-restricted, with neurogenic and oligodendroglial clones arising from distinct lineages.[51] This may be an important aspect in the development of future therapeutic strategies, for it allows the specific targeting of either progeny in the context of endogenous cell recruitment following brain injury.

1.3 Multiple sclerosis: an inflammatory demyelinating disease of the Central Nervous System

1.3.1 Pathology and clinical course of multiple sclerosis

Multiple sclerosis (MS) is the most prevalent demyelinating disease of the CNS. It affects twice as many women as men and typically presents in adults between the ages of 20 to 45. While its aetiology is yet to be established, epidemiological studies suggest it arises from a complex interplay between genetic and environmental factors.[54,55] The comorbidity of other immune-mediated disorders in patients diagnosed with MS and its association with the major histocompatibility complex (MHC) genes have been interpreted as evidence that MS is an autoimmune disease.[56,57,58]

The pathology of MS is characterized by the presence of inflammatory infiltrates within the CNS and concomitant oligodendrocyte death, destruction of myelin, axonal loss and gliosis.[59,60] These lesions are termed plaques and constitute the pathological hallmark of MS. Plaques can occur in both eloquent and non-eloquent areas. Eloquent sites can present in the optic pathways, brain stem, cerebellum or spinal cord and are associated with clinical symptoms such as optic neuritis, paraesthesia, weakness and autonomic motor abnormalities. In contrast, non-eloquent areas are restricted to other white-matter domains, in particular the cerebral periventricular zones, and even the cerebral cortex, often remaining clinically silent.[61,62,63]

The clinical course of MS is highly heterogeneous and uncharacteristic of neurological diseases, instead resembling other auto-immune disorders.[64] In approximately 85% of cases, patients initially present with a relapsing-remitting MS (RRMS) phenotype in which symptomatic episodes are interrupted by periods of recovery. Following 5 to 25 years, the majority of RRMS patients develop a secondary progressive form of MS (SPMS) and the acute disabling events are replaced with a slow but steady increase in symptom severity. However, in 10% of patients the relapse-remission pattern is absent and symptoms gradually worsen since the beginning. This clinical course is termed primary progressive MS (PPMS). An even smaller minority of individuals presents with a progressive-relapsing form of the disease (PRMS), characterized by a steady increase in symptom severity since onset and punctuated by sudden worsening episodes without periods of remission.[65] A schematic representation of the possible disability patterns over time is presented in Figure 1.7.

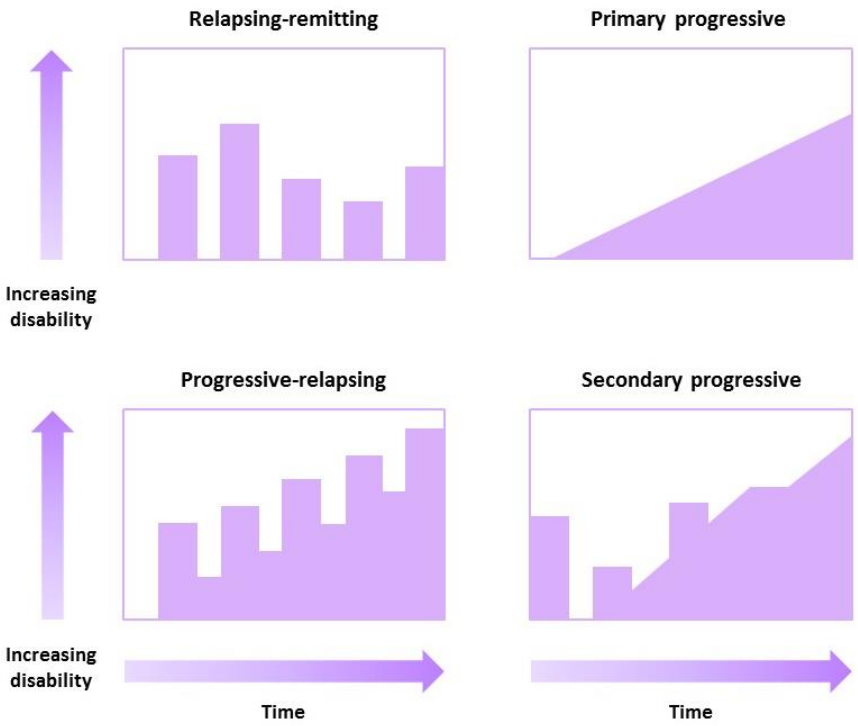

Figure 1.7 – Schematic representation of the disability pattern over time in the clinical phenotypes of MS. Relapsing-remitting MS, the most common clinical phenotype, is characterized by acute symptomatic attacks with recovery periods in-between episodes. In primary progressive MS, a gradual progression of disability is present from onset. Progressive-relapsing MS is characterized by a steady increase in disability but with acute disabling events. In secondary progressive MS, an initial pattern of relapsing-remitting events is observed, which is then replaced with a slow but steady progression in disability. Adapted from [65]*Lublin F.D. et al., 1996.*

Cumulative axonal injury as a result of inflammatory demyelination and transection eventually leads to permanent neurological disability in MS patients.[66] Thus, all available disease-modifying therapies with clinical benefit are immunotherapies aiming to restore a state of immune tolerance in relapsing forms of MS (Table 1.2).[67] However, these are only partially effective and the challenge of addressing the progressive atrophy of demyelinated axons remains.[68]

Remyelination is an observable feature during the course of MS and is associated with clinical remittances, although the extent to which it occurs is extremely variable between individuals.[69] This spontaneous process results in the histological appearance of "shadow plaques", which are characterized by the presence of irregularly thinner and shorter myelin sheaths than would be expected for a given axon's diameter (Figure 1.8).[70,71] In theory, regeneration could be achieved by post-mitotic oligodendrocytes that survive a demyelinating event in spite of losing their myelin sheaths. However, studies have shown this is not the case.[72,73] Instead, myelin repair involves the proliferation and migration of new cells from the oligodendroglial lineage towards injured sites.[74,75] Here, they must increase the expression of Nkx2.2 and Olig2, two transcription factors conserved from developmental myelination, in order to differentiate into functional oligodendrocytes.[76] The majority of recruited oligodendrocytes are derived from $NG2^+$ OPCs present in the parenchyma.[77,78] A smaller contribution arises from adult NSCs present in the SVZ. Examination of human SVZ in post-mortem MS patient brains revealed a two to three-fold increase in cell density and proliferation of progenitors committed

to a glial fate.[79] Enhanced SVZ activation was also demonstrated in experimental autoimmune encephalomyelitis, with mobilized cells generating oligodendrocytes and astrocytes in the lesioned areas.[80]

Table 1.2 – Approved disease-modifying agents for the treatment of multiple sclerosis. There is currently no cure for MS, but therapies exist for the reduction of relapses and management of symptoms.[81]

Drug	Route of Administration	Mechanism of Action
Alemtuzumab	Intravenous	Monoclonal antibody against CD52, a cell surface molecule especially present in T and B lymphocytes[82]
Dimethyl fumarate	Oral	Shifts Th1 cell-based immunity to a Th2 cell response[83]
Fingolimod	Oral	Inhibits the migration of lymphocytes to the CNS, by promoting their retention in the lymph nodes[84]
Glatiramer acetate	Subcutaneous	Binds to MHC molecules and competes with MBP/MHC for T cell-presentation[85]
Interferon β-1a and β-1b	Intramuscular and subcutaneous, respectively	Inhibits T-cell activation and proliferation, as well as leukocyte migration across the BBB[86]
Mitoxantrone	Intravenous	Inhibits the proliferation of T and B lymphocytes, macrophages and other antigen-presenting cells and promotes their apoptosis[87]
Natalizumab	Intravenous	Monoclonal antibody against α4-integrin, preventing the endothelial transmigration of lymphocytes to the CNS[88]
Teriflunomide	Oral	Blocks the *de novo* synthesis of pyrimidines, thus inhibiting the proliferation of T and B cells[89]

Nevertheless, remyelination in MS patients is ultimately inefficient at preventing further disability and the disease continues to progress.[90] The mechanisms responsible for this failure still remain to be completely elucidated, but it is understood that both non-disease-related and disease-specific factors affect this process.[91] For instance, age is known to decrease the effectiveness of myelin repair by impairing OPC recruitment and differentiation. This is an especially important aspect, since the course of MS typically spans several decades.[92] In addition, sustained demyelinating insults seem to deplete the available pool of OPCs.[93,94] A more important contribution, however, stems from environmental cues present in inflamed lesions that inhibit the differentiation of OPCs into myelin-forming cells.[95]

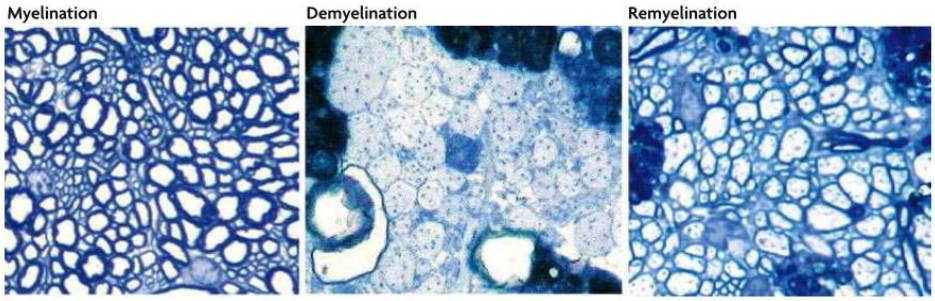

Figure 1.8 – Demyelination and remyelination in MS. These images correspond to transverse sections from the adult rat cerebellar white matter, showing normally myelinated axons, demyelinated axons following injections of ethidium bromide and remyelinated axons with thinner myelin sheaths.[91]

1.3.2 Animal models of multiple sclerosis

Animal models of MS have been extremely important in deciphering the sequence of events that underlie disease development. Since MS is a complex disorder, distinct clinical and pathological aspects are usually recapitulated in different model systems. In the inside-out paradigm, pathological events lead to axonal injury and neurodegeneration, leaving empty myelin sheaths that are subsequently degraded. Conversely, in the outside-in model, loss of trophic support following demyelination leaves the axons susceptible to damage. Autoimmune and viral infection models to either neurons or oligodendrocytes are available to study both pathways of CNS injury.[96]

Experimental autoimmune encephalomyelitis (EAE) is the most extensively used animal model of MS.[97] Incidentally, it was first described in humans as a rare complication of rabies vaccination, developed by Pasteur in the late nineteenth century. The resulting paralysis, histologically characterized by perivascular demyelination, was later proven to arise from an autoimmune response triggered by rabbit spinal cord contaminants present in the vaccine.[98] Based on this knowledge, Thomas Rivers developed EAE as an inflammatory demyelinating animal model in 1933, following immunisation of rhesus monkeys with repeated inoculations of rabbit brain extracts.[99,100] Since then, active EAE has been induced in a variety of animals, notably rodents, by immunisation with CNS tissue or myelin-derived peptides in combination with an adjuvant, which stimulates the host's immune response to the target antigen.[101,102] Alternatively, passive EAE can be induced in naive recipients by transfer of myelin-specific $CD4^+$ T cells from donor animals. More recently, spontaneous EAE models have been established in transgenic animals expressing genes that encode T cell receptors and immunoglobulins specific for myelin proteins.[103,104]

Studies using the EAE model of MS have dictated that following an initial priming and activation in the peripheral lymphoid organs against myelin-specific antigens, $CD4^+$ T cell and monocytes cross the blood-brain barrier (BBB) and invade the CNS parenchyma, initiating a pro-inflammatory cascade.[105] However, the most prevalent immune cell types in MS lesions are $CD8^+$ T cells and macrophages, with $CD4^+$ T cells much less abundant.[106] In this context, the viral demyelinating model induced by infection with Theiler's murine encephalomyelitis virus (TMEV) is a suitable alternative. TMEV, a single-stranded RNA virus from the *Picornaviridae* family, was

first described in 1934 by Max Theiler following observation of spontaneous flaccid paralysis of the hind legs in mice.[107,108] This natural pathogen of mice can be divided into two subgroups, GDVII and TO, based on their ability to damage the CNS. The GDVII subgroup consists of highly virulent strains that cause fatal encephalitis in less than one week. However, infection with strains from the TO subgroup produces a chronic progressive demyelinating inflammatory disease, with the first lesions appearing 3 to 4 weeks following intracerebral inoculation.[109] In this MS model, neurological deficits resulting from demyelination depend on the immune response mediated by $CD8^+$ T cells.[110]

In addition to the well-established models discussed above, toxins are also suitable as demyelinating agents. Toxin models, while not faithfully mimicking the complex aetiology of MS, are nonetheless useful in the study of the mechanisms behind non-autoimmune-induced demyelination and spontaneous remyelination.[111] In this context, demyelination can be caused by focal application or systemic administration of the toxin. First described by Carlton in 1966, the most common agent for systemic demyelination is cuprizone, a copper chelator which is included in the animal's diet at a concentration of 0.2%.[112,113] Copper is an essential metal ion that serves as a cofactor for various metabolic enzymes and its concentration is therefore tightly regulated inside cells. While the precise mechanism by which cuprizone induces demyelination has not yet been deciphered, the most consensual hypothesis proposes that copper deficiency impairs mitochondrial function, leading to increased oxidative stress to which oligodendrocytes are particularly vulnerable.[113,114] Cuprizone ingestion in mice produces a highly reproducible pattern of demyelination and after 5 to 6 weeks of treatment, the corpus callosum is almost entirely void of myelin. Following this acute phase, extensive remyelination occurs within 3 to 4 weeks if cuprizone is removed from the diet. However, if dietary cuprizone consumption persists, remyelination ultimately fails.[115]

Numerous agents have been used to induce focal demyelination in animals, including 6-aminonicotinamide, bacterial endotoxin, ethidium bromide and lysophosphatidylcholine (LPC), also referred to as lysolecithin.[116,117,118,119] The most commonly used of these is LPC and its demyelinating capacity was first demonstrated in CNS tissue *in vitro* in 1950 by Morrison and Zamecnik.[120] The *in vivo* effect of LPC was tested at a concentration of 10 mg/ml in myelinated nerve fibres in the sciatic nerve of adult mice in 1971 and in the white matter of the mouse spinal cord in 1972 by Susan Hall. In both instances, an initial disruption of the myelin sheath occurred within 30 minutes of LPC injection and a subsequent demyelinating lesion was observed.[121] Since then, a 1% solution of LPC in isotonic saline has been used to induce focal demyelination in different areas of the CNS, including the striatum, spinal cord, optic nerve and corpus callosum.[122,123,124,125] Remyelination is an observable occurrence over the following weeks at a rate dependent on the age of the animals.[126,127]

LPC is a minor phospholipid present in cell membranes and plasma and its production is mediated by the action of phospholipase A_2 (PLA_2). This enzyme catalyses the hydrolysis of an ester bond at the *sn-2* position of phospholipids, generating a lysophospholipid and a free fatty acid, such as LPC and arachidonic acid, respectively.[128,129] The metabolism of arachidonic acid by cyclooxygenase and lipoxygenase generates eicosanoids, a known family of inflammatory mediators.[130] On the other hand, LPC is rapidly metabolized by lysophospholipase and LPC-

acyltransferase, lasting only shortly *in vivo*.[128] Although the demyelinating mechanism of LPC is not completely established yet, myelin loss is thought to occur by dissolution into progressively smaller vesicles, rather than as a secondary effect on oligodendrocytes.[131] Moreover, it can act as a chemoattractant agent for immune cells, recruiting T cells, neutrophils, monocytes and activating macrophages and microglia.[123,132,133] These changes were accompanied by disruption of the BBB, upregulation of vascular cell adhesion molecule-1 (VCAM-1) and intercellular adhesion molecule-1 (ICAM-1), and release of chemokines and cytokines.[123,134] However, LPC-induced demyelination is not an immune-mediated event, since it occurs in mice lacking both T and B cells. In addition, efficient CNS remyelination is dependent on the action $CD4^+$ and $CD8^+$ T cells.[135]

More recently, LPC has also been applied to organotypic slices to study the process of de- and remyelination.[136,137,138,139] These *ex vivo* systems preserve CNS explants in long-term cultures which maintain the critical features of *in vivo* studies, namely functional synaptic circuitry and conserved cytoarchitecture, while also allowing control over the extracellular milieu.[140] These aspects are extremely useful in the development of novel active compounds through functional screening without resorting to whole animal studies.[140,141] Specifically in the context of MS, *ex vivo* systems enable the monitoring of the myelin repair process in a more immune-restricted environment, thus providing a method for testing the efficacy of a potential remyelinating therapy.[142,143] Furthermore, organotypic brain slices have been successfully used in the study of adult neurogenesis, both in the hippocampus and in the SVZ.[144,145,146,147]

1.4 Adenosine receptors: a potential target in the treatment of multiple sclerosis

1.4.1 The dual action of adenosine in the Central Nervous System

Adenosine is an endogenous purine nucleoside present in every cell, where it serves as a building block of important molecules involved, for instance, in energy metabolism and signal transduction.[148] It is predominantly produced from the catabolism of adenosine triphosphate (ATP).[149] Intracellular synthesis occurs by dephosphorylation of adenosine 5'-monophosphate (AMP) in a reaction catalysed by cytosolic endo-5'-nucleotidases. An alternative source of intracellular adenosine also arises from the hydrolysis of S-adenyl-L-homocysteine (SAH).[150,151] Subsequently, adenosine can follow several synthetic pathways or be transported out of the cell. In addition, adenosine can also be generated extracellularly from ATP by the action of several enzymes, including ecto-5'-nucleotidase. Since the intracellular concentration of ATP is fifty times higher than AMP's, a small imbalance in the metabolism of ATP leads to a substantial increase in the concentration of AMP. As a result, the intracellular generation of adenosine from cytosolic ATP is considered to represent a sensitive signal of metabolic stress.[152]

In contrast to ATP, adenosine is not traditionally described as a neurotransmitter because it is neither stored nor delivered through synaptic vesicles upon arrival of an electrical impulse. Instead, its release in the nervous system is primarily mediated by the action of equilibrative nucleoside transporters (ENTs) in which the direction of transport depends on the concentration

gradient between the cytoplasm and extracellular space.[153] However, recent evidence showed that adenosine is also released upon electrical stimulation by a calcium-dependent and tetrodotoxin (TTX)-sensitive mechanism, thus suggesting a possible vesicular loading of adenosine into synaptic vesicles.[154] In the extracellular space, adenosine is present at low concentrations and its accumulation in response to metabolic stress and injury acts through a regulatory loop to preserve tissue homeostasis by inhibiting cell metabolism.[155,156,157] Additionally, it influences synaptic transmission at the pre- and postsynaptic level by inhibiting or facilitating neurotransmitter release and de- or hyperpolarising neurons, respectively. Adenosine is thus classified as a neuromodulator.[158,159]

Adenosine exhibits a dual role in the nervous system as a homeostatic regulator and a neuromodulator at the synaptic level, through activation of four metabotropic G-protein coupled receptors (GPCRs): A_1, A_{2A}, A_{2B} and A_3.[160] These receptor subtypes are also known as P1 purinergic receptors and their activation mostly modulates the activity of adenylyl cyclase (AC), an enzyme which catalyses the conversion of adenosine triphosphate (ATP) to cyclic adenosine 3',5'-monophosphate (cAMP) and pyrophosphate (PP_i).[161] cAMP is an important second messenger which upon binding to its main effector – protein kinase A (PKA) – induces the dissociation of the catalytic and regulatory subunits of the latter. Substrates for the catalytic subunits of PKA include metabolic enzymes and transcription factors, such as the cAMP-response element-binding protein (CREB). cAMP-independent transduction pathways, such as phospholipase C (PLC) and phosphoinositide 3-kinase (PI3K), can also be involved (Figure 1.9).[162]

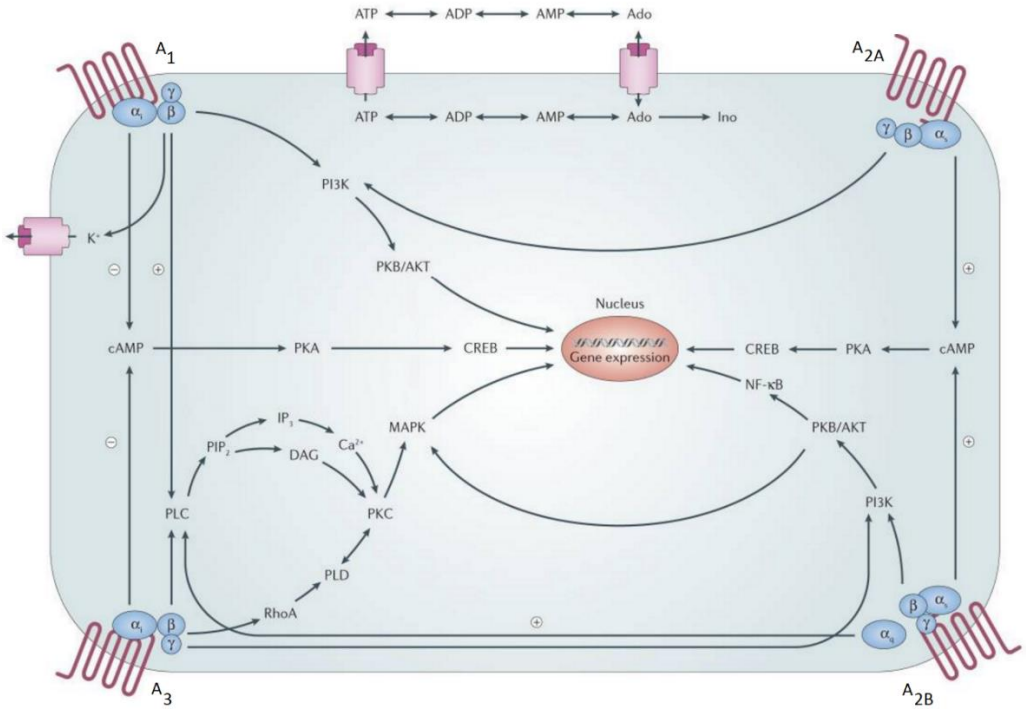

Figure 1.9 – Adenosine receptor signalling pathways. Stimulation of A_1R and A_3R inhibits AC through activation of $G_{i/o}$ proteins and induces PLC-mediated synthesis of inositol 1,4,5-trisphosphate (IP_3) and diacylglycerol (DAG) via $G_{\beta\gamma}$ subunits. In neurons, A_1Rs can also activate K^+ channels. Activation of $A_{2A}R$ and $A_{2B}R$ increases the intracellular concentration of cAMP through $G_{s/olf}$-mediated stimulation of AC. $A_{2A}R$ can also lead to formation of inositol phosphates under certain circumstances. $A_{2B}R$-induced stimulation of PLC occurs through G_q proteins. All four subtypes of ARs can couple to mitogen-activated protein kinase (MAPK), thus giving them a role in cell proliferation, differentiation and apoptosis.[162]

The A_1 receptor (A_1R) is the most abundant of the adenosine receptors (ARs) in the CNS, being highly expressed in the neocortex, cerebellum, hippocampus and dorsal horn of the spinal cord.[163] Activation of this high affinity receptor mediates the $G_{i/o}$-dependent inhibition of AC, thus decreasing the intracellular concentration of cAMP.[164,165] The A_{2A} receptor ($A_{2A}R$) exhibits a widespread distribution in the brain and it is extensively expressed in the olfactory bulb, nucleus accumbens and striatopallidal GABAergic neurons.[166,167,168,169] Similarly to the A_1R, it is also a high affinity receptor but its activation leads to an increase in intracellular cAMP concentration through G_s/G_{olf}-dependent AC stimulation.[170] The A_{2B} receptor ($A_{2B}R$) has a low expression level in the brain and is positively coupled to both AC and PLC through activation of G_s and G_q proteins, respectively.[171,172,173] It is a low affinity receptor and thus remains silent under physiological conditions, becoming activated when the extracellular concentration of adenosine increases.[174] The A_3 receptor (A_3R) has relatively low levels of expression in the brain and is more abundant in the hippocampus and cerebellum.[175,176] Its activation stimulates PLC and leads to a decrease in cAMP through inhibition of AC.[177] All ARs are expressed in both neurons and glia.[178,179]

The synthesis of agonists and antagonists specific for ARs has been a subject of medicinal chemistry in the last four decades. In this context, structure-activity relationship studies of these ligands were crucial to ascertain the biological effects of each AR subtype. Most agonists were designed as derivatives of the adenosine molecule with modifications at the adenine subunit. Similarly, the majority of AR antagonists were developed as analogues of xanthines, a class of compounds to which caffeine belongs (Figure 1.10).[180]

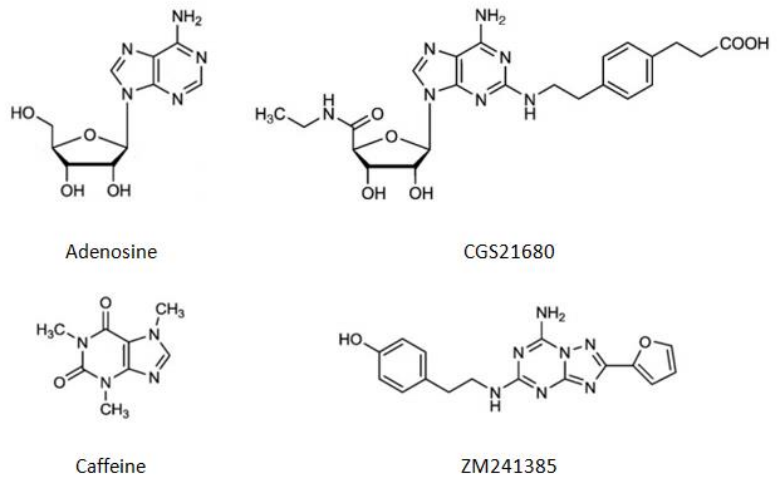

Figure 1.10 – Structural similarity between natural and synthetic ligands of adenosine receptors. CGS21680, a selective agonist of the $A_{2A}R$ (K_i=27 nM), presents a phenylethyl group at the N^2-position of the adenosine molecule. The triazolotriazine ZM241385, a selective antagonist of the $A_{2A}R$ (K_i=1.6 nM), is closely related to caffeine.[162,180]

A_{2A} receptors activate several intracellular signalling pathways. As previously mentioned, $A_{2A}R$ activation promotes the intracellular increase of cAMP, primarily through coupling to members of the G_s subfamily. In the striatum, however, the production of cAMP through $A_{2A}R$ activation was shown to be dependent on its interaction with G_{olf}, the olfactory isoform of the stimulatory G-protein alpha subunit.[181] cAMP produced by downstream GPCR-activation of AC stimulates three main effectors: PKA, the guanine-nucleotide exchange factor EPAC and cyclic-nucleotide-gated ion channels. The most relevant of these is PKA, a heterotetramer composed

of two regulatory and two catalytic subunits which is involved in a wide variety of cellular processes, including metabolism and proliferation. The binding of two molecules of cAMP to each regulatory subunit releases the catalytic subunits, which are now free to phosphorylate serine and threonine residues of target proteins. Some of these are metabolic enzymes and the phosphorylation of glycogen synthase and acetyl CoA carboxylase inhibits glycogen and lipid synthesis, respectively.[182] The catalytic subunits of PKA can also translocate to the nucleus, where they phosphorylate nuclear targets, such as the cAMP response element binding protein (CREB).[183] This transcription factor binds to DNA sequences termed cAMP response elements (CRE) and regulates the expression of downstream genes, namely those involved in neuronal plasticity and long-term memory potentiation (LTP).[184,185]

In addition to the cAMP/PKA pathway, $A_{2A}R$ activation also modulates the MAPK signalling cascade.[186] MAPKs are serine/threonine protein kinases which phosphorylate target substrates implicated in the regulation of cell proliferation, survival and differentiation.[187,188] Finally, activation of A_{2A} receptors also stimulates the phosphatidylinositol-3-kinase (PI3K) signalling pathway.[189] PI3Ks constitute a family of enzymes capable of phosphorylating the 3'-OH group of phosphatidylinositol molecules present in the plasma membrane.[190] These phosphorylated inositol lipids activate various signalling proteins and phosphatidylinositol 3,4,5-trisphosphate (PIP_3) in particular anchors protein kinase B (PKB), a serine/threonine kinase also known as Akt, to the plasma membrane.[191] Downstream effectors of the PI3K/Akt pathway are involved in the regulation of cell proliferation, survival and differentiation.[192] For instance, the activity of pro-apoptotic proteins Bax and Bad is inhibited by PKB.[193] NF-κB, a transcription factor which regulates the expression of anti-apoptotic proteins Bcl-2 and Bcl-X_L, is also an important effector of the PI3K/Akt signalling pathway.[194]

1.4.2 Adenosine receptors in the pathogenesis of multiple sclerosis

The development of both MS and EAE has been associated with dysregulation of the adenosinergic system. A_1R protein expression is significantly decreased in peripheral blood monocytes and brain macrophages in MS patients, potentially leading to increased activation of these cells and subsequent CNS inflammation.[195,196] In the animal model, A_1R null ($A_1R^{-/-}$) mice developed a more severe form of EAE compared to wild-type (WT) ($A_1R^{+/+}$) littermates, which was characterized by exacerbated demyelination, axonal injury and increased activation of microglia and macrophages.[197] Chronic treatment with caffeine, a non-selective antagonist of all subtypes of ARs, was shown to attenuate EAE in both mice and rats by upregulating A_1R expression in microglia.[197,198] Furthermore, high consumption of coffee has been associated with a lower risk of developing MS in two independent case-control studies in humans.[199]

The exact role of the $A_{2A}R$ in MS pathology remains ambiguous. This receptor is regarded as the major mediator of adenosine's anti-inflammatory effects. Its activation supresses key events underlying immune responses, including leukocyte recruitment, pro-inflammatory cytokine production and cell proliferation.[200,201,202,203] Furthermore, $A_{2A}R$ upregulation was observed in lymphocytes from MS patients and *in vitro* stimulation inhibited the release of the pro-inflammatory cytokines IL-1β, IL-6, IL-17, TNF-α and IFN-γ.[204] Expression of $A_{2A}Rs$ is also

increased in cerebral white matter of patients presenting with the SPMS form of the disease, but the significance of this is yet to be unveiled.[205] Surprisingly, a study showed that blockage of the $A_{2A}R$ protected WT mice from EAE induction, most likely by hindering lymphocyte entry to the CNS.[206] However, the most recent evidence on this matter suggests that the $A_{2A}R$ plays a dual and complex role in the progression of EAE. In this animal model, $A_{2A}Rs$ were also found to be upregulated in the CNS, especially in T cells and macrophages/microglia within the inflamed tissue. Preventive treatment in WT animals with an $A_{2A}R$-specific agonist delayed the onset of symptoms, while $A_{2A}R$ activation starting at the peak of EAE exerted the opposite effect and instead worsened the clinical phenotype. Accordingly, $A_{2A}R$ knockout mice showed accelerated disease progression and an exacerbated phenotype in the earlier stages. Following this initial period, $A_{2A}R^{-/-}$ mice quickly recovered to a disease level equivalent to that of WT animals, even exhibiting decreased myelin debris accumulation.[207]

As previously mentioned, the $A_{2B}R$ is a low affinity receptor with reduced levels of expression in brain. While its role in MS remains unknown, it has been demonstrated that antagonism of this receptor ameliorates EAE pathogenesis by inhibiting Th17 differentiation through reduction of IL-6 expression.[208] The involvement of the A_3R in the pathology of MS and EAE is also undetermined. Activation of this receptor has been implicated to mediate the suppression of TNF-α production in microglia following lipopolysaccharide (LPS)-induced inflammation.[209] However, neutralization of TNF-α was shown to be detrimental rather than beneficial to MS patients.[210,211]

1.4.3 Adenosine receptors in the process of oligodendrogenesis

A promising therapeutic strategy in the treatment of MS involves the recruitment of OPCs and their functional maturation in demyelinated sites. In this context, ARs constitute a potential pharmacological target. OPCs express all four subtypes of ARs and adenosine was shown to inhibit cell proliferation, instead promoting their differentiation towards pre-myelinating $O4^+$ oligodendrocytes in a concentration-dependent manner following action potential firing.[212] Furthermore, A_1R activation stimulated OPC migration *in vitro*.[213] In contrast, activation of A_{2A} receptors was discovered to inhibit the differentiation of OPCs isolated from the rat cortex, since treatment with CGS21680 increased the percentage of $NG2^+$ OPCs while decreasing $O4^+$ pre-OLGs and MAG^+ myelinating oligodendrocytes, without affecting cell viability or proliferation.[214] Thus, adenosine appears to act *in vitro* as a dual modulator of cortical oligodendrogenesis through activation of A_1 and A_{2A} receptors.

The SVZ constitutes a long-lasting source of OPCs in the adult mammalian brain. A study has shown that A_1R activation inhibited postnatal neurogenesis by promoting SVZ-derived astrogliogenesis as assayed in neurosphere cultures.[215] However, previous data from our group demonstrated that activation of the $A_{2A}R$ stimulates SVZ-derived oligodendrogenesis in the context of the neurosphere assay, without affecting cell death or proliferation. In particular, pharmacological treatment of SVZ neurospheres with the $A_{2A}R$ agonist CGS21680 (30 nM) increased the number of $Olig2^+$, $NG2^+$, $GalC^+$ and MBP^+ cells. This outcome was blocked by co-incubation with the $A_{2A}R$ antagonist ZM241385 (50 nM).[37]

1.5 Aims

MS is a disease with a profound social impact, since it predominantly affects young adults with progressive neurological disability. Current therapeutic strategies target exclusively its immune component and are, thus, only partially effective as disease continues to advance while typically remaining refractory to non-relapsing-remitting subtypes. During the clinical course of MS, attempts at remyelination occur and new oligodendrocytes are generated from two main sources: OPCs present in the brain parenchyma and a minority from neural stem cells present in the SVZ along the lateral ventricles. As a result, a possible approach in the treatment of MS consists in promoting the remyelination process through increased OPC recruitment, while also facilitating their differentiation into fully mature cells in inflamed sites.

Numerous studies have demonstrated the involvement of the adenosinergic system in the pathogenesis of MS. In particular, A_1 and A_{2A} adenosine receptors regulate the immune response following a demyelination event. OPC migration and differentiation in injured areas also appears to be modulated by these receptors. Indeed, results from our group demonstrated that $A_{2A}R$ activation stimulates SVZ-derived oligodendrogenesis in the neurosphere assay paradigm, without affecting either cell death or proliferation. Thus, the aim of this work was to evaluate whether activation of $A_{2A}Rs$ can promote the generation of oligodendrocytes from the SVZ. For this purpose, two experimental approaches were conducted and the role of $A_{2A}Rs$ in SVZ oligodendrogenesis was studied both *in vivo*, under physiological conditions, and *ex vivo*, following a demyelinating insult with LPC.

2. Methods

2.1 Ethics statement

All the experiments were performed according to European guidelines for the care and use of laboratory animals (86/609/EEC; 2010/63/EU; 2012/707/EU) and Portuguese law (DL 113/2013) concerning the protection of animals for scientific purposes.

2.2 *In vivo* studies

Six-week old adult Wistar rats were implanted with a mini-osmotic pump (Alzet 2004, DURECT Corporation, Cupertino) that was connected to a cannula in the right lateral ventricle (Figure 2.1). Mini-osmotic pumps were filled with artificial cerebrospinal fluid, aCSF (148mM NaCl, 3mM KCl, 1.4mM $CaCl_2$, 0.8mM $MgCl_2$, 1.5mM Na_2HPO_4 and 0.2mM NaH_2PO_4) containing 100nM CGS21680 or with only aCSF, as vehicle (control), with a blunt sterile syringe. The flow moderator, the catheter tube and cannula were assembled to the mini-osmotic pump with surgical glue and the whole drug delivery system was then submerged in sterile saline solution (0.9% NaCl) for 48h at 37°C, in order to ensure a constant pumping prior to pump implantation. Cannulas were inserted in the lateral ventricle of the right hemisphere at the following coordinates: anterior-posterior: -0.4mm, medial-lateral: 1.2mm, dorso-ventral: 3.5mm, having the bregma as a reference. This system delivered CGS21680 (100 nM) or the aCSF at a continuous flow rate of 0.25µl/h for 28 days without restraining the animals. Control rats were infused with aCSF only. Following 28 days, animals were sacrificed in order to evaluate cell proliferation, migration and differentiation. To study cell proliferation, rats received two intraperitoneal injections of 5-bromo-2'-deoxyuridine (BrdU, 100 mg per kg of body weight) in the final day of drug administration at 2-hour intervals. Following the last injection, animals were sacrificed.[80] In contrast, to assess cell migration and differentiation, animals were injected intraperitoneally with BrdU (100 mg per kg of body weight) twice daily, at 12-hour intervals, in the first three days after surgery.[216] BrdU was dissolved in a sterile solution of 0.9% NaCl and 1.75% NaOH (0.4M) and administered at 37°C.

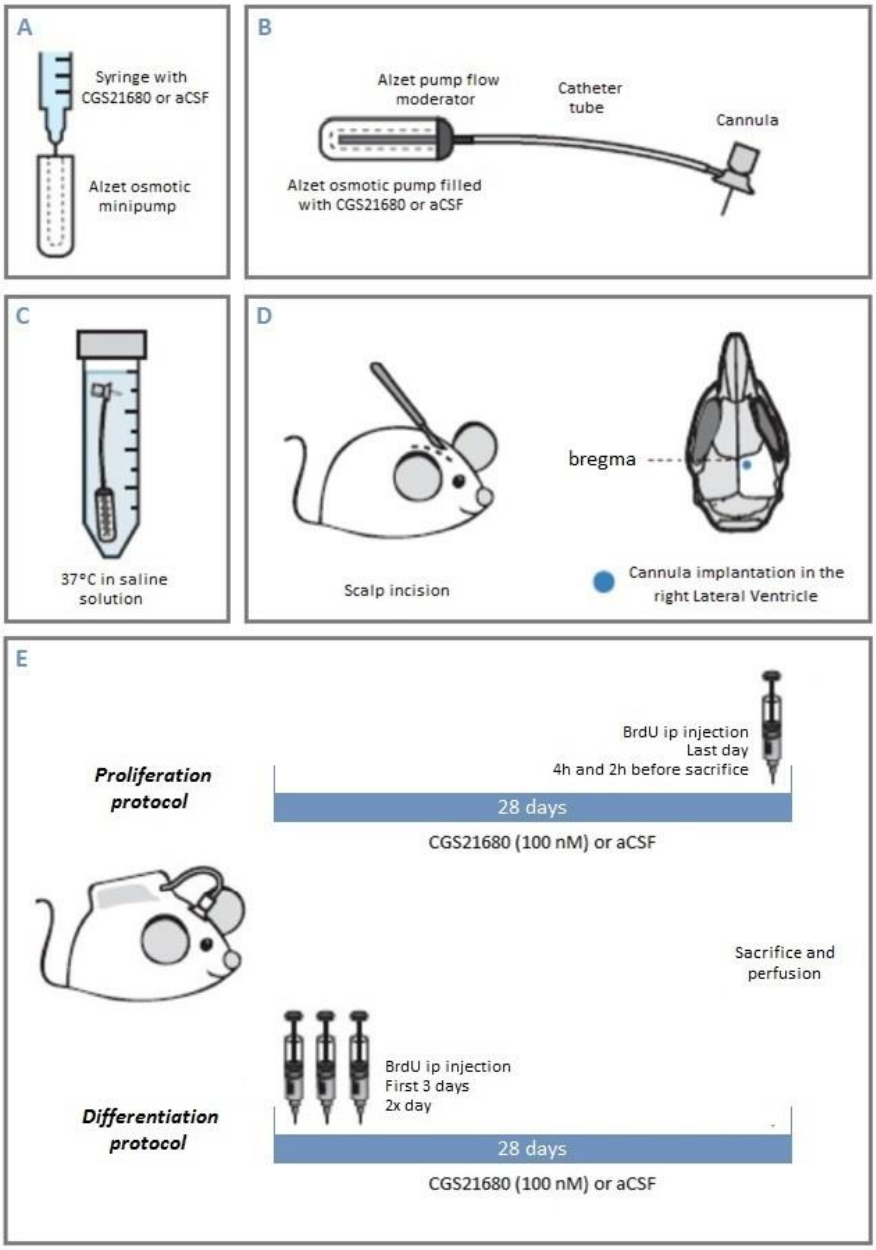

Figure 2.1 – Schematic representation of the experimental protocol employed in the *in vivo* study of SVZ-derived oligodendrogenesis. A. Pump loading with CGS21680 (100 nM) in aCSF or aCSF only for control animals with a sterile syringe. **B.** Assembling the pump flow moderator, catheter tube and cannula. **C.** Pieces were fixed with surgical glue and submerged in sterile saline solution for 48 hours at 37ºC for priming. **D.** The implantation place was set by exposing the skull with a rostro-caudal incision and drilling a hole with precisely the same diameter as the cannula's in the right lateral ventricle. **E.** Experimental design followed for 28 days to study oligodendrogenesis derived from the SVZ, using two BrdU-labelling paradigms to evaluate cell proliferation and differentiation. *Adapted from [217]Eiriz, PhD Thesis, 2013.*

2.2.1 Tissue processing and immunohistochemistry

The procedures regarding surgery, brain fixation and cryosectioning were performed by a PhD student at our group before the start of this master's thesis. Briefly, animals underwent transcardial perfusion under deep anaesthesia with phosphate-buffered saline (PBS) and 4%

paraformaldehyde (PFA). Brains were removed, post-fixed in the same fixative agent and then incubated with 15% and 30% sucrose solutions at 4°C overnight. Subsequently, tissue was embedded in gelatin and cryosectioned into 30-µm-thick coronal serial slices containing the subventricular zone (SVZ), rostral migratory stream (RMS) and olfactory bulb (OB) collected from the contralateral brain hemispheres to perform immunohistochemistry assays. Coronal sections were collected in 10 series on top of Superfrost laminas, each series containing an anterior-posterior reconstruction of the brain formed by sections separated by 300 µm. Serial sectioning allows the visualization of the SVZ's, RMS's and OB's complex morphology and architecture in a single series, while also permitting the unbiased estimation of volume of a brain region of interest and the number of cells within it.[9,218]

Slices from a complete series were rinsed three times with 0.1 M phosphate buffer (PB, 0.081M of Na_2HPO_4 and 0.019M of NaH_2PO_4) at 37°C to remove the gelatin, followed by incubation with hydrochloric acid 2M at the same temperature for 20 minutes to denature DNA and expose the BrdU epitope for antibody labelling. Neutralization was then carried out with 0.1M borate buffer (pH 8.5) for 10 minutes. Slices were washed two times with PB and incubated with blocking solution containing 10% fetal bovine serum (FBS) and 0.2% Triton x-100 in PB for one hour. Subsequently, slices were incubated overnight with the primary antibodies (Table 2.1) diluted in the same blocking solution at room temperature.

Table 2.1 – Primary antibodies and respective working dilutions used in immunohistochemical staining for the *in vivo* experiments

Antigen	Species	Company	Dilution	Reference
BrdU (bromodeoxyuridine)	Mouse	Dako	1:1000	M0744
DCX (doublecortin, C-18)	Goat	Santa Cruz Biotechnology	1:500	Sc-8066
GFAP (glial fibrillary acidic protein)	Mouse	Millipore	1:500	MAB360
Iba1 (ionized calcium-binding adapter molecule 1)	Goat	Abcam	1:500	AB5076
Nestin	Mouse	Abcam	1:500	AB6142
NeuN	Rabbit	Cell Signaling	1:500	D3S3I
Olig2	Rabbit	Millipore	1:1000	AB9610
Sox2 (sex determining region Y-box 2)	Rabbit	Millipore	1:1000	AB5603

Sections were then rinsed three times with 0.1% Triton x-100 in PB (PBT) and incubated with the respective secondary antibodies (Table 2.2) for two hours at room temperature. Following one wash with PBT, nuclei were counterstained with DAPI (1:1000). Slices were rinsed two more times with PBT and once with PB before being mounted in Mowiol medium for fluorescence imaging.

Table 2.2 – Secondary antibodies and respective working dilutions used in the immunohistochemical analysis for the *in vivo* experiments

Antibody	Species	Company	Dilution	Reference
Alexa Fluor 488 anti-goat	Donkey	Life Technologies, Thermo Fisher Scientific	1:1000	A11055
Alexa Fluor 488 anti-rabbit	Donkey	Life Technologies, Thermo Fisher Scientific	1:1000	A21206
Alexa Fluor 568 anti-mouse	Donkey	Life Technologies, Thermo Fisher Scientific	1:1000	A10037
Alexa Fluor 568 anti-rabbit	Donkey	Life Technologies, Thermo Fisher Scientific	1:1000	A10042

2.2.2 Microscopy and cell counting

Fluorescence imaging was performed in two Point Scanning Confocal Microscopes: *Zeiss LSM 710* and *Zeiss LSM 880*. Z-stacks at 2-µm intervals were collected using a 40x objective with a digital zoom of 0.6 and a 1024x1024 resolution.

Cell counting was performed in the SVZ, RMS and randomly selected fields in the granule cell layer of the OB (Figure 2.2). Stereological probes with rectangular frames consisting of two red (rejection) and green (acceptance) lines were manually drawn in serial sections of the OB to count the number of cells.[218] *Zen* and *Fiji* software was used for subsequent image analysis, including area measurements in the designated regions. Volume was estimated by multiplying slice thickness (30 µm) with the area of interest in the respective maximum intensity projection. An extrapolation of total SVZ and RMS volume was performed according to Cavalieri's principle, which states that any volume can be estimated without bias by multiplying the sum of profile areas of the brain region of interest with the distance between sections cut at consistent intervals.[218]

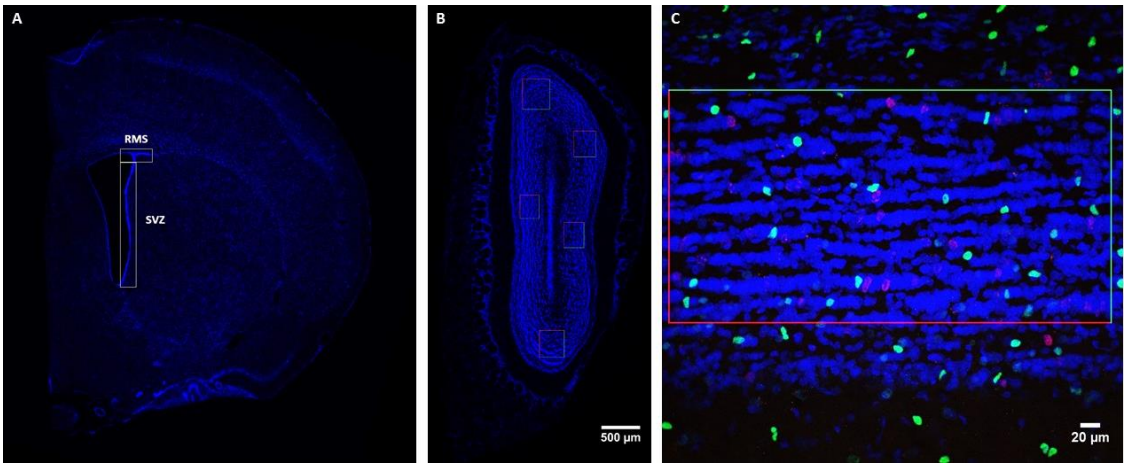

Figure 2.2 – Cell counting in the SVZ, RMS and OB. A. Double-labelled cells for BrdU and Olig2 were counted in coronal sections containing the right lateral wall of the SVZ and RMS. **B, C.** Stereological probes with counting frames consisting of two rejection (red) and acceptance (green) lines were manually drawn in randomly selected fields of the OB.

2.2.3 Statistical analysis

Data are expressed as mean ± standard error of the mean (SEM). Results obtained from control and experimental groups were analysed using an unpaired Student's t-test, with $p<0.05$ considered to represent statistical significance. *GraphPad Prism* software (version 6.01) was used for the analysis of parametric data.

2.3 Forebrain organotypic slice cultures

To study the role of A_{2A} receptors during a demyelinating event, forebrain organotypic slice cultures containing the SVZ and corpus callosum (CC) were prepared per the interface method. Briefly, the brains of Sprague-Dawley rats were removed following decapitation and 400 µm-thick coronal slices were obtained using a McIlwain tissue chopper. While rinsed in ice-cold modified Gey's balanced salt solution (GBSS, Gibco) with 1% D-glucose (Sigma), two slices were carefully separated and placed in each semi-porous membrane insert (Millipore). Cell culture inserts were kept in six-well trays, each with 1 ml of medium, at 37°C in a controlled atmosphere of 5% CO_2 (Figure 2.3).

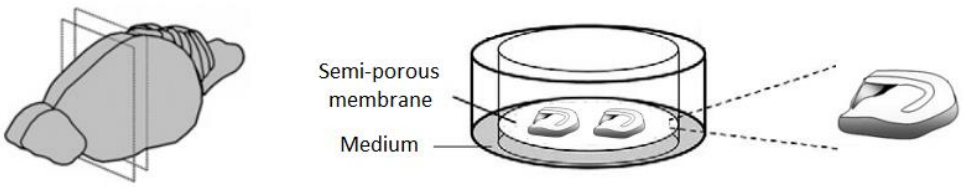

Figure 2.3 – Experimental procedure for obtaining forebrain organotypic slices containing the SVZ and CC. Brains were cut into coronal sections and slices containing the SVZ and CC were isolated and placed onto semi-porous membrane inserts for culturing. Adapted from [219]*Armentano et al., 2011*.

Two experimental designs with forebrain organotypic cultures were performed in rats of different ages, the first with P9 and the second with P14 animals. In protocol 1 (Figure 2.4), isolated slices were maintained in 50% minimal essential media (MEM, Gibco), 25% of heat-inactivated horse serum and Earle's balanced salt solution (EBSS, Gibco), 25 mM HEPES, 36 mM D-glucose, 1% L-glutamine and 1% antibiotic-antimycotic (Sigma). This MEM medium was renewed in the first day *in vitro* (DIV 1) and replaced at DIV 4 by a chemically defined serum-free Neurobasal-A medium (NB-A, Gibco), supplemented with 25 mM HEPES, 36 mM D-glucose, 2% B-27, 1% L-glutamine, 1% antibiotic-antimycotic (Sigma). NB-A medium was renewed at DIV 6 and slices were incubated with 0.5 mg/ml of lysophosphatidylcholine (LPC, Sigma) in ethanol at DIV 7 for 18 hours.[139] Slices were then incubated with the $A_{2A}R$ agonist CGS21680 (30 nM, Tocris) and/or antagonist ZM241385 (50 nM, Tocris) in NB-A medium for 36 hours, following which fixation was performed.

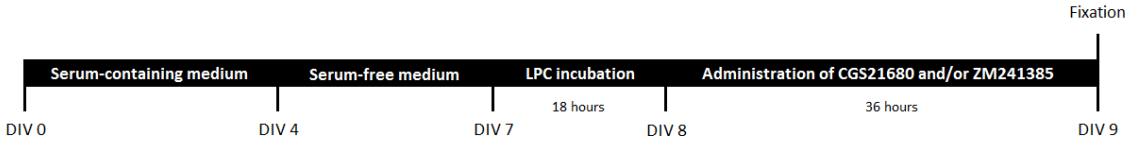

Figure 2.4 – Schematic representation of the culturing protocol 1 using P9 rats. In the first experimental design, forebrain organotypic slices were placed in serum-containing medium for four days, which was then replaced with serum-free medium for three days. Incubation with LPC in serum-free medium for 18 hours followed, after which slices were treated with the $A_{2A}R$ agonist CGS21680 (30 nM) or antagonist ZM241385 (50 nM) for 36 hours.

In protocol 2 (Figure 2.5), slices were isolated and maintained in MEM for one day. Medium was changed to NB-A the next day and slices were incubated with 0.5 mg/ml of LPC for 18 hours. At DIV 2, medium was renewed and treatment with the $A_{2A}R$ agonist CGS21680 (30 nM, Tocris) and/or antagonist ZM241385 (50 nM, Tocris) for 36 hours followed, after which fixation was performed.

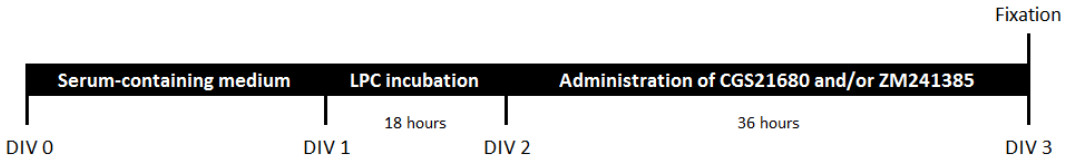

Figure 2.5 – Schematic representation of the culturing protocol 2 using P14 rats. In this experimental design, slices remain only one day in serum-containing medium before being incubated with LPC in serum-free medium for 18 hours. Slices were then treated with the $A_{2A}R$ agonist CGS21680 (30 nM) or antagonist ZM241385 (50 nM) for 36 hours.

2.3.1 Tissue processing and immunohistochemistry

Slices were fixed for one hour with 4% PFA diluted in PBS at room temperature, followed by one-hour incubations in 10% and 20% sucrose solutions. Finally, slices were kept at 4°C in a 30% sucrose solution in PBS until immunostaining was performed.

Following fixation, membranes containing tissue sections were cut from cell culture inserts and put in 24-well plates. Following two PBS washes, slices were incubated in blocking solution (5% horse serum, 5% FBS and 1% Triton x-100 in PBS) for three hours at room temperature with gently agitation on an orbital shaker, ensuring blocking and permeabilization of the tissue in a single step. Subsequently, sections were incubated with the primary antibodies (Table 2.3) diluted in blocking solution (5% horse serum, 5% FBS and 0.2% Triton x-100 in PBS) for one day at 4°C.

Table 2.3 – Primary antibodies and respective working dilutions used in the immunohistochemical analysis of forebrain organotypic slices

Antibody	Company	Dilution	Reference
Rabbit anti-MBP (myelin basic protein)	Cell Signaling	1:200	D8X4Q
Mouse anti-GFAP (glial fibrillary acidic protein)	Millipore	1:750	MAB360
Goat anti-Iba1 (ionized calcium-binding adapter molecule 1)	Abcam	1:750	AB5076
Mouse anti-BrdU (bromodeoxyuridine)	Dako	1:1000	M0744
Rabbit anti-NeuN	Cell Signaling	1:750	D3S3I
Rabbit anti-GFAP (glial fibrillary acidic protein)	Sigma	1:750	G9269
Mouse anti-MAP2 (microtubule-associated protein 2)	Sigma-Aldrich	1:250	M44C3
Rabbit anti-Olig2	Millipore	1:750	AB9610

Slices were then rinsed three times with 0.1% Triton x-100 in PBS (PBST) and incubated with the respective conjugated secondary antibodies (Table 2.4) for one day at 4°C. Following three washes in PBST, nuclei were stained with DAPI (1:1000), rinsed and mounted in Mowiol medium.

Table 2.4 – Secondary antibodies and respective working dilutions used in the immunohistochemical analysis of forebrain organotypic slices.

Antibody	Species	Company	Dilution	Reference
Alexa Fluor 488 anti-goat	Donkey	Life Technologies, Thermo Fisher Scientific	1:1000	A11055
Alexa Fluor 488 anti-rabbit	Donkey	Life Technologies, Thermo Fisher Scientific	1:1000	A21206
Alexa Fluor 568 anti-mouse	Donkey	Life Technologies, Thermo Fisher Scientific	1:1000	A10037
Alexa Fluor 568 anti-rabbit	Donkey	Life Technologies, Thermo Fisher Scientific	1:1000	A10042

2.3.2 Microscopy

To study the role of A_{2A}Rs in oligodendrogenesis within the parenchyma and SVZ following a demyelinating insult with LPC, whole-mount imaging of forebrain slices was performed in the *Leica Z6 APO* Macroscope and in the Widefield Fluorescence Microscope *Zeiss Axio Observer*. For the purpose of widefield imaging of MBP immunofluorescent staining, the intensity of the HXP-120 light source and exposure time in the channel of interest were kept at 79.16% and 150 milliseconds, respectively, in every experiment. Area and fluorescence intensity measurements were performed in the CC region using *Zen* and *Fiji* software. Corrected total fluorescence intensity measurements were performed by subtracting the background noise in three distinct areas to the integrated density of MBP-staining in the CC. Additionally, representative images of CNS cell types in these slices were acquired with the Point Scanning Confocal Microscope *Zeiss LSM 880* using a 20x objective and a digital zoom of 2.0.

2.3.3 Statistical analysis

Data are expressed as mean ± SEM. Results obtained from control and experimental groups were analysed using a one-way analysis of variance (ANOVA) followed by Bonferroni's multiple comparison test and an unpaired Student's t-test, with $p<0.05$ considered to represent statistical significance. *GraphPad Prism* software (version 6.01) was used for the analysis of parametric data.

3. Results

The putative modulatory role of A_{2A}Rs in rat subventricular zone (SVZ) oligodendrogenesis was investigated using *in vivo* and *ex vivo* approaches. In the *in vivo* studies, the proliferation of $Olig2^{+}BrdU^{+}$ cells in the SVZ and their migration along the rostral migratory stream (RMS) to the olfactory bulb (OB) were evaluated under physiological conditions. Moreover, in the *ex vivo* experiments the ability of OPCs, within the parenchyma and SVZ, to remyelinate the corpus callosum (CC) following a demyelinating insult with lysophosphatidylcholine (LPC) was explored.

3.1 *In vivo* studies

3.1.1 The expression of SVZ cellular markers is not altered following activation of A_{2A} receptors

The postnatal SVZ is characterized by the expression of specific cellular markers, as described in the introduction chapter. A qualitative characterization of the SVZ region was performed by immunohistochemical analysis against different cell markers.

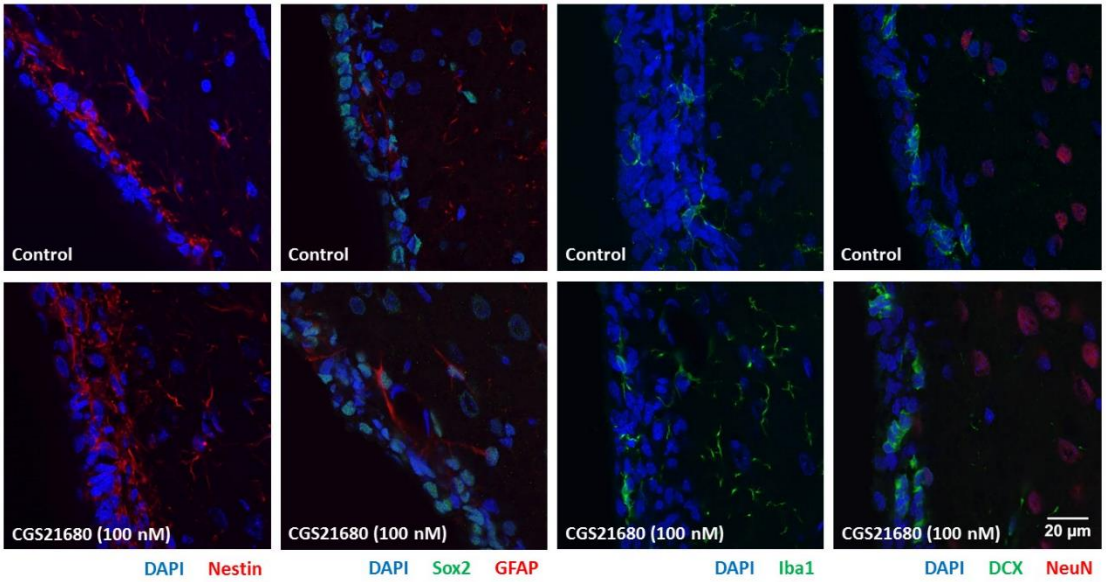

Figure 3.1 – The expression of SVZ cellular markers is not altered following activation of A_{2A} receptors with CGS21680 (100 nM). Representative confocal microscopy images of SVZ molecular markers in control and treated animals, where nuclei were stained with DAPI (**blue**), immature cells with nestin (**red**) and Sox2 (**green**), astrocytes with GFAP (**green**), microglia with Iba1 (**green**), immature neurons with DCX (**green**) and mature neurons with NeuN (**red**). Abbreviations: DCX doublecortin, GFAP glial fibrillary acidic protein, Iba1 ionized calcium-binding adaptor molecule 1, Sox2 sex determining region Y-box 2.

Continuous administration of the $A_{2A}R$ selective agonist CGS21680 (100 nM) during 28 days induced no observable effect in the expression of the intermediate filament Nestin, present in B1 astrocytes and transit-amplifying C cells.[220] Similarly, sex determining region Y-box 2 (Sox2), a transcription factor involved in the self-renewal capacity of NSCs[221], and glial fibrillary acidic protein (GFAP), an intermediate filament expressed in astrocytes[222], was also present in both control and treated animals. The expression of ionized calcium-binding adaptor molecule 1 (Iba1), an actin-binding protein specific of microglia/macrophages[223], is not altered in the SVZ following administration with CGS21680. Finally, doublecortin (DCX), a microtubule-associated protein unique to neuroblasts[224], and NeuN, a marker of mature neurons[225], are also similarly expressed in control and CGS21680-treated animals (Figure 3.1).

3.1.2 $Olig2^+BrdU^+$ cells migrate out of the SVZ along the RMS to the OB under physiological conditions

Proliferation and migration/differentiation of SVZ NSCs promoted by $A_{2A}R$ activation was studied using two different protocols of BrdU administration. To evaluate proliferation, animals received two BrdU injections in the last day of pharmacological treatment. In contrast to the paradigm used to evaluate proliferation in the SVZ, BrdU injections in the first three days of experimental course allowed the study of cell migration of double-labelled NSCs for Olig2, a transcription factor which is expressed throughout the oligodendroglial lineage, from immature to myelin-forming oligodendrocytes, and BrdU. Although a minority of these are found within the striatum and corpus callosum, most $Olig2^+BrdU^+$ cells born in the SVZ travel to the OB along the RMS under physiological conditions (Figure 3.2).

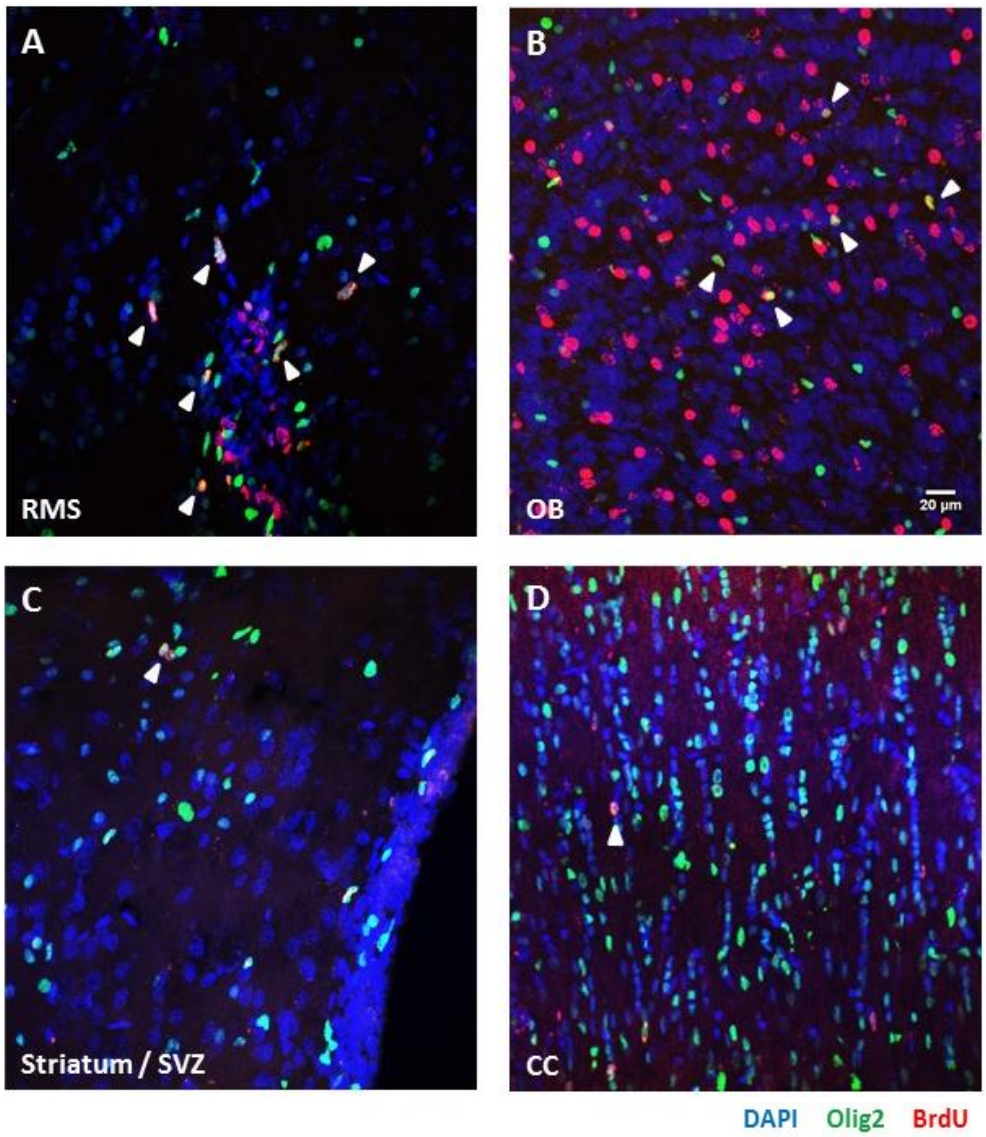

Figure 3.2 – The majority of Olig2⁺BrdU⁺ cells migrate along the RMS to the OB under physiological conditions. Representative images obtained by confocal microscopy of Olig2⁺ (**green**) and BrdU⁺ (**red**) cells, with DAPI (**blue**) allowing the visualization of nuclei. Most Olig2⁺BrdU⁺ cells from the SVZ travel through the RMS **(A)** until reaching the OB **(B)**, while a minority migrates to the striatum surrounding the SVZ **(C)** and to the CC **(D)**. Scale bar, 20 µm.

Their migration out of the SVZ becomes evident when comparing the number of cells double-labelled for Olig2 and BrdU in the SVZ of animals subjected to the proliferation *versus* differentiation protocols. By normalizing the data to control rats from the proliferation paradigm, a drastic reduction was observed in the number of Olig2⁺BrdU⁺ cells per volume of SVZ in control animals from the differentiation protocol (control-proliferation: (6.32±1.01) x 10^{-3} mm^{-3}; control-differentiation: (2.69±0.2) x 10^{-4} mm^{-3}) (Figure 3.3.A). By expressing this data as a percentage of the control-proliferation mean, a reduction of 95.7%±16.1 was observed in the number of Olig2⁺BrdU⁺ cells (control-proliferation: 100.0%±16.1; control-differentiation: 4.3%±0.4, N=3, **p=0.0040) (Figure 3.3.B). Furthermore, a significant decrease in the number of Olig2⁺BrdU⁺ cells between proliferation and differentiation protocols in rats administered with CGS21680 was also observed (CGS21680-proliferation: (2.15±0.54) x 10^{-3} mm^{-3}; CGS21680-differentiation: (3.06±0.27) x 10^{-4} mm^{-3}) (Figure 3.4.A). Similarly, by expressing this data as a

percentage of the control-proliferation mean, a difference of 29.2%±8.6 was observed in the number of Olig2⁺BrdU⁺ cells between proliferation and differentiation protocols following $A_{2A}R$ activation (CGS21680-proliferation: 34.0%±8.6; CGS21680-differentiation: 4.8%±0.4; N=3, *p=0.0273) (Figure 3.4.B).

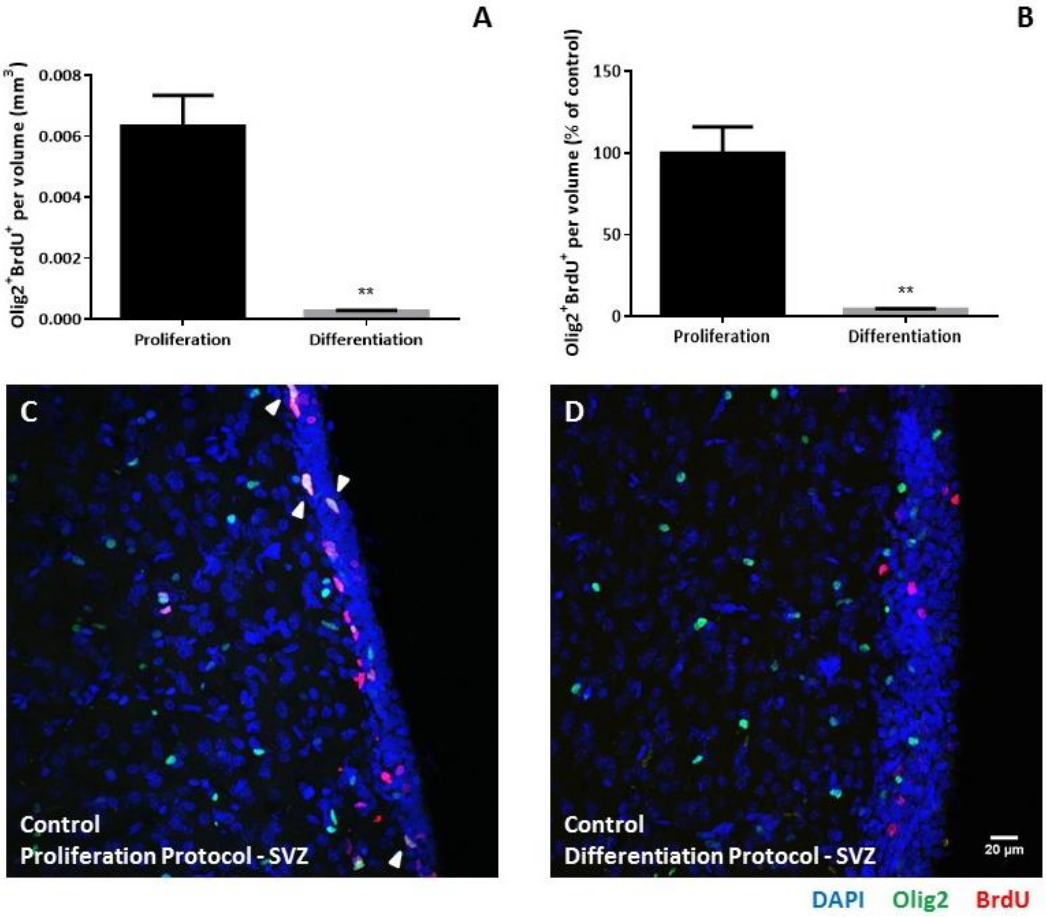

Figure 3.3 – Olig2⁺BrdU⁺ cells migrate out of the SVZ in control animals. Bar graphs depict the number of Olig2⁺BrdU⁺ cells expressed per volume of SVZ in mm^3 **(A)** and as a percentage of the control-proliferation mean **(B)**. Data are expressed as mean ± SEM from three animals per group. Statistical significance was assessed by an unpaired Student's t-test for comparison with the control: **p<0.01. Representative images obtained by confocal microscopy of Olig2⁺ (**green**) and BrdU⁺ (**red**) cells in the SVZ of control-proliferation **(C)** and control-differentiation **(D)** animals, with DAPI (**blue**) allowing the visualization of nuclei. Scale bar, 20 µm.

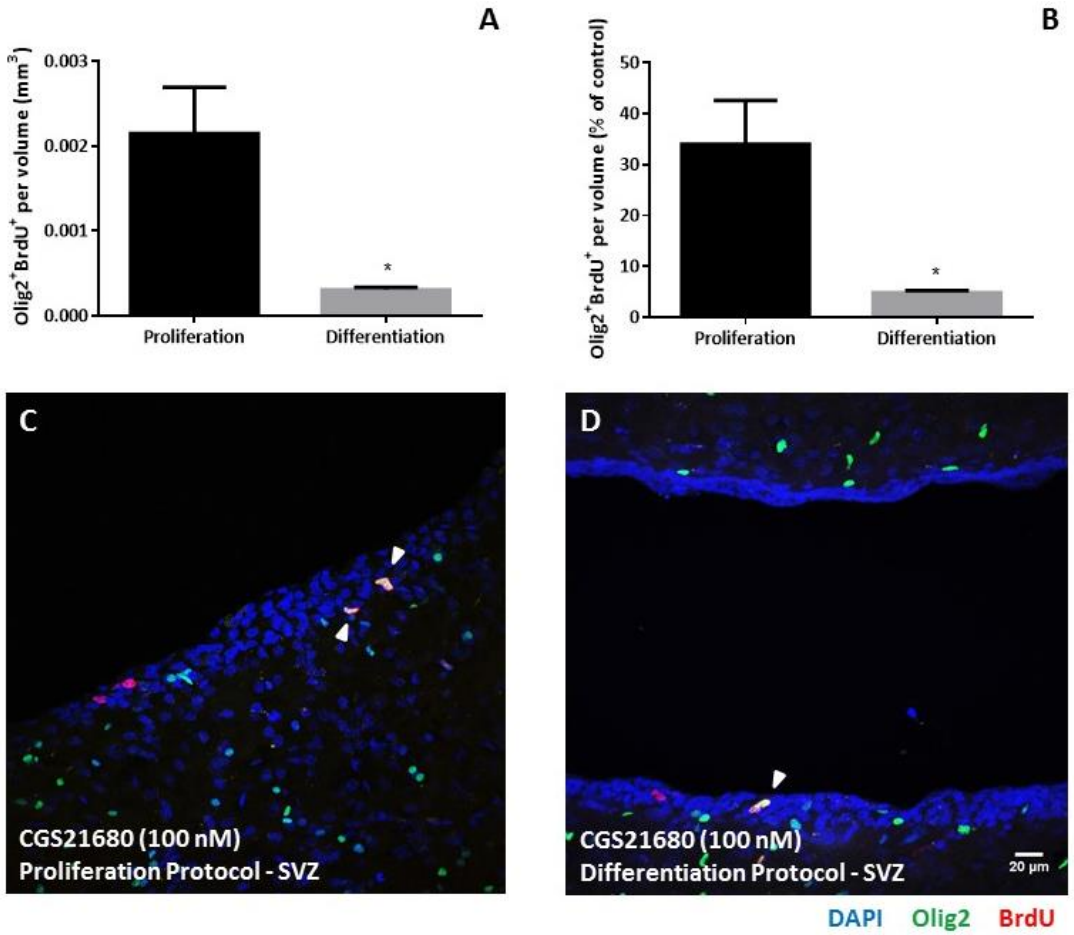

Figure 3.4 – Olig2⁺BrdU⁺ cells migrate out of the SVZ in CGS21680-treated animals. Bar graphs depict the number of Olig2⁺BrdU⁺ cells expressed per volume of SVZ in mm³ **(A)** and as a percentage of the control-proliferation mean **(B)**. Data are expressed as mean ± SEM from three animals per group. Statistical significance was assessed by an unpaired Student's t-test for comparison with the control: *p<0.05. Representative images obtained by confocal microscopy of Olig2⁺ (**green**) and BrdU⁺ (**red**) cells in the SVZ of CGS21680-proliferation **(C)** and CGS21680-differentiation **(D)** animals, with DAPI (**blue**) allowing the visualization of nuclei. Scale bar, 20 µm.

3.1.3 Effect of $A_{2A}R$ activation on the proliferation of NSCs in the SVZ: proliferation protocol

To evaluate the ability of $A_{2A}R$ activation in regulating SVZ oligodendrogenesis, we first studied its effect in regulating NSC proliferation *in vivo*. For this purpose, animals received two BrdU injections in the last day of drug administration, before being sacrificed and BrdU-positive cells in control and treatment groups were then counted. It was observed that administration of the $A_{2A}R$ selective agonist CGS21680 during 28 days resulted in a tendency towards a reduction in the number of BrdU-labelled cells in the SVZ (control: (7.78±1.04) x 10^{-2} mm^{-3}; CGS21680: (5.43±0.62) x 10^{-2} mm^{-3}; N=3, ns, p=0.1236) (Figure 3.5.A). By expressing this data as a percentage of the control mean, this decrease was estimated to be 30.2% (control: 100.0%±13.3; CGS21680: 69.8%±7.9) (Figure 3.5.B).

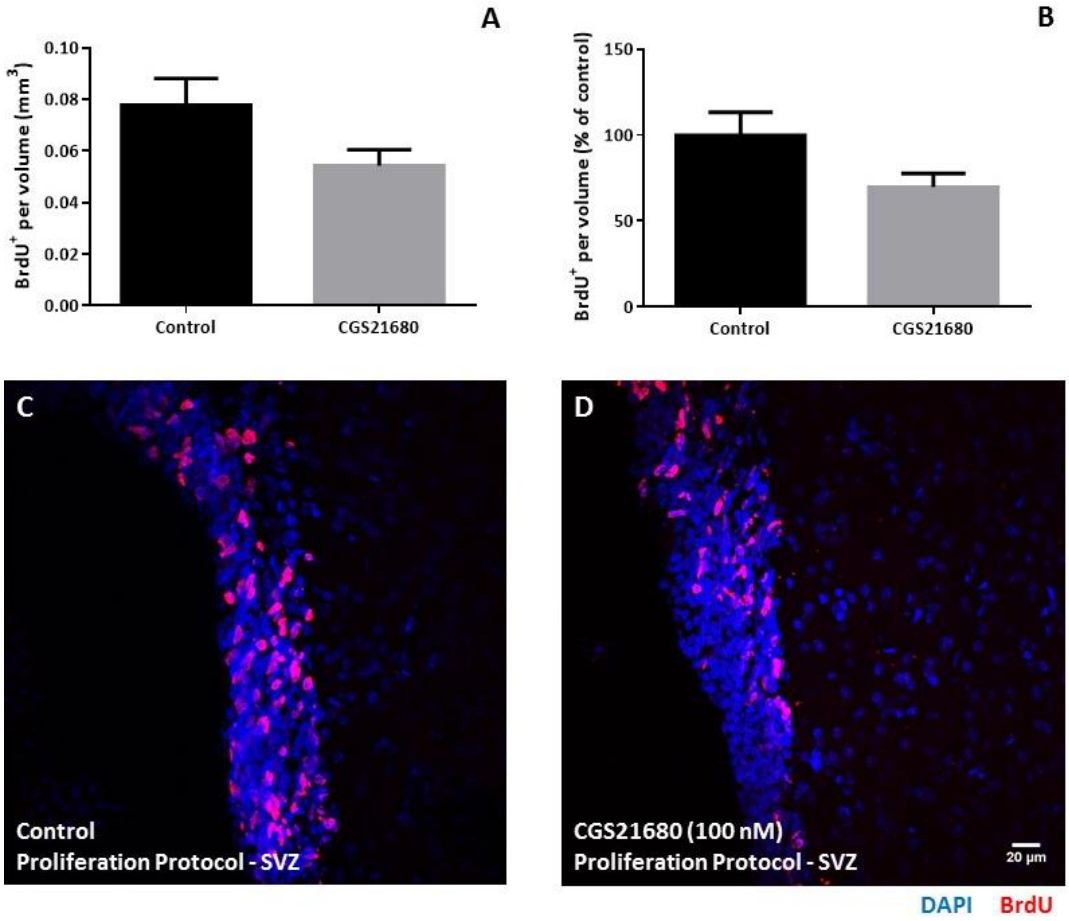

Figure 3.5 – Effect of $A_{2A}R$ activation on the proliferation of SVZ NSCs. Bar graphs depict the number of $BrdU^+$ cells expressed per volume in mm^3 **(A)** and as percentage of the control mean **(B)**. Data are expressed as mean ± SEM from three animals per group. Statistical significance was assessed by an unpaired Student's t-test for comparison with the control. Representative images obtained by confocal microscopy show proliferative cells stained with BrdU (**red**) in the SVZ of control **(C)** and CGS21680-treated **(D)** animals, with DAPI (**blue**) allowing the visualization of nuclei. Scale bar, 20 µm.

3.1.4 $BrdU^+$ cells display unaltered migratory activity along the RMS following $A_{2A}R$ activation: proliferation *versus* differentiation protocols

In contrast, the migration of $BrdU^+$ cells along the RMS is unaltered in rats administered with CGS21680. Indeed, the number of $BrdU^+$ cells present in the RMS of animals subjected to the proliferation protocol is only slightly lower following $A_{2A}R$ activation (control: (7.08±0.68) x 10^{-2} mm^{-3}; CGS21680: (6.10±1.20) x 10^{-2} mm^{-3}) (Figure 3.6.A). By expressing this data as a percentage of the control, this non-significant difference was found to be 13.8%±19.4 (control: 100.0%±9.6; CGS21680: 86.2%16.9; N=3, ns, p=0.5164) (Figure 3.6.B). Moreover, using the differentiation protocol no meaningful differences were observed in the number of $BrdU^+$ cells in the SVZ (control: 100.0%±25.2; CGS21680: 85.7%±31.7; N=3, ns, p=0.7422) (Figure 3.7.B) or in the RMS (control: 100.0%±17.2; CGS21680: 80.8%±42.1; N=3, ns, p=0.6954) (Figure 3.8.B) of control and CGS21680-treated animals.

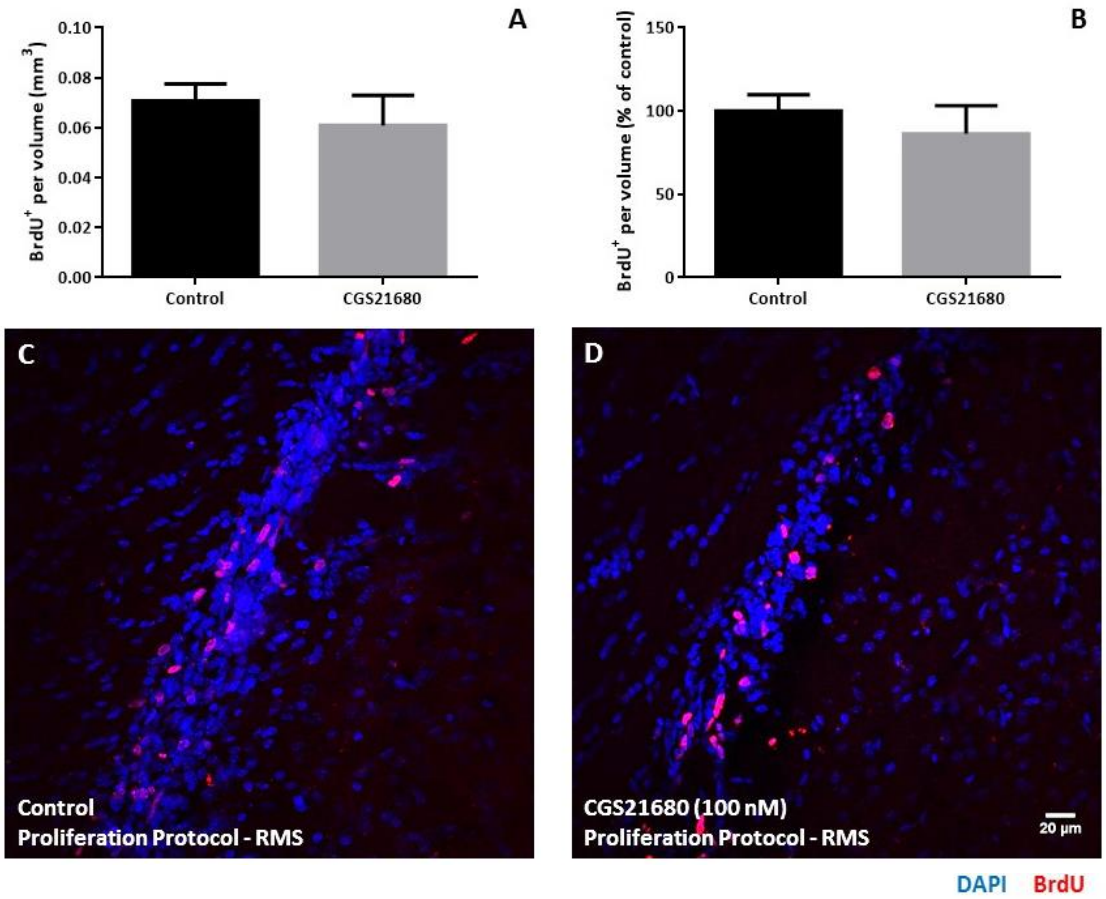

Figure 3.6 – The migration of BrdU⁺ cells along the RMS of control and CGS21680-treated animals from the proliferation protocol. Bar graphs depict the number of BrdU⁺ cells expressed per volume of RMS in mm^3 **(A)** and as a percentage of the control mean **(B)**. Data are expressed as mean ± SEM from three animals per group. Statistical significance was assessed by an unpaired Student's t-test for comparison with the control. Representative images obtained by confocal microscopy of BrdU⁺ (**red**) cells in the RMS of control **(C)** and CGS21680-treated **(D)** animals, with DAPI (**blue**) allowing the visualization of nuclei. Scale bar, 20 µm.

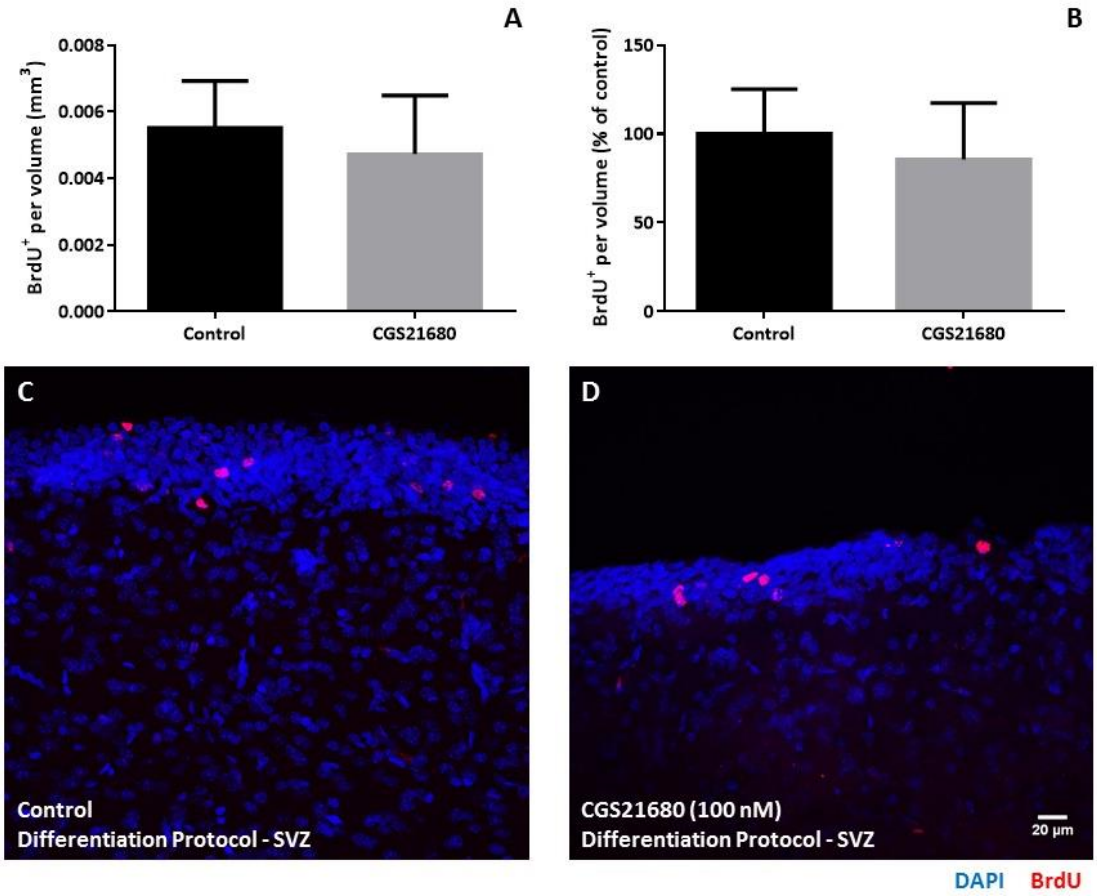

Figure 3.7 – The number of BrdU⁺ cells in the SVZ of CGS21680-treated animals is not altered using the differentiation protocol. Bar graphs depict the number of BrdU⁺ cells expressed per volume of SVZ in mm^3 **(A)** and as a percentage of the control mean **(B)**. Data are expressed as mean ± SEM from three animals per group. Statistical significance was assessed by an unpaired Student's t-test for comparison with the control. Representative images obtained by confocal microscopy of BrdU⁺ (**red**) cells in the SVZ of control **(C)** and CGS21680-treated **(D)** animals, with DAPI (**blue**) allowing the visualization of nuclei. Scale bar, 20 µm.

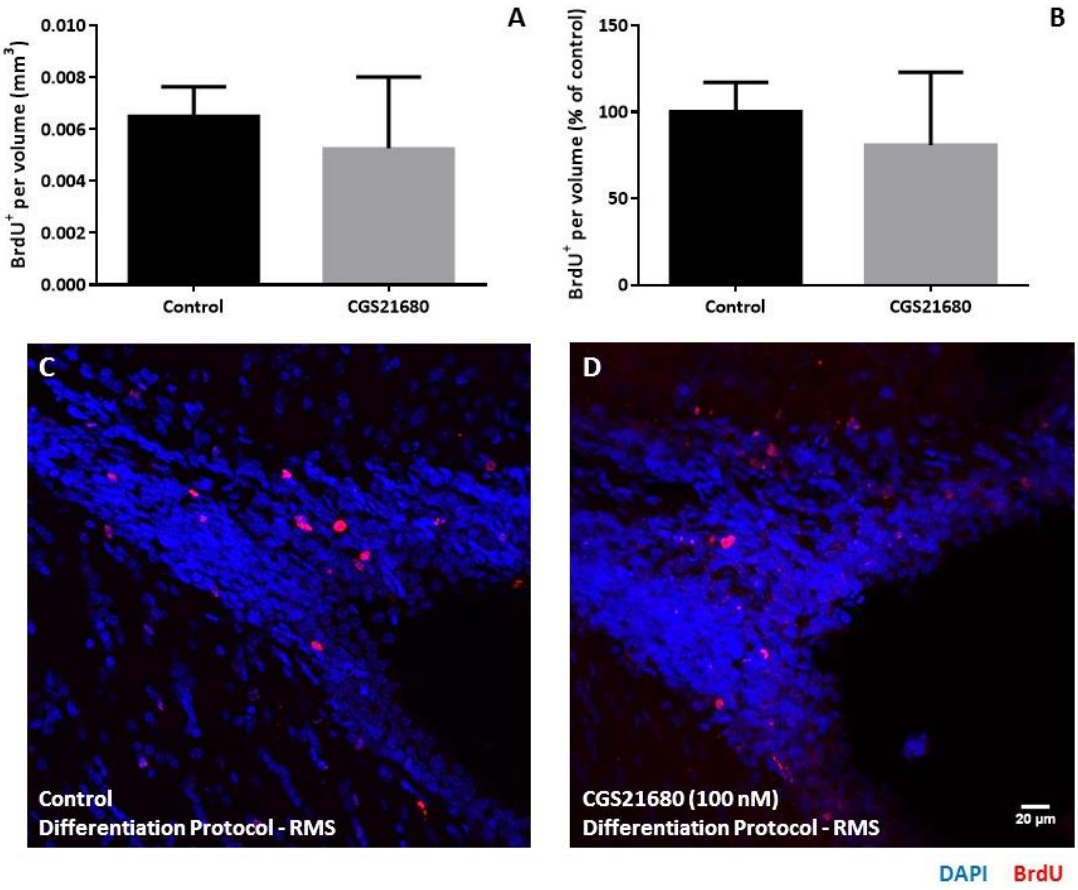

Figure 3.8 – The number of BrdU⁺ cells in the RMS of CGS21680-treated animals is not altered using the differentiation protocol. Bar graphs depict the number of BrdU⁺ cells expressed per volume of RMS in mm^3 **(A)** and as a percentage of the control mean **(B)**. Data are expressed as mean ± SEM from three animals per group. Statistical significance was assessed by an unpaired Student's t-test for comparison with the control. Representative images obtained by confocal microscopy of BrdU⁺ (**red**) cells in the RMS of control **(C)** and CGS21680-treated **(D)** animals, with DAPI (**blue**) allowing the visualization of nuclei. Scale bar, 20 µm.

Supporting the previous observation that migration of BrdU-labelled cells along the RMS following $A_{2A}R$ activation in rats remains unaltered, no significant differences were found in the number of BrdU⁺ cells per volume in the OB of control and CGS21680-treated animals subjected to the differentiation paradigm (control: (9.58±2.11) x 10^{-3} mm^{-3}); CGS21680: (9.02±2.46) x 10^{-3} mm^{-3})) (Figure 3.9.A). Moreover, by normalizing the data in regard to number of BrdU⁺ cells in the OB of control rats, no differences between control and CGS21680-treated animals were observed using the differentiation protocol (control: 100.0%±22.1; CGS21680: 94.1%±13.1, N =3, ns, p=0.8296) (Figure 3.9.B).

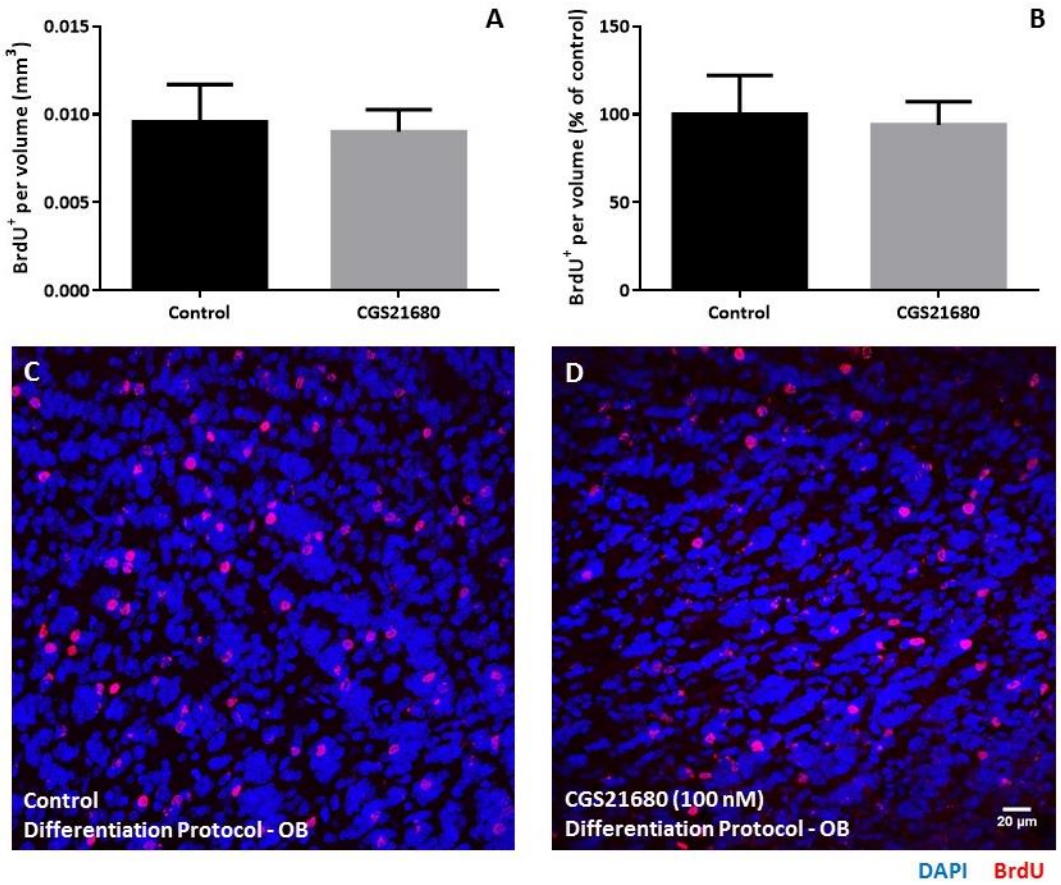

Figure 3.9 – The number of BrdU⁺ cells in the OB is not altered following CGS21680 treatment using the differentiation protocol. Bar graphs depict the number of BrdU-labelled cells per volume **(A)** and expressed as a percentage of control **(B)** in the OB using the differentiation protocol. Data are expressed as mean ± SEM from three animals per group. Statistical significance was assessed by an unpaired Student's t-test for comparison with the control. Representative confocal images show BrdU⁺ (**red**) cells in the OB of control **(C)** and CGS21680-treated rats **(D)** from the differentiation protocol, with DAPI (**blue**) allowing the visualization of nuclei. Scale bar, 20 µm.

3.1.5 $A_{2A}R$ activation decreases the proliferation of Olig2⁺ cells in the SVZ: proliferation protocol

The role of $A_{2A}Rs$ in SVZ oligodendrogenesis *in vivo* was then studied by double-immunostaining against BrdU and Olig2.

It was observed that treatment with CGS21680 (100 nM) for 28 days promoted a reduction in the percentage of Olig2⁺BrdU⁺ relative to total BrdU⁺ cells when compared with the control group (control: 8.3%±1.2; CGS21680: 4.2%±1.2; N=3, ns, p=0.072) (Figure 3.10.A). Moreover, the number of double-labelled cells per volume of SVZ is also decreased in treated animals (control: (6.32±1.01) x 10^{-3} mm^{-3}; CGS21680: (2.15±0.54) x 10^{-3} mm^{-3}) (Figure 3.10.B). Therefore, when data were normalized to the control group, a statistically significant reduction of 66.0%±18.2 in proliferating Olig2⁺ cells was observed (control: 100.0%±16.1; CGS21680: 34.0%±8.6; N=3, *p=0.0222) (Figure 3.10C).

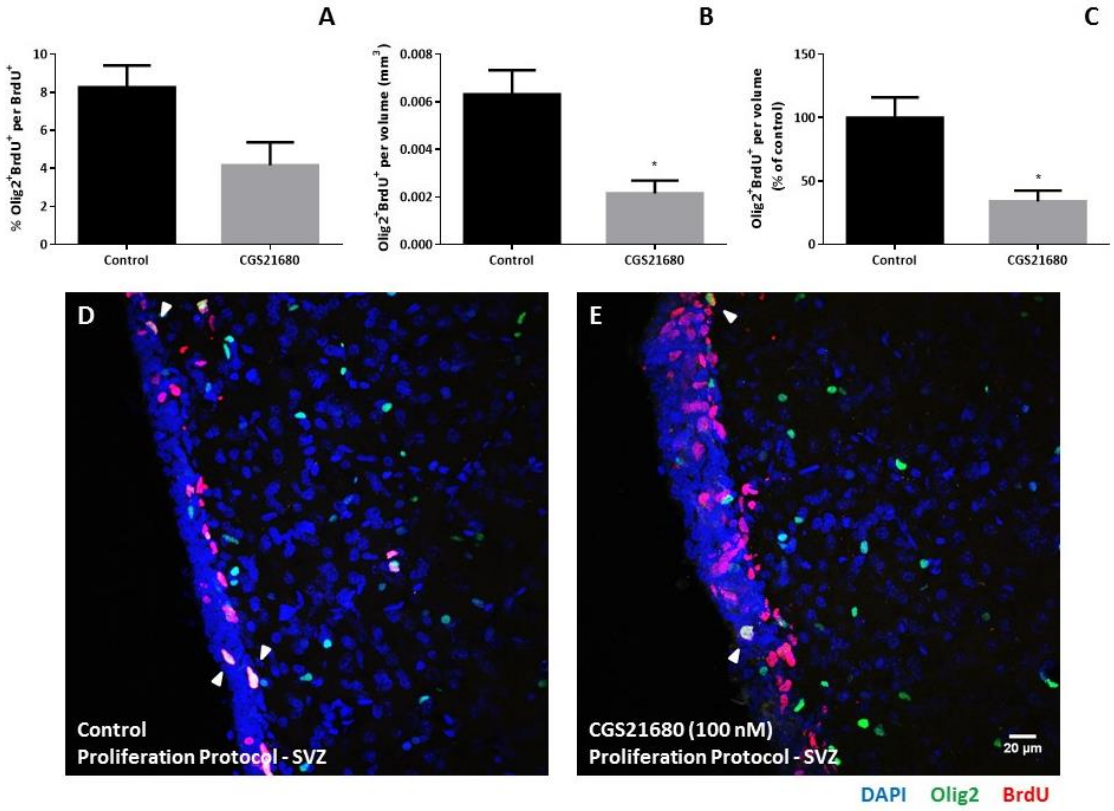

Figure 3.10 – A_{2A} receptor activation decreases the proliferation of Olig2⁺BrdU⁺ cells in the SVZ. Bar graphs depict the number of Olig2⁺BrdU⁺ cells expressed as a percentage of total BrdU⁺ cells **(A)**, per volume of SVZ in mm^3 **(B)** and as a percentage of the control mean **(C)**. Data are expressed as mean ± SEM from three animals per group. Statistical significance was assessed by an unpaired Student's t-test for comparison with the control: *p<0.05. Representative images obtained by confocal microscopy of Olig2⁺ (**green**) and BrdU⁺ (**red**) cells in the SVZ of control **(D)** and CGS21680-treated **(E)** animals, with DAPI (**blue**) allowing the visualization of nuclei. Scale bar, 20 µm.

3.1.6 Olig2⁺BrdU⁺ cells display a slower migratory activity along the RMS following A_{2A}R activation: proliferation *versus* differentiation protocols

Interestingly, the migration of Olig2⁺BrdU⁺ cells is inhibited by the activation of A_{2A} receptors. Indeed, using the proliferation protocol, it was possible to observe that in the RMS the percentage of Olig2⁺BrdU⁺ relative to total BrdU⁺ cells in the RMS is similar in control and CGS21680-treated animals (control: 17.7%±0.7; CGS21680: 16.2%±0.6; N=3, ns, p=0.1914, Figure 3.11.A). However, the number of double-labelled cells per volume of RMS is slightly diminished in treated animals comparing with controls (control: (1.25±0.12) x 10^{-2} mm^{-3}; CGS21680: (9.78±1.67) x 10^{-3} mm^{-3}) (Figure 3.11.B). Moreover, when expressing this data as a percentage of the control mean, there is a tendency towards a reduction of 21.9%±16.4 in the number of Olig2⁺BrdU⁺ cells (control: 100%±9.5, CGS21680: 78.1%±13.4, N=3, ns, p=0.2529) (Figure 3.11.C).

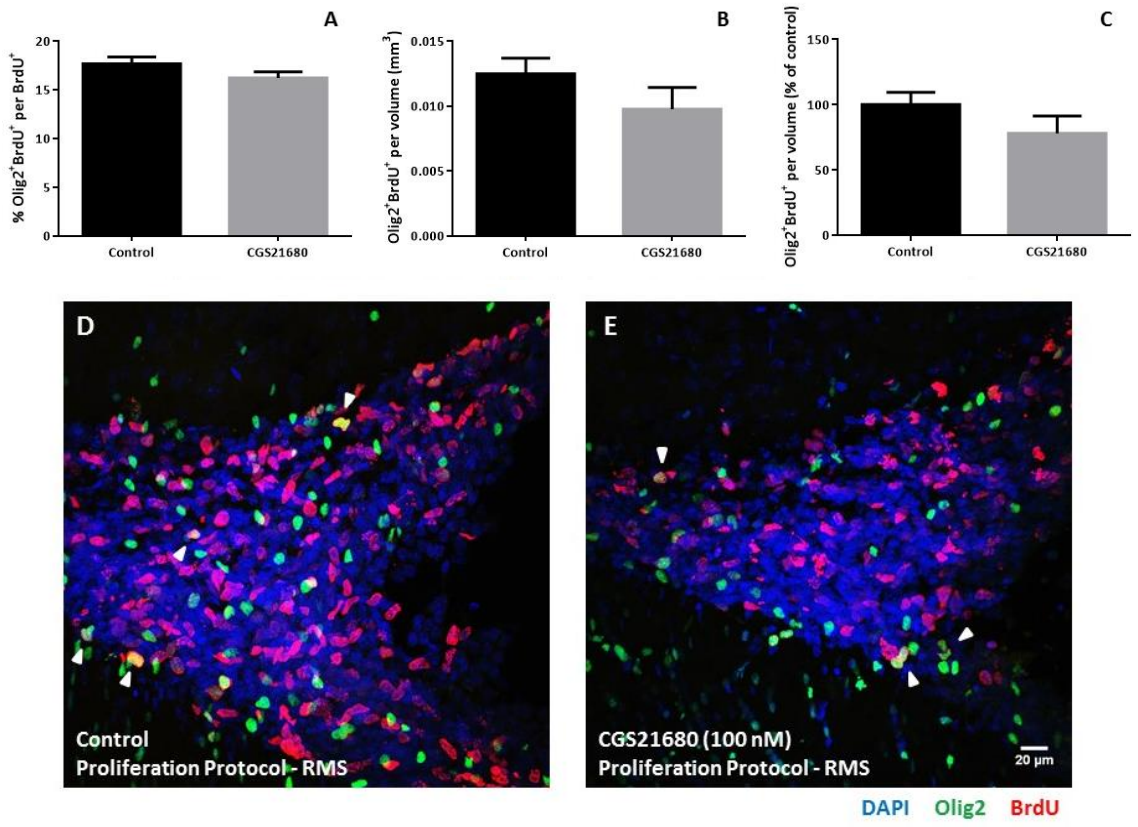

Figure 3.11 – Migration of Olig2⁺BrdU⁺ cells along the RMS of control and CGS21680-treated animals from the proliferation protocol. Bar graphs depict the number of Olig2⁺BrdU⁺ cells expressed as a percentage of total BrdU⁺ cells **(A)**, per volume of SVZ in mm^3 **(B)** and as a percentage of the control mean **(C)**. Data are expressed as mean ± SEM from three animals per group. Statistical significance was assessed by an unpaired Student's t-test for comparison with the control. Representative images obtained by confocal microscopy of Olig2⁺ (**green**) and BrdU⁺ (**red**) cells in the RMS of control **(D)** and CGS21680-treated **(E)** animals, with DAPI (**blue**) allowing the visualization of nuclei. Scale bar, 20 µm.

These differences become greater and thus statistically significant when analysing immunostaining results from animals subjected to the differentiation protocol since there is more time to allow cell migration (Figure 3.12). As such, the percentage of Olig2⁺BrdU⁺ relative to total BrdU⁺ cells in the RMS is significantly lower following activation of A_{2A} receptors when compared with control rats (control: 17.2%±2.6, CGS21680: 5.0%±0.5, N=3, *p=0.0105) (Figure 3.12.A). Moreover, the number of Olig2⁺BrdU⁺ cells per volume of RMS is also diminished in CGS21680-treated animals (control: (1.08±0.11) x 10^{-3} mm^{-3}; CGS21680: (2.43±1.06) x 10^{-4} mm^{-3}; N=3) (Figure 3.12.B). By expressing this data as a percentage of the control mean, a reduction of 77.5%±14.5 was observed in the number of Olig2⁺BrdU⁺ cells in the RMS of CGS21680-administered rats from the differentiation protocol (control: 100%±8.7, CGS21680: 22.5%±9.8, N=3, **p=0.0060) (Figure 3.12.C).

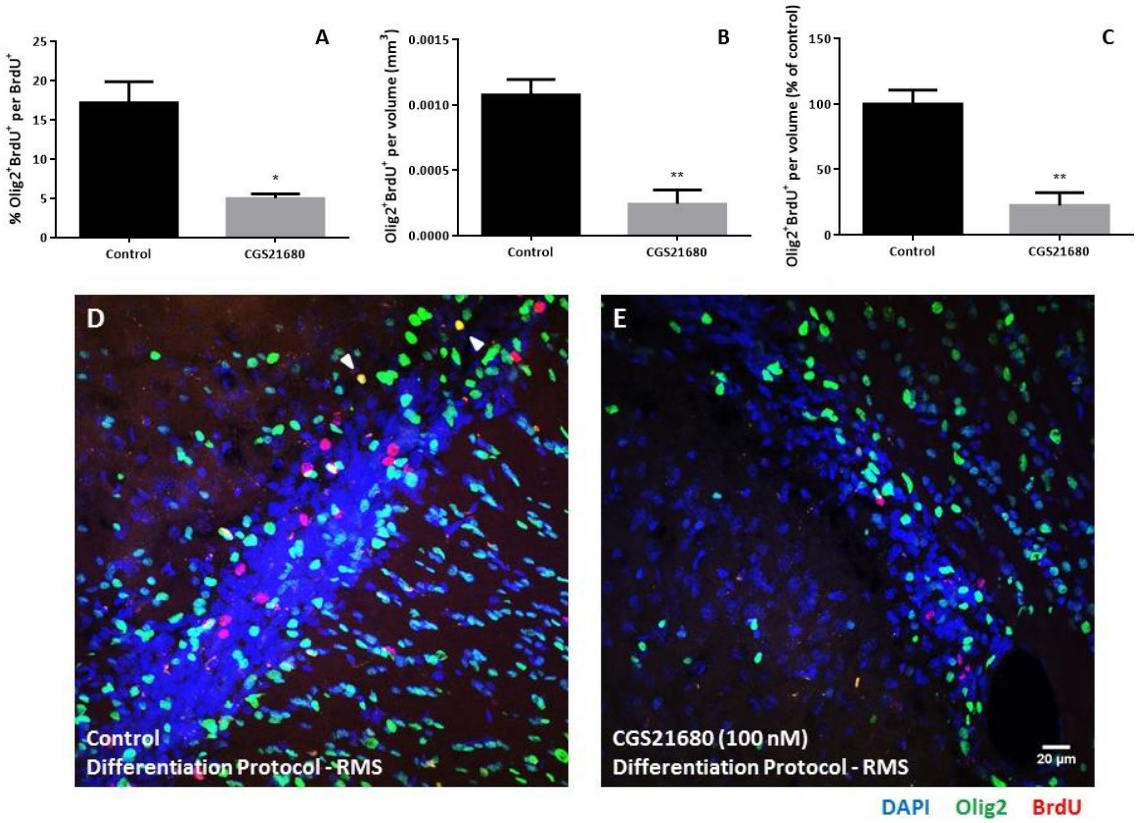

Figure 3.12 – The migratory ability of Olig2⁺BrdU⁺ cells along the RMS is impaired in CGS21680-treated rats using the differentiation protocol. Bar graphs depict the number of Olig2⁺BrdU⁺ cells expressed as a percentage of total BrdU⁺ cells **(A)**, per volume of SVZ in mm^3 **(B)** and as a percentage of the control mean **(C)**. Data are expressed as mean ± SEM from three animals per group. Statistical significance was assessed by an unpaired Student's t-test for comparison with the control: *p<0.05 and **p<0.01. Representative images obtained by confocal microscopy of Olig2⁺ (**green**) and BrdU⁺ (**red**) cells in the RMS of control **(D)** and CGS21680-treated **(E)** animals, with DAPI (**blue**) allowing the visualization of nuclei. Scale bar, 20 µm.

This effect of A_{2A} receptors in impairing Olig2⁺BrdU⁺ cell migration along the RMS is further supported by an increased tendency towards their presence in the SVZ of CGS21680-treated animals from the differentiation protocol (Figure 3.13), as observed by their percentage relative to total BrdU⁺ cells (control: 5.8%±1.8; CGS21680: 9.0%±3.5; N=3, ns, p=0.4616) (Figure 3.13.A), number per volume of SVZ (control: (2.69±0.24) x 10^{-4} mm^{-3}; CGS21680: (3.05±0.28) x 10^{-4} mm^{-3}) (Figure 3.13.B) and normalization to the control mean (control: 100.0%±9.0; CGS21680: 113.5%±10.3; N=3, ns, p=0.3790) (Figure 3.13.C).

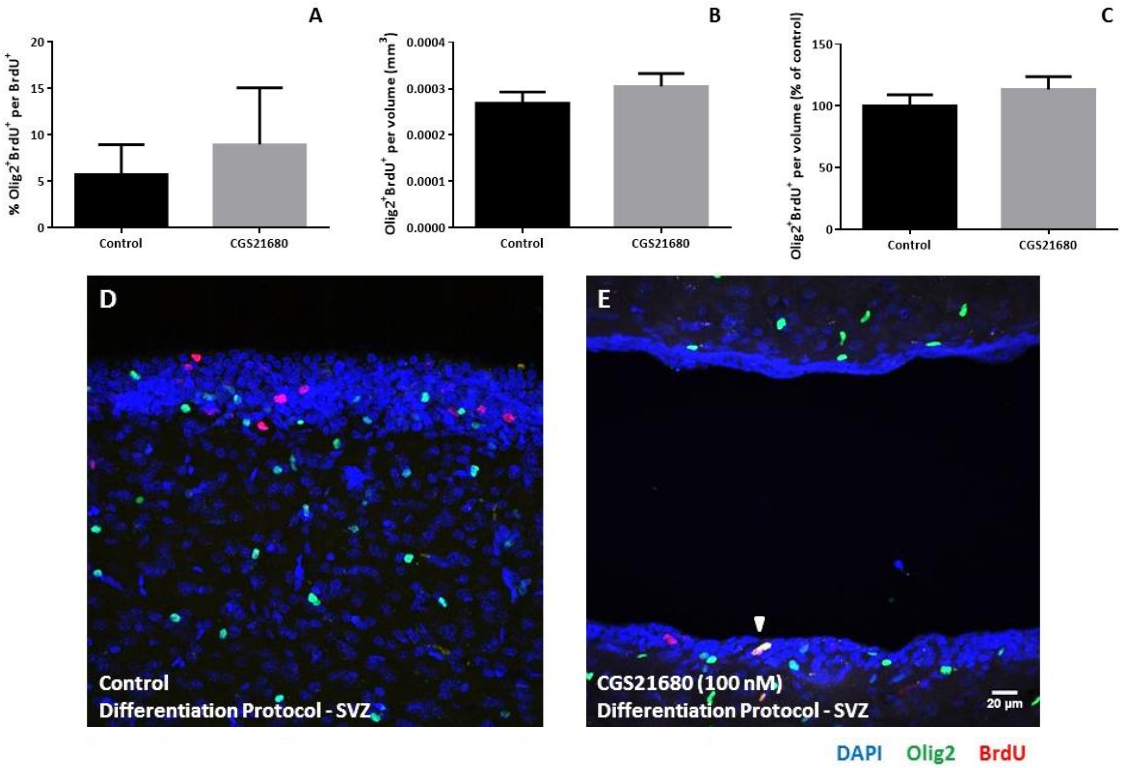

Figure 3.13 – The presence of Olig2⁺BrdU⁺ cells is increased in the SVZ of CGS21680-treated animals from the differentiation protocol. Bar graphs depict the number of Olig2⁺BrdU⁺ cells expressed as a percentage of total BrdU⁺ cells **(A)**, per volume of SVZ in mm^3 **(B)** and as a percentage of the control mean **(C)**. Data are expressed as mean ± SEM from three animals per group. Statistical significance was assessed by an unpaired Student's t-test for comparison with the control. Representative images obtained by confocal microscopy of Olig2⁺ (**green**) and BrdU⁺ (**red**) cells in the SVZ of control **(D)** and CGS21680-treated **(E)** animals, with DAPI (**blue**) allowing the visualization of nuclei. Scale bar, 20 µm.

3.1.7 Only a minority of Olig2⁺BrdU⁺ cells born in the SVZ are retained in the Olfactory Bulb

Lastly, the role of $A_{2A}R$ activation in the differentiation of Olig2⁺BrdU⁺ cells from the SVZ was investigated in the OB of healthy rats. For this purpose, the same labelling paradigm used to evaluate cell migration was employed and double-labelled cells in control and treatment groups were then counted in the OB.

The number of Olig2⁺BrdU⁺ cells present in the OB using the differentiation protocol was significantly scarcer comparatively to the SVZ+RMS of both control and CGS21680-treated animals that underwent the proliferation paradigm. More specifically, a reduction of 65.8% in the percentage of double-labelled cells relative to total BrdU⁺ cells was observed in the OB of control rats (control SVZ+RMS proliferation: 11.1%±0.7; control OB differentiation: 3.8%±0.3; N=3, ***p=0.0009) (Figure 3.14). Likewise, a decrease of 63.5% in the percentage of Olig2⁺BrdU⁺ cells relative to total BrdU⁺ cells was found in the OB of CGS21680-treated animals from the differentiation protocol in regard to the SVZ+RMS of experimental animals using the

proliferation paradigm (CGS21680 SVZ+RMS proliferation: 8.5%±0.4; CGS21680 OB differentiation: 3.1%±0.2; N=3, ***p=0.0004) (Figure 3.15).

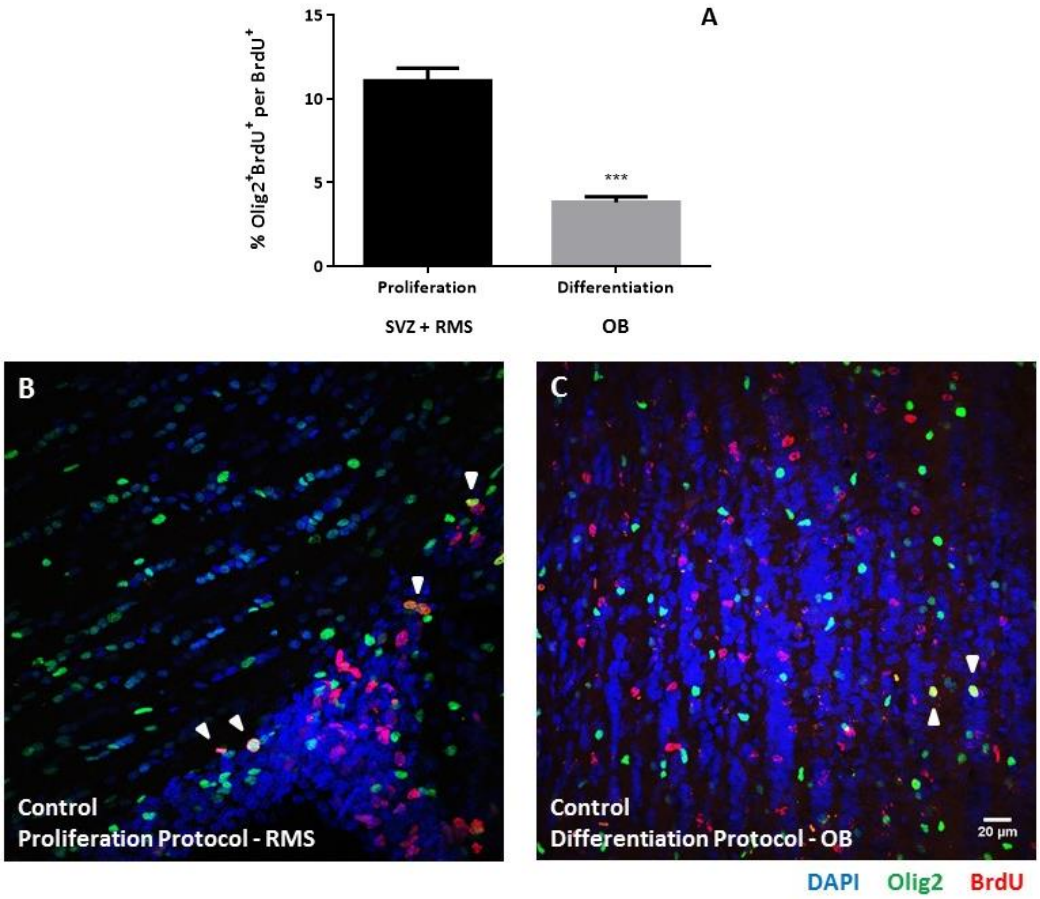

Figure 3.14 – The presence of Olig2⁺BrdU⁺ cells in the OB using the differentiation protocol is decreased in comparison to the SVZ+RMS with the proliferation protocol in control animals. Bar graph depicts the number of Olig2⁺BrdU⁺ cells expressed as a percentage of total BrdU⁺ cells **(A)**. Data are expressed as mean ± SEM from three animals per group. Statistical significance was assessed by an unpaired Student's t-test for comparison with the control: ***p<0.001. Representative images obtained by confocal microscopy of Olig2⁺ (**green**) and BrdU⁺ (**red**) cells in the SVZ+RMS using the proliferation protocol **(B)** and OB using the differentiation paradigm **(C)** in control animals, with DAPI (**blue**) allowing the visualization of nuclei. Scale bar, 20 µm.

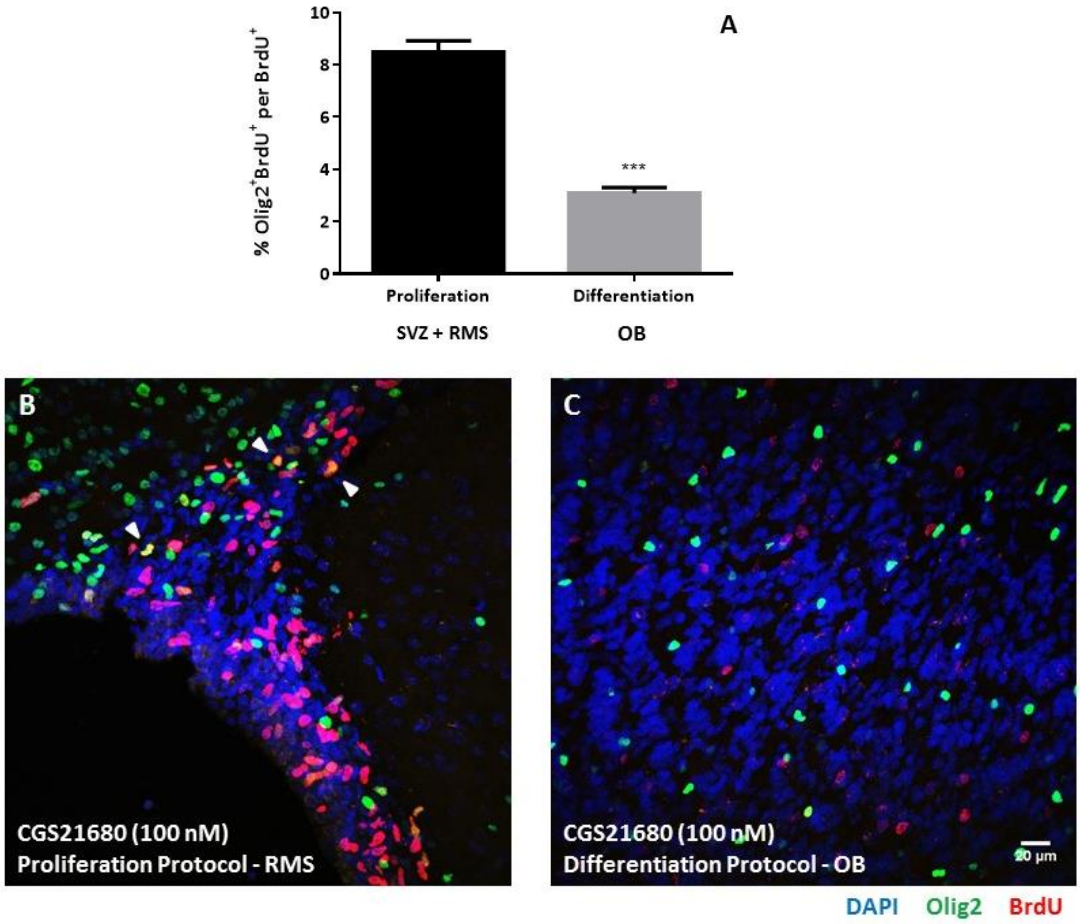

Figure 3.15 – The presence of Olig2⁺BrdU⁺ cells in the OB using the differentiation protocol is decreased in comparison to the SVZ+RMS with the proliferation protocol in CGS21680-treated animals. Bar graph depicts the number of Olig2⁺BrdU⁺ cells expressed as a percentage of total BrdU⁺ cells **(A)**. Data are expressed as mean ± SEM from three animals per group. Statistical significance was assessed by an unpaired Student's t-test for comparison with the control: ***p<0.001. Representative images obtained by confocal microscopy of Olig2⁺ (**green**) and BrdU⁺ (**red**) cells in the SVZ+RMS using the proliferation protocol **(B)** and OB using the differentiation paradigm **(C)** in CGS21680-treated animals, with DAPI (**blue**) allowing the visualization of nuclei. Scale bar, 20 µm.

Additionally, the decreased proliferation of double-labelled Olig2 and BrdU cells in the SVZ following $A_{2A}R$ activation is considerably less evident in the OB only. Particularly, by normalizing the data in regard to control rats from the proliferation protocol, a reduction of 42.6%±16.0 was observed in the number of Olig2⁺BrdU⁺ cells per volume in the SVZ and RMS of CGS21680-treated rats (control SVZ+RMS proliferation: 100.0%±14.2; CGS21680 SVZ+RMS proliferation: 57.4%±7.4, N=3, ns, p=0.0563) using the same proliferation paradigm (Figure 3.16.A). Furthermore, the percentage of double-labelled cells relative to total BrdU⁺ cells was decreased by 2.6%±0.9 in the SVZ and RMS of CGS21680-treated animals when comparing with the SVZ and RMS from control animals using the proliferation protocol (control SVZ+RMS proliferation: 11.1%±0.7; CGS21680 SVZ+RMS proliferation: 8.5%±0.4; N=3, *p=0.0396) (Figure 3.16.B). However, when comparing the OB of animals from the differentiation protocol normalized to the mean of controls from the proliferation paradigm, the difference in number of Olig2⁺BrdU⁺ cells between control and CGS21680-treated rats (control OB differentiation:

4.3%±0.7; CGS21680 OB differentiation: 3.4%±0.6; N=3, ns, p=0.3780) is remarkably smaller (Figure 3.16.A). Similarly, there is no difference in the percentage of double-labelled cells relative to total number of $BrdU^+$ cells in the OB between control and CGS21680-treated rats using the differentiation protocol (control OB differentiation: 3.8%±0.3; CGS21680 OB differentiation: 3.1%±0.2; N=3, ns, p=0.1262) (Figure 3.16.B). Importantly, it was possible to observe that the number of $Olig2^+BrdU^+$ cells when expressed per volume and total $BrdU^+$ cells is much smaller in the OB compared with the SVZ and RMS in both control and CGS21680-treated animals.

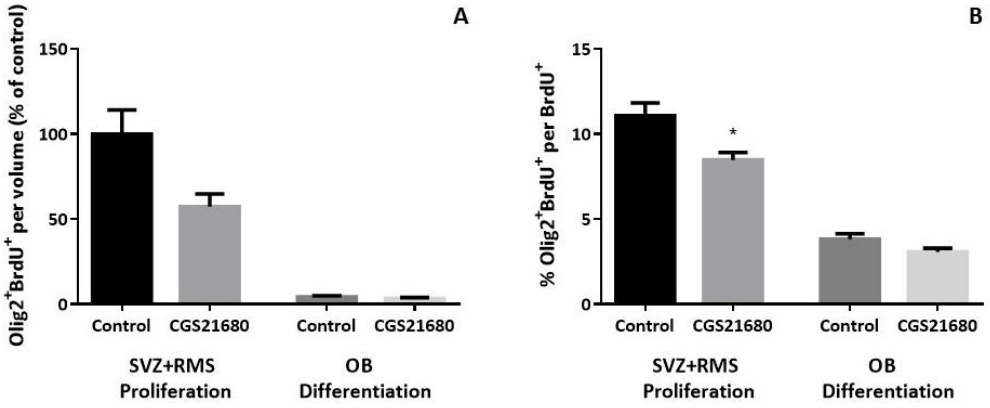

Figure 3.16 – $Olig2^+BrdU^+$ cells in the OB are much sparser when comparing with the SVZ+RMS. Bar graphs depict the number of $Olig2^+BrdU^+$ cells expressed as a percentage of the control mean from the proliferation protocol **(A)** and of total $BrdU^+$ cells **(B)**. Data are expressed as mean ± SEM from three animals per group. Statistical significance was assessed by an unpaired Student's t-test for comparison with the control: *p<0.05.

3.1.8 Activation of A_{2A} receptors induces no effect in SVZ or RMS volume

The observed effects in proliferation and migration of $Olig2^+BrdU^+$ cells could be due to changes in SVZ and/or RMS volumes following $A_{2A}R$ activation. However, this was shown not to be the case, since no differences between control and CGS21680-treated animals in volume of SVZ (control: 17151±1902 mm^3; CGS21680: 16708±2103 mm^3; N=6, ns, p=0.8790) (Figure 3.17.A) and RMS (control: 7836±1138 mm^3, CGS21680: 8401±1144 mm^3, N=6, ns, p=0.7334) (Figure 3.17.B) were found.

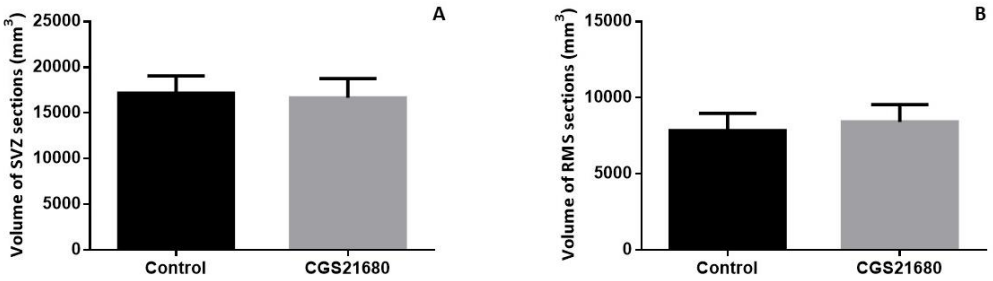

Figure 3.17 – SVZ and RMS volumes are not altered following CGS21680 treatment. Bar graphs depict SVZ **(A)** and RMS **(B)** volume in mm^3. Data are expressed as mean ± SEM from six animals per group. Statistical significance was assessed by an unpaired Student's t-test for comparison with the control.

Additionally, an extrapolation of global SVZ and RMS volumes was performed according to Cavalieri's principle (Figure 3.18). The latter states that any volume can be estimated without bias by multiplying the sum of profile areas of the brain region of interest with the distance between sections cut at consistent intervals.[218] Thus, volumes were extrapolated by multiplying the sum of SVZ or RMS areas with the distance between sections (300 µm). Therefore, the total volume of SVZ for controls was estimated to be $1.48x10^6 \pm 2.90x10^5$ mm^3 and for CGS21680-treated animals was $1.47x10^6 \pm 2.94x10^5$ mm^3 (N=6, ns, p=0.9798) (Figure 3.18.A), while the RMS global volume was $6.90x10^5 \pm 1.53x10^5$ mm^3 while CGS21680-treated animals was $7.28x10^5 \pm 1.44x10^5$ mm^3, respectively (N=6, ns, p=0.8603) (Figure 3.18.B).

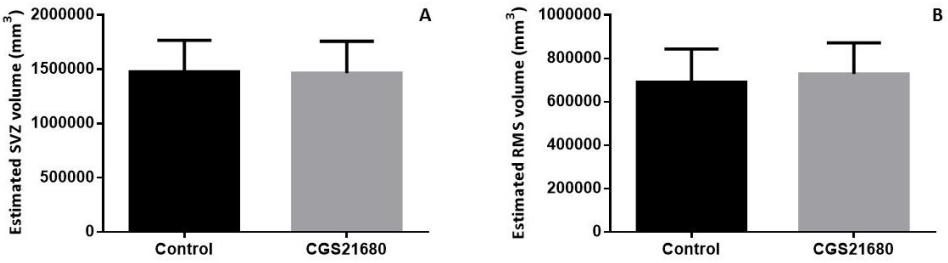

Figure 3.18 – Total SVZ and RMS volumes are not altered following CGS21680 treatment as estimated based on Cavalieri's principle. Bar graphs depict SVZ **(A)** and RMS **(B)** estimated total volume in mm^3. Data are expressed as mean ± SEM from six animals per group. Statistical significance was assessed by an unpaired Student's t-test for comparison with the control.

Since the results mentioned previously regarding the number of $Olig2^+$ and $BrdU^+$ cells in the OB could be due to differences in sampling volume of this region, a final comparison between the two groups was made. No statistically significant difference was observed between the means of OB volume sampled from control and CGS21680-treated animals (control: 70559±17545 mm^3, CGS21680: 69333±19378 mm^3, N=3, ns, p=0.9648) (Figure 3.19A). Furthermore, by normalizing to the mean sampling volume from control animals no differences were observed in OB volume (control: 100.0%±24.9; CGS21680: 98.3%±27.5; N=3, ns, p=0.9648) (Figure 3.19B).

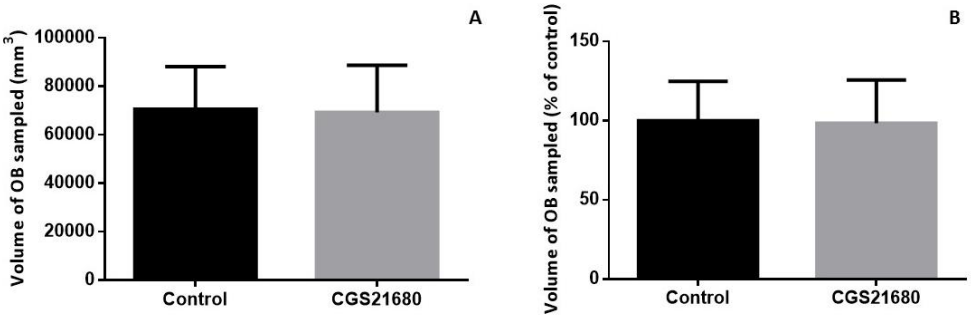

Figure 3.19 – OB volume is not altered following CGS21680 treatment. Bar graphs depict the volume of OB **(A)** and expressed as percentage of control **(B)**. Data are expressed as mean ± SEM from three animals per group. Statistical significance was assessed by an unpaired Student's t-test for comparison with the control.

3.2 *Ex vivo* studies

3.2.1 Culturing conditions affect SVZ architecture and organization

Forebrain SVZ-containing organotypic slices from P9 rats maintained in culture for 9 days revealed a rearrangement which was macro- and microscopically different from freshly dissected slices. In fact, tissue re-organization was remarkably conspicuous in the SVZ, with cells occupying the space of the lateral ventricle. Moreover, heterogeneity in rearrangement between slices was observed, as demonstrated by the high degree of variability in SVZ areas (Figure 3.20).

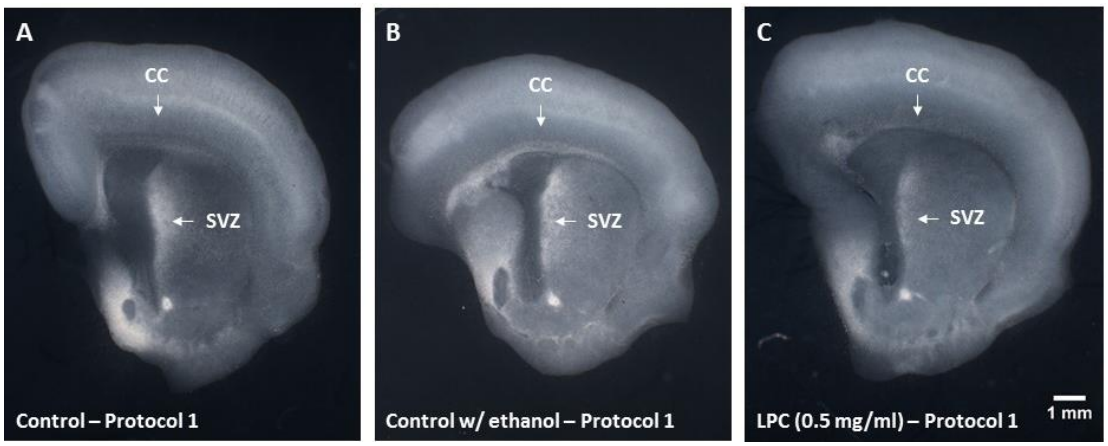

Figure 3.20 – Organotypic forebrain slice cultures obtained from P9 rats are macroscopically rearranged when maintained in culture for 9 days (Protocol 1). Tissue rearrangement is independent of experimental condition (**A:** control; **B:** vehicle, ethanol; **C:** LPC, 0.5 mg/ml) and is entirely evident in the SVZ of these slices. Abbreviations: CC corpus callosum, SVZ subventricular zone. Scale bar, 1 mm.

Therefore, we hypothesized that this unexpected reorganization could be dependent on culturing time. Consequently, a shorter experimental design in which slices obtained from P14 rats were maintained in culture for 3 days was implemented. In this new protocol, slice architecture is considerably more preserved, with the SVZ clearly distinguishable from the surrounding striatum and corpus callosum. However, heterogeneity between slices persists (Figure 3.21) and the morphology of the SVZ appears altered in these slices comparatively to its *in vivo* counterpart, as analysed by immunofluorescent staining in the previous sections. Interestingly, organotypic slices, obtained using protocol 2, remain thicker than those from protocol 1.

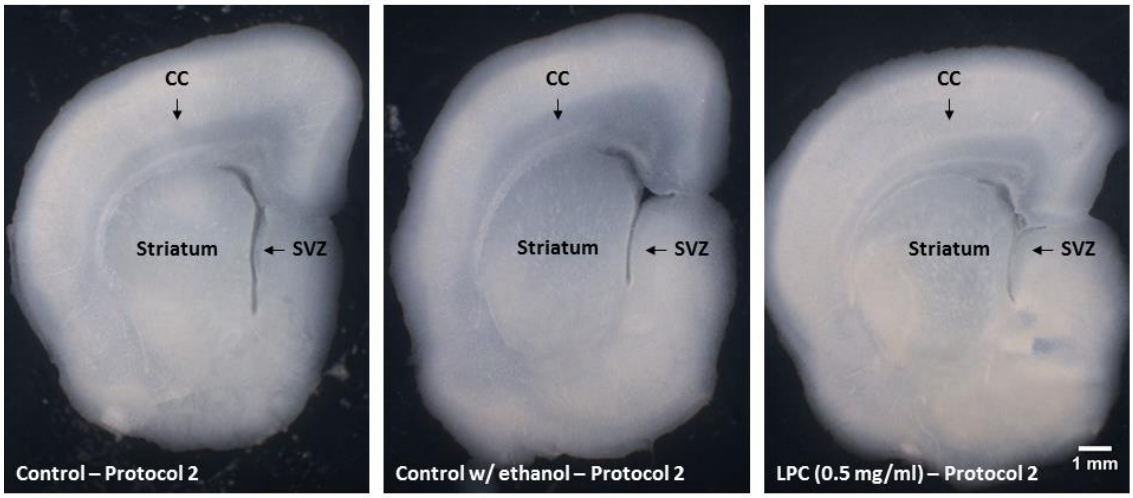

Figure 3.21 – Organotypic forebrain slice cultures obtained from P14 rats are not macroscopically rearranged when maintained in culture for 3 days (Protocol 2). Tissue architecture is more preserved in slices from this second experimental design. Abbreviations: CC corpus callosum, SVZ subventricular zone. Scale bar, 1 mm.

3.2.2 The expression of neuron, astrocyte, microglia and oligodendrocyte markers is retained in organotypic slices following treatment with LPC

A qualitative assessment of CNS cell types present in slices obtained from P9 (Protocol 1) and P14 (Protocol 2) rats in the corpus callosum (CC) was performed by immunofluorescent staining against typical markers of neurons, astrocytes, oligodendrocytes and microglia.

Neurons in organotypic slice cultures were visualized with an antibody against NeuN, a protein exclusively located in the nuclei and perinuclear cytoplasm of CNS neurons.[225] No apparent differences in either size or number of $NeuN^+$ cells appear to exist above the CC between control and LPC-incubated slices in their respective culturing protocols (Figure 3.22). However, neurons using protocol 1 seem considerably more numerous and larger than their counterparts from protocol 2.

Additionally, neurons in organotypic slices were also stained with an antibody against the microtubule-associated protein-2 (MAP-2), a cytoskeleton protein present in the dendrites of functional neurons.[226] Regarding the culturing protocols, no significant differences were seen in the number and morphology of dendrites above the CC between control and LPC-incubated slices. However, dendrites in the first protocol appear to be denser and more numerous than those from the second one (Figure 3.23).

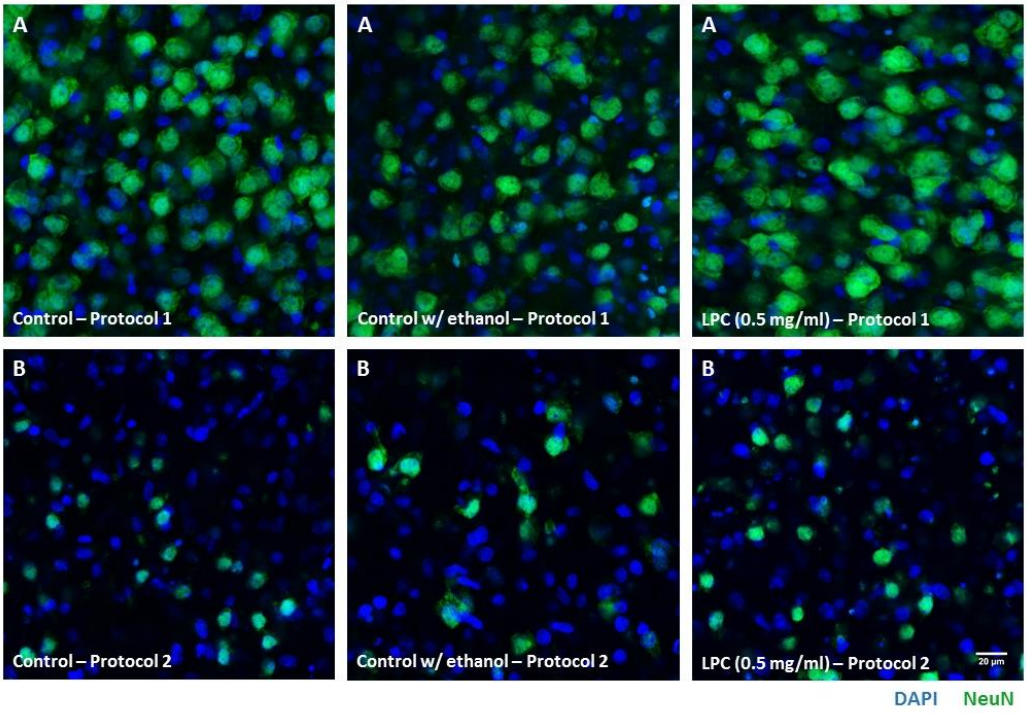

Figure 3.22 – Neuronal size and number is not altered by LPC treatment. Representative images obtained by confocal microscopy of NeuN$^+$ (**green**) cells above the corpus callosum of forebrain organotypic slice cultures, with DAPI (**blue**) allowing the visualization of nuclei. No apparent differences in size or number between control and LPC-treated slices were discerned in protocol 1 **(A)** or 2 **(B)**. Scale bar, 20 µm.

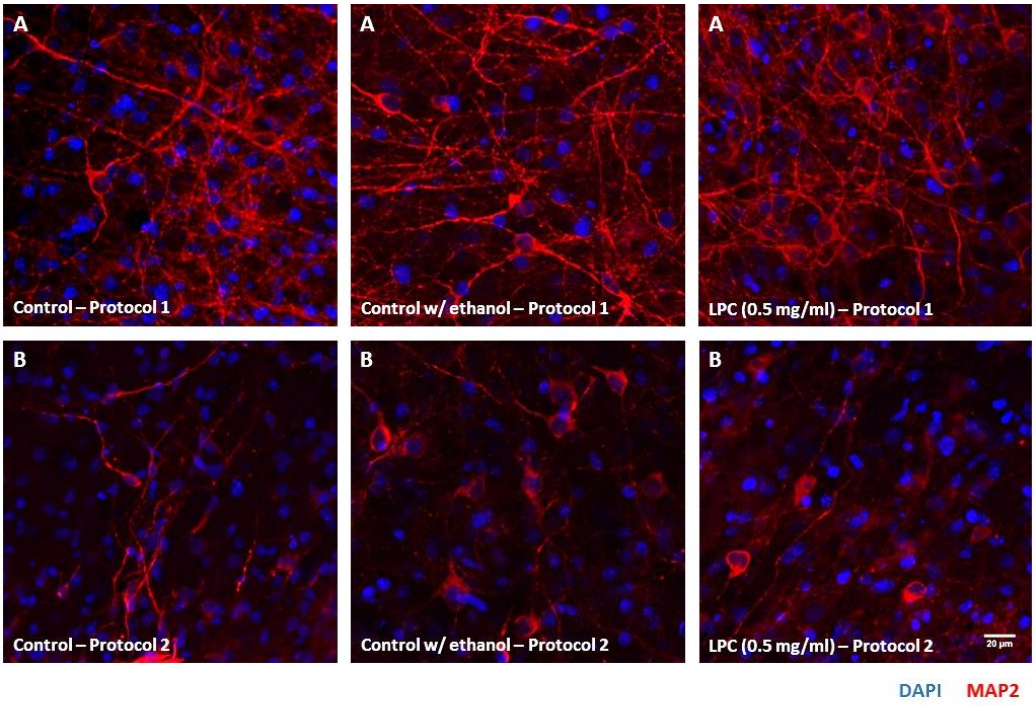

Figure 3.23 – Neuronal morphology is not altered by LPC treatment. Representative images obtained by confocal microscopy of MAP2$^+$ (**red**) cells above the corpus callosum of forebrain organotypic slice cultures, with DAPI (**blue**) allowing the visualization of nuclei. No differences in the number and morphology of dendrites between control and LPC-treated slices were observed in protocol 1 **(A)** or 2 **(B)**. Scale bar, 20 µm.

Subsequently, astrocytes in organotypic slices were observed with an antibody against the glial fibrillary acidic protein (GFAP). The upregulation of this intermediate filament protein is necessary for astrogliosis, a process following injury in which astrocytes acquire a reactive phenotype characterized by hypertrophy of their soma and thicker cellular processes.[227,228] When comparing the morphology of GFAP$^+$ astrocytes between control and LPC-incubated slices in respect to the culturing conditions, no differences in size of their soma and cellular processes were observed beneath the CC. However, the expression of GFAP appears to be increased in slices from the first protocol in comparison to those from the second one (Figure 3.24).

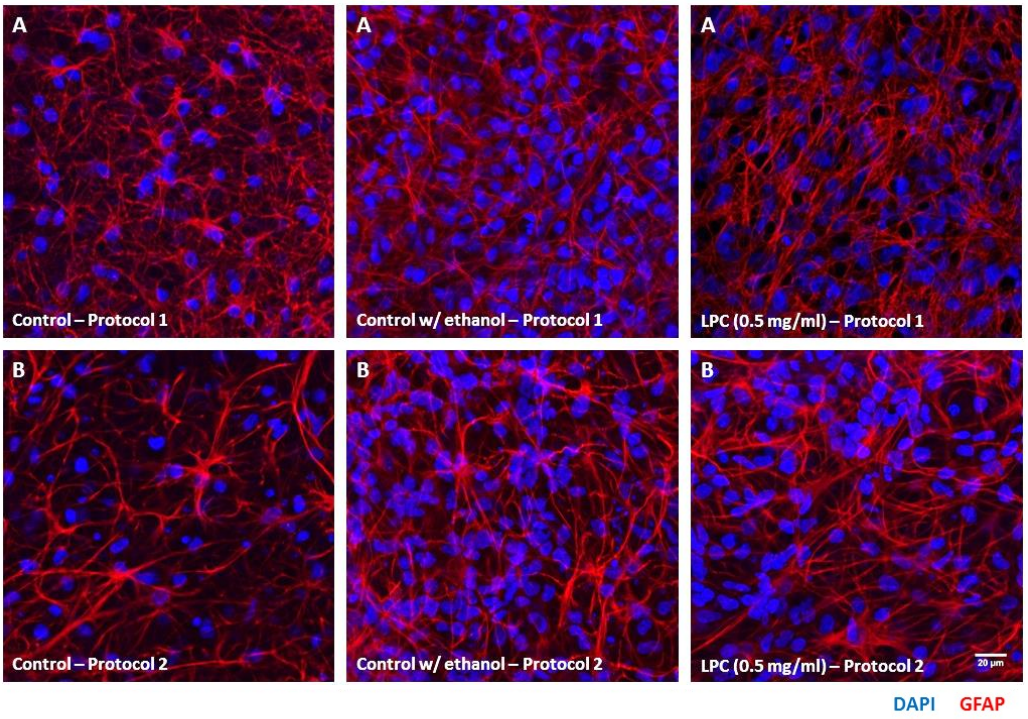

Figure 3.24 – Astrocyte morphology is not altered by LPC treatment. Representative images obtained by confocal microscopy of GFAP$^+$ (**red**) cells beneath the corpus callosum of forebrain organotypic slice cultures, with DAPI (**blue**) allowing the visualization of nuclei. No distinction in the number and morphology of astrocytic processes and expression of GFAP between control and LPC-treated slices in protocol 1 **(A)** and 2 **(B)** was observed. Scale bar, 20 µm.

The presence of microglia in organotypic slices was evaluated by immunohistochemistry against the ionized calcium-binding adaptor molecule 1 (Iba1). In the CNS, this protein is exclusively expressed in resting and activated microglia.[229,230] When analysing the number and morphology of Iba1$^+$ cells between control and LPC-incubated slices, no apparent differences were observed above the CC with respect to the culturing protocols (Figure 3.25). Microglia appear to have a ramified morphology, with thin processes branching from their soma, characteristic a resting state.[231]

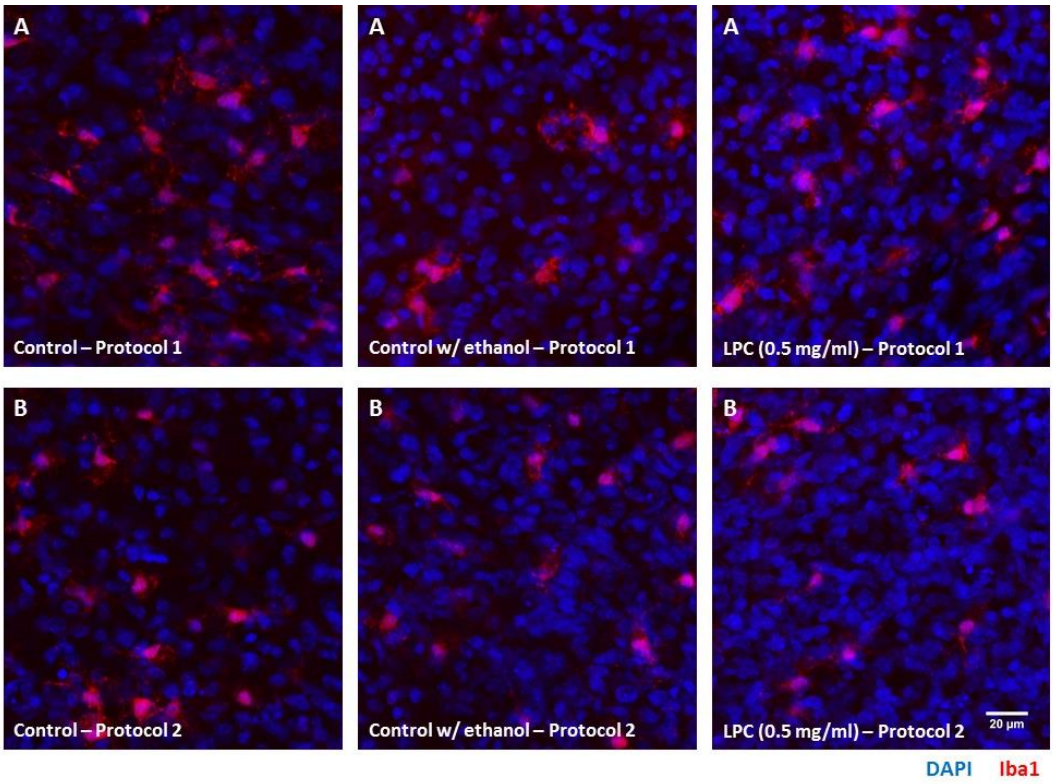

Figure 3.25 – Microglial number and morphology are not altered by LPC treatment. Representative images obtained by confocal microscopy of Iba1$^+$ (**red**) cells above the corpus callosum of forebrain organotypic slice cultures, with DAPI (**blue**) allowing the visualization of nuclei. No apparent differences in the morphology and number of microglia between control and LPC-treated slices were discerned in protocol 1 **(A)** or 2 **(B)**. Scale bar, 20 µm.

Finally, oligodendrocytes in organotypic slices were observed by immunostaining against the oligodendroglial lineage marker Olig2. No apparent distinction in the number of Olig2$^+$ cells was observed beneath the CC between control and LPC-incubated slices within each culturing protocol (Figure 3.26). However, slices from P14 rats (protocol 2) seem to exhibit a higher percentage of Olig2$^+$ cells in regard to those obtained from P9 animals (protocol 1).

Therefore, since the general morphology of organotypic slices containing the SVZ is better preserved using protocol 2, we have pursued the project with this protocol.

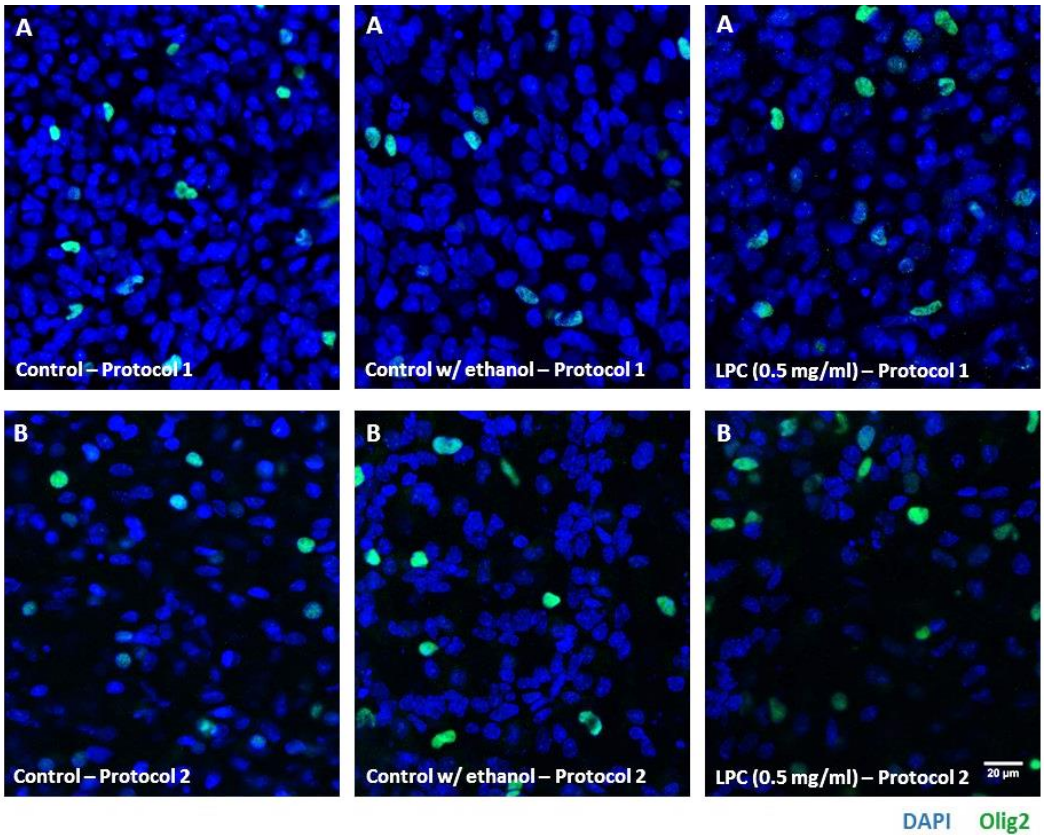

Figure 3.26 – Oligodendrocyte size and number is not altered by LPC treatment. Representative images obtained by confocal microscopy of Olig2$^+$ (**green**) cells beneath the corpus callosum of forebrain organotypic slice cultures, with DAPI (**blue**) allowing the visualization of nuclei. No apparent distinction in the number of oligodendrocytes between control and LPC-treated slices was discerned in protocol 1 **(A)** or 2 **(B)**. Scale bar, 20 µm.

3.2.3 Most proliferative cells in forebrain organotypic slices belong to the astrocytic, oligodendroglial and microglial lineage

As previously mentioned in section 3.2.1., organotypic slices containing the SVZ are remarkably proliferative in culture. Attempting to identify the cells which are proliferating, slices were incubated with BrdU in the last 36 hours of culture and a double immunostaining against BrdU together with NeuN, GFAP, Olig2 and Iba1 was performed. Proliferative cells from SVZ-containing organotypic slices do not give rise to neurons in culture in the CC, since double-labelled cells for BrdU and NeuN were not observed (Figure 3.27.A). However, double-positive cells for BrdU and either GFAP (Figure 3.27.B), Olig2 (Figure 3.27.C) and Iba1 (Figure 3.27.D) were visualized, indicating that proliferative cells in the CC of these slices are astrocytes (BrdU$^+$GFAP$^+$), oligodendrocytes (BrdU$^+$Olig2$^+$) and microglia (BrdU$^+$Iba1$^+$).

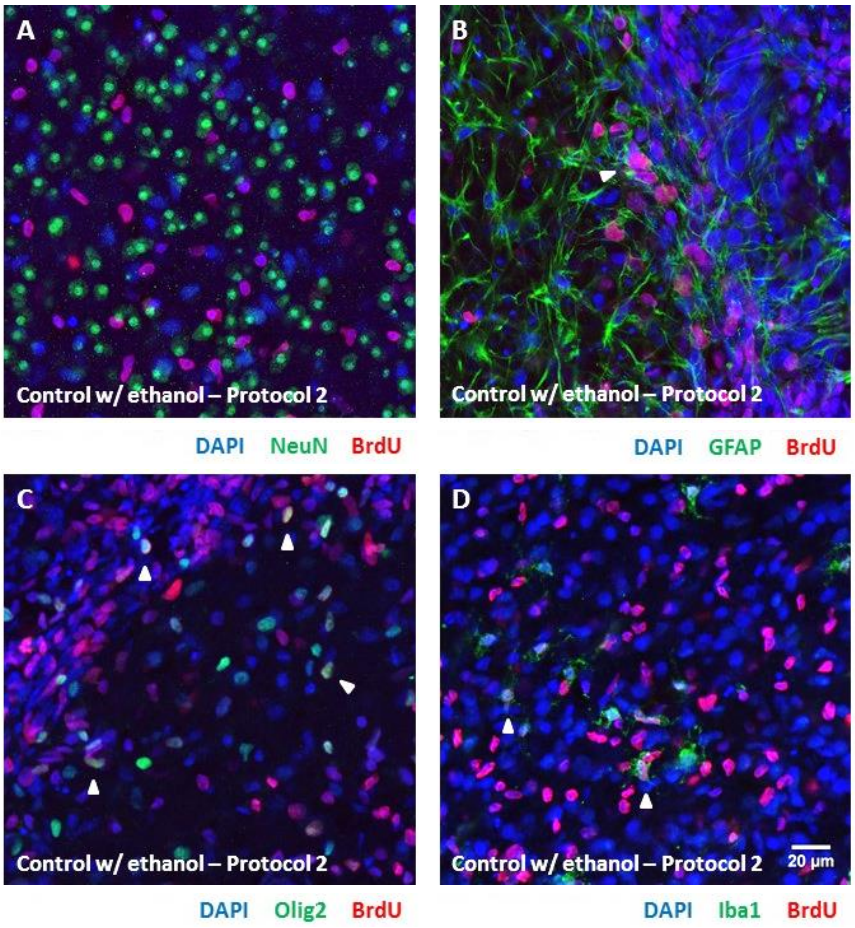

Figure 3.27 – Proliferative cells in forebrain organotypic slices from P14 rats are astrocytes, oligodendrocytes or microglia. Representative images obtained by confocal microscopy of BrdU-labelled cells in the corpus callosum of organotypic control slice cultures. Proliferative cells were identified by double-immunostaining against BrdU (**red**) and NeuN (**A**, **green**), GFAP (**B**, **green**), Olig2 (**C**, **green**) or Iba1 (**D**, **green**). White arrows indicate double-labelled cells. Scale bar, 20 µm.

3.2.4 $A_{2A}R$ activation promotes myelination in the corpus callosum in the absence of a demyelinating event

The initial aim of the current project was to evaluate the effect of $A_{2A}R$ activation upon the ability of SVZ-derived OPCs to remyelinate the CC following a demyelinating insult. However, since BrdU incorporation occurs throughout the entire extent of forebrain slice cultures and an unexpected high number of BrdU-labelled cells in control conditions are also immune-reactive for Olig2, it was decided to assess the entire pool of OPCs, comprising both parenchyma and SVZ-derived precursors. For this purpose, the fluorescence intensity of myelin basic protein (MBP) was measured in the corpus callosum of forebrain organotypic slice cultures (Figure 3.28).

Before evaluating the outcome of $A_{2A}R$ activation in the process of remyelination, the role of these receptors in myelinogenesis was first assessed. It was observed that incubation of forebrain organotypic slices with the selective agonist CGS21680 (30 nM) for 36 hours resulted in a tendency towards an increase in total fluorescence intensity of MBP per area of corpus callosum regarding controls (control: 100.0%±27.6; CGS21680: 136.6%±12.7; N=3, ns,

p=0.8355). In contrast, blocking of A_{2A}Rs with the selective antagonist ZM241385 (50 nM) did not alter the MBP-staining intensity in the corpus callosum of forebrain organotypic slices (ZM241385: 116.0%±22.2, N=3, ns, p>0.9999) (Figure 3.28).

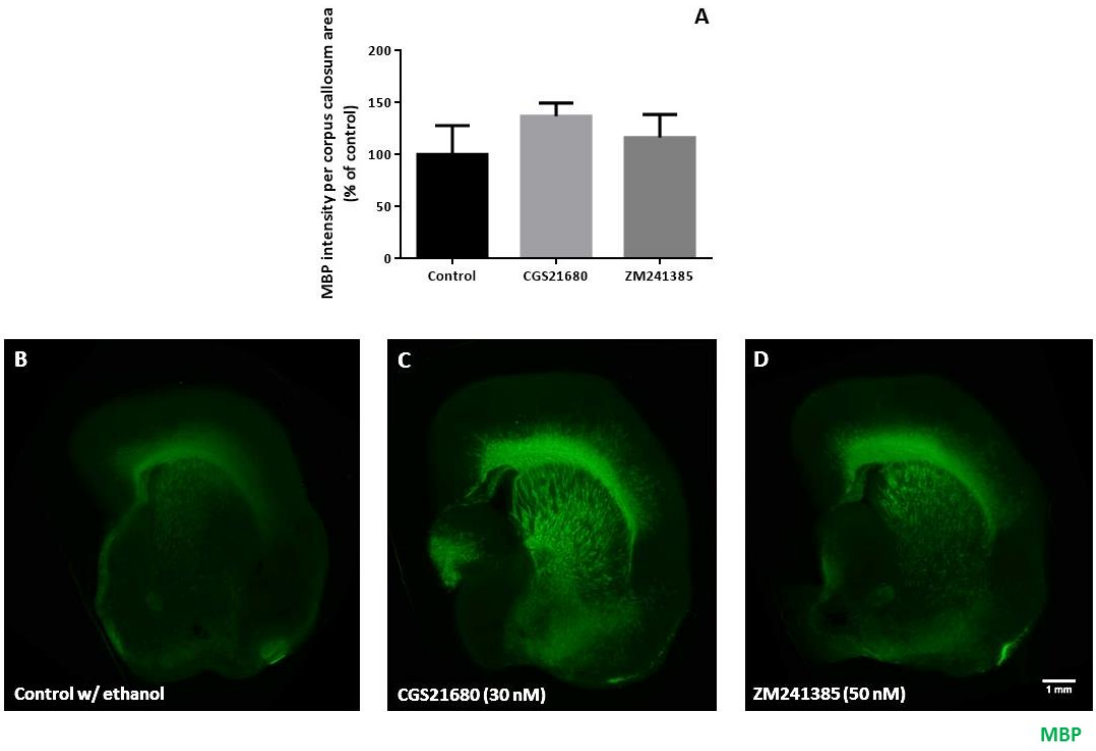

Figure 3.28 – A_{2A}R activation promotes myelination in the corpus callosum in the absence of a demyelinating event. A. Bar graph depicts the corrected total fluorescence intensity of MBP per corpus callosum area in SVZ-containing organotypic slices, expressed as a percentage of control. Data are expressed as mean ± SEM from three slices per group. Statistical significance was assessed by a one-way ANOVA followed by Bonferroni's correction for multiple comparisons with the control. Representative images obtained by widefield fluorescence microscopy of MBP-stained (**green**) organotypic slices incubated with ethanol **(B)**, CGS21680 **(C)** and ZM241385 **(D)**. Scale bar, 1 mm.

3.2.5 Treatment with LPC for 18 hours at a concentration of 0.5 mg/ml does not induce demyelination in rat forebrain slices

Subsequently, the effect of incubation with LPC (0.5 mg/ml) during 18 hours in the fluorescence intensity of MBP staining in the corpus callosum of *ex vivo* slices was evaluated (Figure 3.29). Treatment with LPC (0.5 mg/ml) for 18 hours in slices from P14 rats did not induce demyelination, since no significant differences were observed in the intensity of MBP staining in the CC. By normalizing the corrected total fluorescence intensity of MBP per area of corpus callosum in LPC-incubated slices it was possible to observe that, indeed, LPC treatment did not induce demyelination when compared to control slices (control: 100.0%±27.6; LPC: 108.7%±21.2; N=3, ns, p=0.8141).

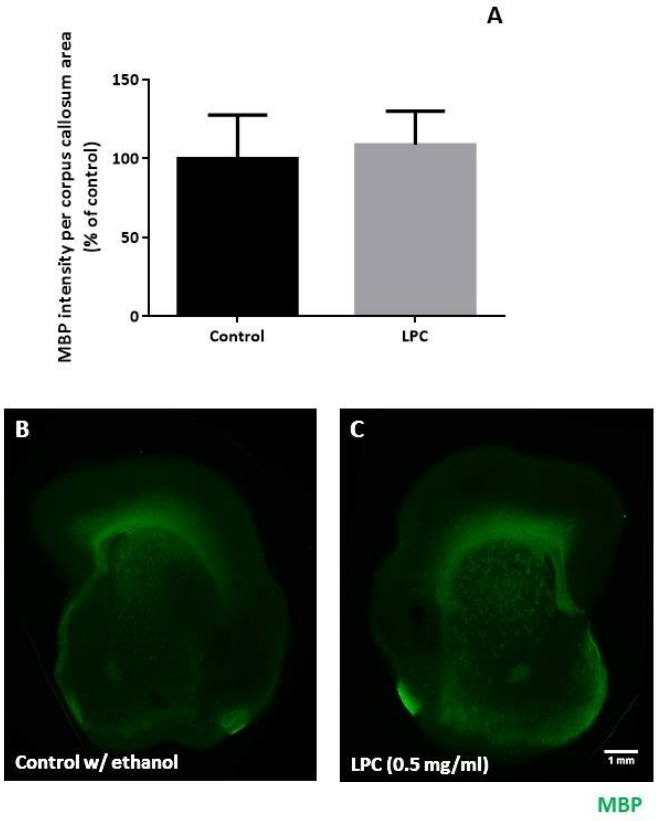

Figure 3.29 – LPC did not induce demyelination of forebrain organotypic slices. A. Bar graph depicts the corrected total fluorescence intensity of MBP per corpus callosum area in SVZ-containing organotypic slices, expressed as a percentage of control. Data are expressed as mean ± SEM from three slices per group. Statistical significance was assessed by an unpaired Student's t-test for comparison with the control. Representative images obtained by widefield fluorescence microscopy of MBP-stained (**green**) organotypic slices incubated with ethanol **(B)** and LPC **(C)**. Scale bar, 1 mm.

3.2.6 $A_{2A}R$ activation or inhibition did not promote myelination in the corpus callosum following LPC incubation

Although LPC did not induce demyelination, we studied whether $A_{2A}R$ modulation could induce myelination following exposure to this toxin (Figure 3.30).

It was observed that treatment with the selective agonist CGS21680 (30 nM) in slices incubated with LPC did not alter the fluorescence intensity of MBP in regard to the respective control (LPC: 108.7%±21.2; LPC + CGS21680: 80.0%±14.0; N=3, ns, p>0.9999). Similarly, incubation with the selective $A_{2A}R$ antagonist ZM241385 (50 nM) after exposure to LPC did not modify the staining intensity of MBP comparatively to LPC-treated slices (LPC: 108.7%±21.2; LPC + ZM241386: 121.9%±7.3; N=3, ns, p>0.9999). Finally, simultaneous treatment with the $A_{2A}R$ agonist and antagonist, CGS21680 (30 nM) and ZM241385 (50 nM), respectively, also did not change the fluorescence intensity of MBP in regard to the corresponding control (LPC: 108.7%±21.2; LPC + CGS21680 + ZM241385: 65.8%±12.8, N=3, ns, p>0.9999).

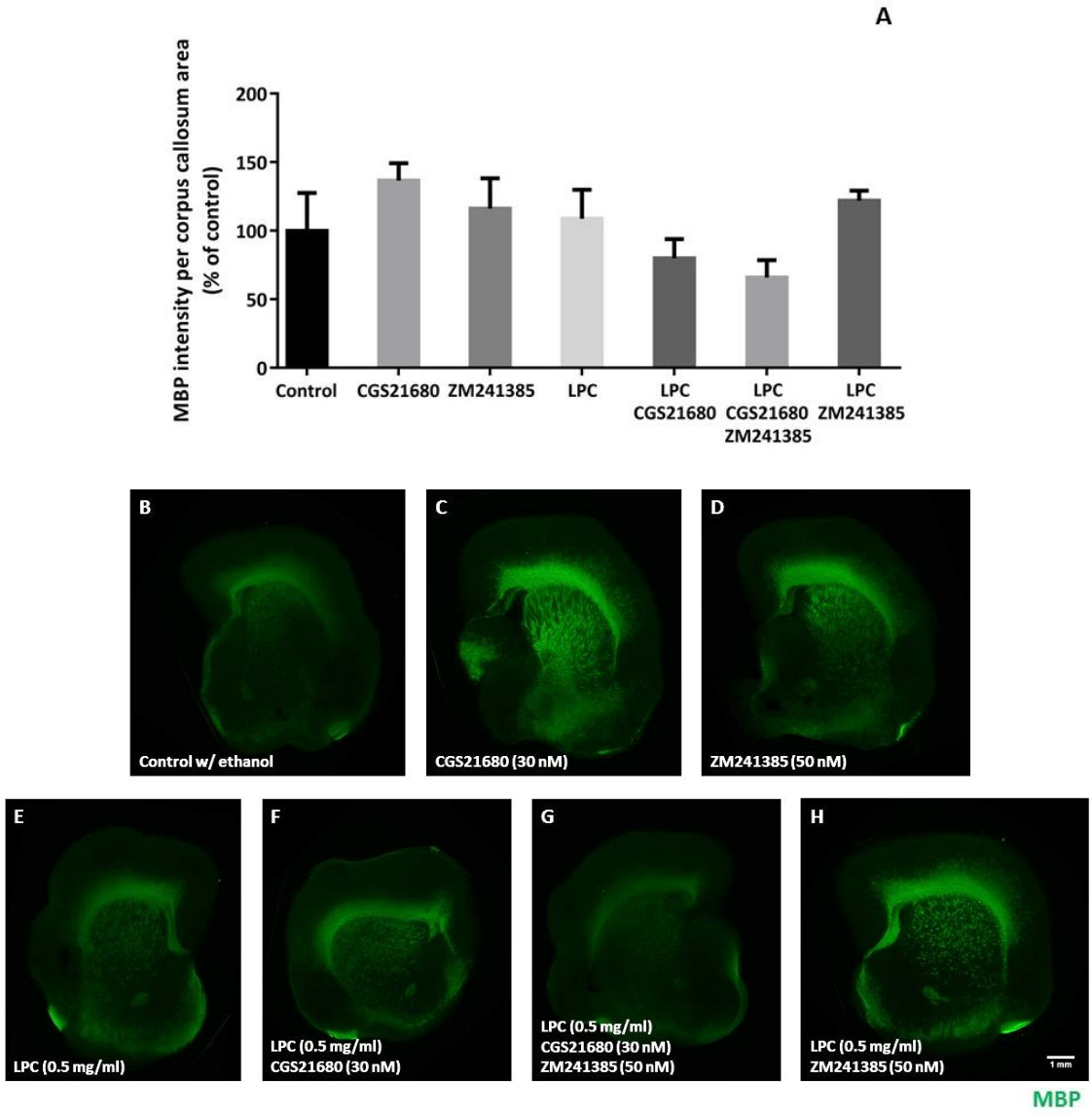

Figure 3.30 – $A_{2A}R$ activation or inhibition did not promote myelination in the corpus callosum following LPC incubation. A. Bar graph depicts the corrected total fluorescence intensity of MBP per corpus callosum area in SVZ-containing organotypic slices. Data are expressed as mean ± SEM from three slices per group. Statistical significance was assessed by a one-way ANOVA followed by Bonferroni's correction for multiple comparisons with the control. Representative images obtained by widefield fluorescence microscopy of MBP-stained (**green**) slices incubated with ethanol **(B)**, CGS21680 **(C)**, ZM241385 **(D)**, LPC **(E)**, LPC + CGS21680 **(F)**, LPC + CGS21680 + ZM241385 **(G)** and LPC + ZM241385 **(H)**. Scale bar, 1 mm.

Since the results obtained above could be due to variations in size, a final comparison between groups regarding corpus callosum area relative to total slice area was performed (Figure 3.31). However, no significant differences were found between groups (control: 100.0%±17.3; CGS21680: 98.8%±6.1; ZM241385: 102.4%±5.5; LPC: 110.6%; LPC + CGS21680: 95.3%±11.2; LPC + CGS + ZM: 98.0±0.8; LPC + ZM: 91.2%±3.3; N=3, ns, p>0.9999).

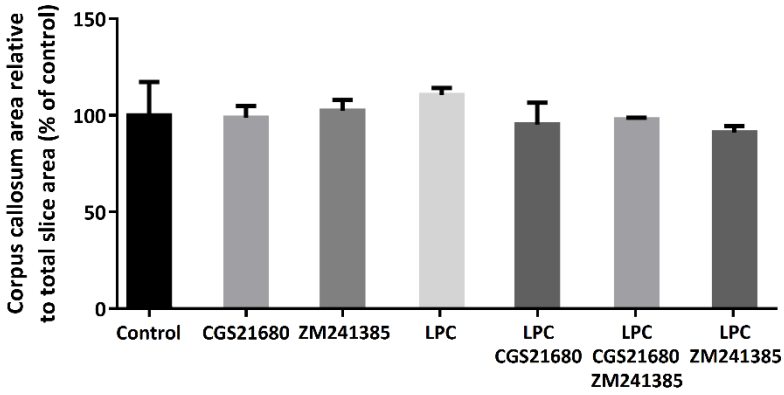

Figure 3.31 – Corpus callosum area relative to total *ex vivo* slice area is not altered. Bar graph depicts the corpus callosum area per total slice area in SVZ-containing organotypic slices. Data are expressed as mean ± SEM from three slices per group. Statistical significance was assessed by a one-way ANOVA followed by Bonferroni's correction for multiple comparisons with the control.

4. Discussion

The subventricular zone (SVZ) is the largest stem cell niche in the adult mammalian brain capable of generating both glial and neuronal precursors. A potential strategy in the treatment of neurodegenerative disorders involves the recruitment of these SVZ progenitors towards sites of injury. Multiple sclerosis (MS), the most prevalent demyelinating disease of the CNS, has a profound social impact, since it predominantly affects young adults, particularly women, with progressive motor and cognitive disabilities. No cure is available and current therapeutic strategies target exclusively its immune component, thus being only partially effective as disease continues to progress, while non-relapsing-remitting subtypes of MS remain refractory. During the clinical course of MS, attempts at remyelination occur, with new oligodendrocytes generated from brain parenchymal OPCs and a minority from NSCs in the SVZ. Therefore, this spontaneous repair process raises reasonable hopes that recruitment of OPCs towards sites of injury may constitute a novel therapeutic approach in MS at overcoming remyelination failure.

Numerous studies have independently established the involvement of the adenosinergic system in the pathogenesis of MS, specifically of A_1 and A_{2A} adenosine receptors. Moreover, previous data from our group has demonstrated that activation of A_{2A}Rs with the agonist CGS21680 (30 nM) promotes the differentiation of oligodendrocytes from neurosphere cultures derived from rat postnatal SVZ. Thus, the present thesis aimed to explore the role of A_{2A}Rs in modulating oligodendrogenesis in the SVZ, both *in vivo* under physiological conditions and *ex vivo* following a demyelinating insult with LPC.

To investigate the outcome of A_{2A}R activation in modulating SVZ oligodendrogenesis *in vivo*, proliferation and migration/differentiation were assessed separately using two different labelling strategies with BrdU. While proliferation in the SVZ was evaluated following two intraperitoneal injections of BrdU in the last day of drug administration, separated by 2-hour intervals, NSC migration and differentiation were examined by injecting rats with BrdU twice a day at 12-hour intervals in the first three days of treatment. Immunohistochemical processing was performed for BrdU and Olig2, the latter a marker of the entire oligodendroglial lineage.

Unexpectedly, *in vivo* administration of the A_{2A}R agonist CGS21680 (100 nM) promoted a significant decrease in the proliferation of $Olig2^+BrdU^+$ cells in the SVZ. Simultaneously, a tendency towards a reduction in the number of proliferating cells in the SVZ was also observed upon activation of A_{2A}Rs, which might explain the results concerning the diminished proliferation of $Olig2^+BrdU^+$ cells. Under non-pathological conditions, $Olig2^+BrdU^+$ cells derived from the SVZ migrate mostly towards the OB, instead of the CC or striatum. However, their migratory ability along the RMS is impaired following continuous activation of A_{2A} receptors for 28 days. The migration of $BrdU^+$ cells, on the contrary, is not altered in animals which were administered with the A_{2A}R agonist CGS21680. The observed results were shown not be due to variations in size and volume of the aforementioned brain regions following A_{2A}R activation, since no differences were found between the two groups of animals.

No published evidence exists regarding the role of A_{2A}Rs in SVZ oligodendrogenesis yet. However, recent literature has demonstrated that A_1R activation negatively modulates SVZ

neurogenesis *in vivo*, as observed by a decrease in the number of DCX^+BrdU^+ neuroblasts in the SVZ and OB and $NeuN^+BrdU^+$ neurons in the OB. In turn, A_1Rs promote SVZ astrogliogenesis *in vivo*, as seen by an increase in the number of $S100\beta^+BrdU^+$ cells in the OB.[215] Since A_1Rs are negatively coupled to cAMP and A_{2A}Rs positively modulate the intracellular concentration of this second messenger, these adenosine receptors are usually related to opposing effects in numerous biological events, including maturation of oligodendrocyte progenitors. Indeed, as previously mentioned in the introduction chapter, it has been demonstrated that A_1Rs inhibit the proliferation of cortical OPCs in culture, while promoting their differentiation into pre-myelinating $O4^+$ cells.[215] However, A_{2A}R activation was shown to inhibit OPC differentiation, since treatment with CGS21680 (100 nM) increased the percentage of $NG2^+$ progenitors while decreasing $O4^+$ pre-OLGs and MAG^+ myelinating cells.[214] Moreover, A_1R activation was also shown to promote the migration of isolated OPCs *in vitro*.[213] As such, the published literature indirectly corroborates the results regarding proliferation and migration of $Olig2^+BrdU^+$ cells in the SVZ and RMS following activation of A_{2A}Rs. However, the therapeutic potential of A_{2A}Rs needs to be considered also in the larger and more complex framework of MS, not only in its ability to interfere with the process of SVZ oligodendrogenesis. It should be remembered that MS is an immune-mediated disease and animal studies using the EAE model suggest that these receptors exert a dual function, with peripheral A_{2A}R lymphocyte expression being beneficial and A_{2A}R activation in the CNS detrimental.[206,207]

Although most literature describes that OPCs migrate radially from the SVZ and RMS to populate the overlying white matter tracts, particularly in the CC and striatum following a demyelinating event, no relevant numbers of $Olig2^+BrdU^+$ cells were found in these brain regions. Moreover, a study has shown that $NG2^+$ progenitors from the SVZ in mice migrate along the RMS, differentiating into $O4^+$ and CNP^+ oligodendrocytes in the GCL of the OB.[232] Thus, it is likely that under physiological circumstances, which do not activate the SVZ, the RMS represents the default migratory pathway for $BrdU^+$ cells derived from the SVZ, which explains the near absence of $Olig2^+BrdU^+$ progenitors in the CC or striatum.

Only a minority of $Olig2^+BrdU^+$ cells derived from the SVZ are found in the OB of both control and treated rats following the experimental time course of 28 days, an observation which may have different possible explanations. For instance, it could reflect the loss of Olig2 marker expression as these cells begin to differentiate. Indeed, while the transcription factor Olig2 is present throughout the entire oligodendroglial lineage, its expression is not exclusive of oligodendroglial cells. In the early embryonic stages, $Olig2^+$ cells from the medial ganglionic eminence (MGE) of the basal forebrain mostly differentiate into inhibitory GABAergic and excitatory cholinergic neurons.[233,234] By contrast, $Olig2^+$ cells constitute a mixed population of glial progenitors in the late fetal telencephalon.[235] In the neonatal forebrain, most $GFAP^+$ astrocytes express Olig2, with a gradual downregulation of this transcription factor occurring as these cells complete their development at later stages.[236] Moreover, $Olig2^+$ cells in the postnatal SVZ differentiate entirely into astrocytes and oligodendrocytes, with migratory progenitors lining the RMS and possibly encompassing part of the astrocyte population which forms the glial tubes that support neuroblast migration towards the OB.[237] Consequently, in this scenario, the negligible number of $Olig2^+BrdU^+$ cells that reach the OB reflects the loss of Olig2 expression as these progenitors differentiate into astrocytes. Alternatively, or perhaps even simultaneously, it could reflect the survival rate of new incoming cells, which is modulated by both intrinsic and

extrinsic mechanisms acting in the local environment to maintain homeostasis. As a matter of fact, proliferating and migrating cells exceed the growth rate of the OB, with a peak of new cells reaching this structure one month following BrdU labelling in the SVZ. Programmed cell death of these young cells has been demonstrated to co-exist with neurogenesis to regulate the growth of neuronal populations in the OB.[238]

To investigate the outcome of $A_{2A}R$ activation in modulating SVZ oligodendrogenesis *ex vivo*, forebrain organotypic slice cultures containing the SVZ and CC were performed according to the interface method. *Ex vivo* cultures have been widely used in neuroscience to investigate the cellular and molecular mechanisms involved in different processes of the brain, including those of adult neurogenesis, in a three-dimensional system that preserves tissue architecture. Surprisingly, however, SVZ-containing organotypic slices from P9 rats and maintained in culture for 9 days (Protocol 1) underwent extensive reorganization, with cells proliferating and migrating to occupy the space of the lateral ventricles. This aberrant behaviour rendered the architecture of the slices macro- and microscopically unrecognizable, thus preventing the use of this *ex vivo* system as a model for the study of SVZ oligodendrogenesis. Rearrangement was hypothesized and later shown to be dependent on culturing time, since a shorter experimental design of 3 days with slices obtained from P14 rats (Protocol 2) allowed these to better preserve their original morphology. However, some degree of tissue disorganization at the level of the SVZ was also observed. Myelination is essentially a postnatal process, which is not yet completed in P9 rats and is recapitulated *in vitro* throughout most of the culturing time of organotypic slices.[239] Furthermore, the onset of myelination in the corpus callosum of rats, as evaluated by MBP^+ immunohistochemistry, was previously described to occur at postnatal day (PD) 7, with a statistically significant increase in myelin deposition observed at PD 14.[240] When Protocol 2 was implemented, the switch from P9 to P14 rats was necessary.

As organotypic slices are placed onto the semi-porous membrane inserts, these tend to flatten with culturing time, reducing their thickness and closing the space corresponding to the lateral ventricles. Moreover, NSCs are multipotent cells endowed with an extraordinary ability to proliferate and migrate. Indeed, although not shown in the results section, a tremendous number of proliferative $BrdU^+$ cells were observed in slices from both protocols. When slices from protocol 2 were incubated with BrdU for 36 hours and later double-stained against common neuronal, astrocytic, oligodendroglial and microglial markers, it was observed that these proliferative cells mostly differentiated into astrocytes, oligodendrocytes and microglia in the CC. This is not a surprising result, since it is known that culture of organotypic hippocampal slices strongly promotes the activation of glial cells.[241] From this perspective, the rearrangement of the SVZ is not an unreasonable result, although it should be noted that cell proliferation in our slices does not exclusively occur in the SVZ. Literature on *ex vivo* systems aimed at investigating SVZ neurogenesis exist[242,243,244,245,246,247,248] and except for one article[219], none refer the reorganization seen in this thesis. However, it must be referred that many of these studies used acute sagittal instead of long-term coronal sections, instead evaluating neuroblast migration along the RMS, and thus the number of proliferative NSCs in such cases is consistently less abundant.[242,243,244] Moreover, in studies which reported the use of long-term coronal cultures, no images from the SVZ were in fact shown.[245,246,247,248]

A qualitative analysis of CNS cells types present in slices obtained from both protocols was performed by immunofluorescent staining against common markers for neurons (NeuN and MAP2), astrocytes (GFAP), oligodendrocytes (Olig2) and microglia (Iba1). No differences in either number or morphology of neurons, astrocytes or microglia in the CC were seen between control and LPC-incubated slices of each culturing protocol. However, neurons appeared more abundant and the expression of GFAP was upregulated in slices from protocol 1. As already described, organotypic slices flatten with culturing time and, therefore, their thickness decreases, as observed in this thesis and reported by different studies.[249,250] Since slices from the protocols 1 and 2 were maintained in culture for nine and three days, respectively, the decreased thickness of slices from the former might account for these observations. In contrast, the percentage of $Olig2^+$ oligodendrocytes seemed higher in slices from protocol 2, which might be correlated with the more extensively myelinated CC of P14 animals in regard to P9 rats. No differences were observed between protocols in the number of microglia, with cells appearing to retain a ramified morphology both in control and LPC-treated slices.

Since the complex three-dimensional architecture of the SVZ is not maintained in culture and a high number of proliferative cells is present in the entire forebrain slice following BrdU incubation, with a considerable percentage of these immune-reactive for Olig2, the initial aim of establishing an *ex vivo* model for the study SVZ oligodendrogenesis was abandoned. Instead, the role of A_{2A}Rs in modulating the ability of both parenchymal and SVZ-derived OPCs to remyelinate the CC following an insult with LPC was investigated using protocol 2. It should be noted, however, that most OPCs present in these slices are derived from the parenchyma and not from the SVZ.

Rather than counting $Olig2^+BrdU^+$ cells, the fluorescence intensity of MBP, a marker of mature myelinating oligodendrocytes, was measured in the CC of forebrain organotypic slices. In the absence of a prior insult with LPC, incubation of slices with the A_{2A}R agonist CGS21680 (30 nM) promoted a tendency towards myelination in the CC, as observed by increased MBP fluorescence intensity, which was not observed following treatment with the antagonist ZM241385 (50 nM). These results appear to be in disagreement with the paper authored by Coppi and collaborators, in which A_{2A}R activation was demonstrated to inhibit OPC differentiation. However, it should be noted that isolated cortical OPCs were used in this study, instead of organotypic slice cultures. It has been shown that organotypic slices exhibit progressive astrogliosis, which in turn delays OPC differentiation in these cultures.[251] Indeed, the effect of A_{2A}Rs in modulating immune responses is well documented. A_{2A}R activation inhibits nitric oxide production by astrocytes in response to stimulation with LPS/IFN-gamma or TNF-α/IL-1β. In microglia, activation of A_{2A}Rs promotes their proliferation, increases the production of cyclooxygenase 2 (COX-2) and induces the retraction of their processes, which in turn can be beneficial to the resolution of inflammation.[252] Thus, in this scenario, A_{2A}R activation inhibits the differentiation of oligodendrocytes in isolated cortical OPCs, while promoting their maturation in the more complex environment of organotypic slices, through an indirect effect mediated by other cells.

Surprisingly, incubation with LPC at a concentration of 0.5 mg/ml during 18 hours did not induce demyelination in forebrain organotypic slices obtained from P14 rats. Literature on this matter is consensual in that in every single study using LPC to demyelinate organotypic slices, a

concentration of 0.5 mg/ml was used during 17-18 hours.[139,253] However, these studies were performed in cerebellar slices obtained from P8/P10 mice and it is likely that the forebrain organotypic slices obtained from P14 rats used in this thesis are in fact more myelinated.

Although LPC did not induce demyelination in our slices, we investigated the modulatory effect of A_{2A}Rs in oligodendrogenesis following incubation with this agent. Neither activation nor inhibition of A_{2A}Rs induced myelination in the CC of slices. However, the increased MBP fluorescence intensity observed after incubation with CGS21680 was not replicated when A_{2A}R activation followed treatment with LPC, which might indicate that even at a concentration that is not sufficient to induce measurable demyelination, LPC is indeed having some effect.

In summary, the results presented in this thesis indicate that activation of A_{2A}Rs modulates oligodendrogenesis in the SVZ by inhibiting OPC proliferation and migration *in vivo*. However, A_{2A}R activation appears to play a positive role in parenchymal oligodendrogenesis through increased OPC differentiation. This dual role of A_{2A}Rs might prove to be important for the development of novel therapeutic strategies in MS.

5. Conclusions and Future Perspectives

Multiple sclerosis (MS) is the most common demyelinating disease worldwide and is characterized by the presence of inflammatory infiltrates, oligodendrocyte death and myelin destruction in areas known as plaques. No cure is available and current therapeutic strategies target exclusively its immune component, thus being only partially effective as disease develops. During its clinical course, remyelination attempts occur with new oligodendrocytes generated mostly from brain parenchymal oligodendrocyte progenitor cells (OPCs). However, a minority of OPCs is derived from neural stem cells (NSCs) present in the subventricular zone (SVZ) along the lateral ventricles. This spontaneous repair process raises reasonable hopes that OPC recruitment towards sites of injury may constitute a novel therapeutic approach in MS. In this context, the adenosine $A_{2A}R$ has assumed a significant role, since numerous studies have independently established its ability to modulate oligodendrogenesis *in vitro* and its involvement in the pathogenesis of MS animal models.

The results presented in this dissertation demonstrate that adenosine $A_{2A}Rs$ are capable of modulating oligodendrogenesis *in vivo* and *ex vivo*. Specifically, $A_{2A}R$ activation inhibits the proliferation and migration to the olfactory bulb of OPCs derived from the SVZ, while promoting the differentiation of oligodendrocytes in the parenchyma. Thus, $A_{2A}Rs$ may constitute a novel and promising therapeutic approach in the treatment of MS. However, future work is necessary to properly dissect the complex interplay between $A_{2A}Rs$ and oligodendrogenesis. In the context of this thesis, further immunohistochemical analysis in the *in vivo* experiments with markers specific of cells in the final stages of oligodendrocyte development would elucidate the effect of $A_{2A}R$ activation in the differentiation of OPCs from the SVZ. Moreover, since incubation with LPC at 0.5 mg/ml proved to be insufficient to demyelinate forebrain organotypic slices from P14 rats, evaluating the fluorescence intensity of MBP with increasing concentrations of LPC would help to determine the optimal concentration of this agent to induce demyelination. Subsequently, treatment of slices with the agonist and/or antagonist of $A_{2A}Rs$ would provide new insights into the biological effects of these receptors following a demyelinating event.

6. Bibliography

1. Alvarez-Buylla A, Lim DA. For the long run: maintaining germinal niches in the adult brain. Neuron. 2004 Mar 4;41(5):683-6.

2. Taupin P. Adult neural stem cells, neurogenic niches, and cellular therapy. Stem Cell Reviews. 2006 Sep 1;2(3):213-9.

3. Stolp HB, Molnár Z. Neurogenic niches in the brain: help and hindrance of the barrier systems. Frontiers in neuroscience. 2015 Feb 3;9(20):1-7

4. Ehninger D, Kempermann G. Neurogenesis in the adult hippocampus. Cell and tissue research. 2008 Jan 1;331(1):243-50.

5. Alvarez-Buylla A, Garcia-Verdugo JM. Neurogenesis in adult subventricular zone. The Journal of Neuroscience. 2002 Feb 1;22(3):629-34.

6. Götz M, Huttner WB. The cell biology of neurogenesis. Nature reviews Molecular cell biology. 2005 Oct 1;6(10):777-88.

7. Malatesta P, Appolloni I, Calzolari F. Radial glia and neural stem cells. Cell and tissue research. 2008 Jan 1;331(1):165-78.

8. Merkle FT, Tramontin AD, García-Verdugo JM, Alvarez-Buylla A. Radial glia give rise to adult neural stem cells in the subventricular zone. Proceedings of the National Academy of Sciences of the United States of America. 2004 Dec 14;101(50):17528-32.

9. Fiorelli R, Azim K, Fischer B, Raineteau O. Adding a spatial dimension to postnatal ventricular-subventricular zone neurogenesis. Development. 2015 Jun 15;142(12):2109-20.

10. Merkle FT, Mirzadeh Z, Alvarez-Buylla A. Mosaic organization of neural stem cells in the adult brain. Science. 2007 Jul 20;317(5836):381-4.

11. Mamber C, Kozareva DA, Kamphuis W, Hol EM. Shades of gray: The delineation of marker expression within the adult rodent subventricular zone. Progress in neurobiology. 2013 Dec 31;111:1-16.

12. Lim DA, Alvarez-Buylla A. The Adult Ventricular–Subventricular Zone (V-SVZ) and Olfactory Bulb (OB) Neurogenesis. Cold Spring Harbor Perspectives in Biology. 2016 May 2;8(5).

13. Alvarez-Buylla A, García-Verdugo JM, Tramontin AD. A unified hypothesis on the lineage of neural stem cells. Nature Reviews Neuroscience. 2001 Apr 1;2(4):287-93.

14. Lledo PM, Merkle FT, Alvarez-Buylla A. Origin and function of olfactory bulb interneuron diversity. Trends in neurosciences. 2008 Aug 31;31(8):392-400.

15. Cayre M, Canoll P, Goldman JE. Cell migration in the normal and pathological postnatal mammalian brain. Progress in neurobiology. 2009 May 31;88(1):41-63.

16. Menn B, Garcia-Verdugo JM, Yaschine C, Gonzalez-Perez O, Rowitch D, Alvarez-Buylla A. Origin of oligodendrocytes in the subventricular zone of the adult brain. The Journal of Neuroscience. 2006 Jul 26;26(30):7907-18.

17. Nait-Oumesmar B, Decker L, Lachapelle F, Avellana-Adalid V, Bachelin C, Evercooren V, Baron A. Progenitor cells of the adult mouse subventricular zone proliferate, migrate and differentiate into oligodendrocytes after demyelination. European Journal of Neuroscience. 1999 Dec 1;11(12):4357-66.

18. Walton NM, Sutter BM, Laywell ED, Levkoff LH, Kearns SM, Marshall GP, Scheffler B, Steindler DA. Microglia instruct subventricular zone neurogenesis. Glia. 2006 Dec 1;54(8):815-25.

19. Altman J, Das GD. Autoradiographic and histological evidence of postnatal hippocampal neurogenesis in rats. Journal of Comparative Neurology. 1965 Jun 1;124(3):319-35.

20. Altman J. Autoradiographic and histological studies of postnatal neurogenesis. IV. Cell proliferation and migration in the anterior forebrain, with special reference to persisting neurogenesis in the olfactory bulb. Journal of Comparative Neurology. 1969 Dec 1;137(4):433-57.

21. Taupin P. BrdU immunohistochemistry for studying adult neurogenesis: paradigms, pitfalls, limitations, and validation. Brain research reviews. 2007 Jan 31;53(1):198-214.

22. Wojtowicz JM, Kee N. BrdU assay for neurogenesis in rodents. Nature protocols. 2006 Nov 1;1(3):1399-405.

23. Moreno MM, Linster C, Escanilla O, Sacquet J, Didier A, Mandairon N. Olfactory perceptual learning requires adult neurogenesis. Proceedings of the National Academy of Sciences. 2009 Oct 20;106(42):17980-5.

24. Sakamoto M, Kageyama R, Imayoshi I. The functional significance of newly born neurons integrated into olfactory bulb circuits. Frontiers in Neuroscience. 2014 May 26; 8(121):1-9.

25. Bergmann O, Liebl J, Bernard S, Alkass K, Yeung MS, Steier P, Kutschera W, Johnson L, Landén M, Druid H, Spalding KL. The age of olfactory bulb neurons in humans. Neuron. 2012 May 24;74(4):634-9.

26. Ernst A, Alkass K, Bernard S, Salehpour M, Perl S, Tisdale J, Possnert G, Druid H, Frisén J. Neurogenesis in the striatum of the adult human brain. Cell. 2014 Feb 27;156(5):1072-83.

27. Curtis MA, Faull RL, Eriksson PS. The effect of neurodegenerative diseases on the subventricular zone. Nature Reviews Neuroscience. 2007 Sep 1;8(9):712-23.

28. Zhang RL, Zhang ZG, Zhang L, Chopp M. Proliferation and differentiation of progenitor cells in the cortex and the subventricular zone in the adult rat after focal cerebral ischemia. Neuroscience. 2001 Jul 16;105(1):33-41.

29. Taupin P. Potential of adult neural stem cells for cellular therapy. Biologics. 2007 Mar 1;1(1):53-8.

30. Castelfranco AM, Hartline DK. The evolution of vertebrate and invertebrate myelin: a theoretical computational study. Journal of computational neuroscience. 2015 Jun 1;38(3):521-38.

31. Simons M, Nave KA. Oligodendrocytes: myelination and axonal support. Cold Spring Harbor perspectives in biology. 2016 Jan 1;8(1):a020479.

32. Aggarwal S, Yurlova L, Simons M. Central nervous system myelin: structure, synthesis and assembly. Trends in cell biology. 2011 Oct 31;21(10):585-93.

33. Simons M, Trotter J. Wrapping it up: the cell biology of myelination. Current opinion in neurobiology. 2007 Oct 31;17(5):533-40.

34. Barateiro A, Fernandes A. Temporal oligodendrocyte lineage progression: in vitro models of proliferation, differentiation and myelination. Biochimica et Biophysica Acta (BBA)-Molecular Cell Research. 2014 Sep 30;1843(9):1917-29.

35. Coppi E, Cellai L, Maraula G, Dettori I, Melani A, Pugliese AM, Pedata F. Role of adenosine in oligodendrocyte precursor maturation. Frontiers in cellular neuroscience. 2015 Apr 24;9(155):1-8.

36. Reynolds RI, Wilkin GP. Development of macroglial cells in rat cerebellum. II. An in situ immunohistochemical study of oligodendroglial lineage from precursor to mature myelinating cell. Development. 1988 Feb 1;102(2):409-25.

37. Moreira AM, Exploring the modulatory role of A_{2A} receptors in oligodendrogenesis derived from neural stem/progenitor cells of the subventricular zone. MSc Dissertation, Faculdade de Medicina, Universidade de Lisboa, 2015.

38. Pringle NP, Yu WP, Guthrie S, Roelink H, Lumsden A, Peterson AC, Richardson WD. Determination of neuroepithelial cell fate: induction of the oligodendrocyte lineage by ventral midline cells and sonic hedgehog. Developmental biology. 1996 Jul 10;177(1):30-42.

39. Lu QR, Yuk DI, Alberta JA, Zhu Z, Pawlitzky I, Chan J, McMahon AP, Stiles CD, Rowitch DH. Sonic hedgehog–regulated oligodendrocyte lineage genes encoding bHLH proteins in the mammalian central nervous system. Neuron. 2000 Feb 29;25(2):317-29.

40. Tekki-Kessaris N, Woodruff R, Hall AC, Gaffield W, Kimura S, Stiles CD, Rowitch DH, Richardson WD. Hedgehog-dependent oligodendrocyte lineage specification in the telencephalon. Development. 2001 Jul 1;128(13):2545-54.

41. Kessaris N, Fogarty M, Iannarelli P, Grist M, Wegner M, Richardson WD. Competing waves of oligodendrocytes in the forebrain and postnatal elimination of an embryonic lineage. Nature neuroscience. 2006 Feb 1;9(2):173-9.

42. Richardson WD, Kessaris N, Pringle N. Oligodendrocyte wars. Nature Reviews Neuroscience. 2006 Jan 1;7(1):11-8.

43. Yeung MS, Zdunek S, Bergmann O, Bernard S, Salehpour M, Alkass K, Perl S, Tisdale J, Possnert G, Brundin L, Druid H. Dynamics of oligodendrocyte generation and myelination in the human brain. Cell. 2014 Nov 6;159(4):766-74.

44. Dawson MR, Polito A, Levine JM, Reynolds R. NG2-expressing glial progenitor cells: an abundant and widespread population of cycling cells in the adult rat CNS. Molecular and Cellular Neuroscience. 2003 Oct 31;24(2):476-88.

45. Levine JM, Reynolds R, Fawcett JW. The oligodendrocyte precursor cell in health and disease. Trends in neurosciences. 2001 Jan 1;24(1):39-47.

46. Clarke LE, Young KM, Hamilton NB, Li H, Richardson WD, Attwell D. Properties and fate of oligodendrocyte progenitor cells in the corpus callosum, motor cortex, and piriform cortex of the mouse. The Journal of Neuroscience. 2012 Jun 13;32(24):8173-85.

47. Dawson MR, Levine JM, Reynolds R. Mini-Review-NG2-Expressing Cells in the Central Nervous System: Are They Oligodendroglial Progenitors?. Journal of Neuroscience Research. 2000 Sep 1;61(5):471-9.

48. Butt AM, Duncan A, Hornby MF, Kirvell SL, Hunter A, Levine JM, Berry M. Cells expressing the NG2 antigen contact nodes of Ranvier in adult CNS white matter. Glia. 1999 Mar 1;26(1):84-91.

49. Polito A, Reynolds R. NG2-expressing cells as oligodendrocyte progenitors in the normal and demyelinated adult central nervous system. Journal of Anatomy. 2005 Dec 1;207(6):707-16.

50. Hughes EG, Kang SH, Fukaya M, Bergles DE. Oligodendrocyte progenitors balance growth with self-repulsion to achieve homeostasis in the adult brain. Nature neuroscience. 2013 Jun 1;16(6):668-76.

51. Ortega F, Gascón S, Masserdotti G, Deshpande A, Simon C, Fischer J, Dimou L, Lie DC, Schroeder T, Berninger B. Oligodendrogliogenic and neurogenic adult subependymal zone neural stem cells constitute distinct lineages and exhibit differential responsiveness to Wnt signalling. Nature cell biology. 2013 Jun 1;15(6):602-13.

52. Azim K, Berninger B, Raineteau O. Mosaic Subventricular Origins of Forebrain Oligodendrogenesis. Frontiers in neuroscience. 2016 Mar 24;10(107):1-7.

53. Colak D, Mori T, Brill MS, Pfeifer A, Falk S, Deng C, Monteiro R, Mummery C, Sommer L, Götz M. Adult neurogenesis requires Smad4-mediated bone morphogenic protein signaling in stem cells. The Journal of Neuroscience. 2008 Jan 9;28(2):434-46.

54. Love S. Demyelinating diseases. Journal of Clinical Pathology. 2006 Nov 1;59(11):1151-9.

55. Goldenberg MM. Multiple sclerosis review. Pharmacy and Therapeutics. 2012 Mar;37(3):175-184.

56. Edwards LJ, Constantinescu CS. A prospective study of conditions associated with multiple sclerosis in a cohort of 658 consecutive outpatients attending a multiple sclerosis clinic. Multiple sclerosis. 2004 Oct 1;10(5):575-81.

57. Haines JL, Terwedow HA, Burgess K, Pericak-Vance MA, Rimmler JB, Martin ER, Oksenberg JR, Lincoln R, Zhang DY, Banatao DR, Gatto N. Linkage of the MHC to familial multiple sclerosis suggests genetic heterogeneity. Human molecular genetics. 1998 Aug 1;7(8):1229-34.

58. Constantinescu CS, Gran B. Multiple sclerosis: Autoimmune associations in multiple sclerosis. Nature Reviews Neurology. 2010 Nov 1;6(11):591-2.

59. Podbielska M, Banik NL, Kurowska E, Hogan EL. Myelin recovery in multiple sclerosis: the challenge of remyelination. Brain sciences. 2013 Aug 28;3(3):1282-324.

60. Haines JD, Inglese M, Casaccia P. Axonal damage in multiple sclerosis. Mount Sinai Journal of Medicine: A Journal of Translational and Personalized Medicine. 2011 Mar 1;78(2):231-43.

61. Frohman EM, Racke MK, Raine CS. Multiple sclerosis – the plaque and its pathogenesis. New England Journal of Medicine. 2006 Mar 2;354(9):942-55.

62. Lucchinetti C, Bruck W, Parisi J, Scheithauer B, Rodriguez M, Lassman H. Heterogeneity of multiple sclerosis lesions: implications for the pathogenesis of demyelination. Annals of neurology. 2000 Jun 1;47(6):707-17.

63. Van der Valk P, De Groot CJ. Staging of multiple sclerosis (MS) lesions: pathology of the time frame of MS. Neuropathology and applied neurobiology. 2000 Jan 1;26(1):2-10.

64. Ransohoff RM, Hafler DA, Lucchinetti CF. Multiple sclerosis – a quiet revolution. Nature Reviews Neurology. 2015 Mar 1;11(3):134-42.

65. Lublin FD, Reingold SC. Defining the clinical course of multiple sclerosis results of an international survey. Neurology. 1996 Apr 1;46(4):907-11.

66. Bjartmar C, Wujek JR, Trapp BD. Axonal loss in the pathology of MS: consequences for understanding the progressive phase of the disease. Journal of the neurological sciences. 2003 Feb 15;206(2):165-71.

67. Torkildsen Ø, Myhr KM, Bø L. Disease-modifying treatments for multiple sclerosis – a review of approved medications. European journal of neurology. 2016 Jan 1;23(S1):18-27.

68. Hemmer B, Hartung HP. Toward the development of rational therapies in multiple sclerosis: what is on the horizon?. Annals of Neurology. 2007 Oct 1;62(4):314-26.

69. Patrikios P, Stadelmann C, Kutzelnigg A, Rauschka H, Schmidbauer M, Laursen H, Sorensen PS, Brück W, Lucchinetti C, Lassmann H. Remyelination is extensive in a subset of multiple sclerosis patients. Brain. 2006 Dec 1;129(12):3165-72.

70. Albert M, Antel J, Brück W, Stadelmann C. Extensive cortical remyelination in patients with chronic multiple sclerosis. Brain Pathology. 2007 Apr 1;17(2):129-38.

71. Hanafy KA, Sloane JA. Regulation of remyelination in multiple sclerosis. FEBS Letters. 2011 Dec 1;585(23):3821-8.

72. Keirstead HS, Blakemore WF. Identification of post-mitotic oligodendrocytes incapable of remyelination within the demyelinated adult spinal cord. Journal of Neuropathology & Experimental Neurology. 1997 Nov 1;56(11):1191-201.

73. Targett MP, Sussmant J, Scoldingt N, O'Leary MT, Compston DA, Blakemore WF. Failure to achieve remyelination of demyelinated rat axons following transplantation of glial cells obtained from the adult human brain. Neuropathology and applied neurobiology. 1996 Jun 1;22(3):199-206.

74. Godfraind C, Friedrich VL, Holmes KV, Dubois-Dalcq M. In vivo analysis of glial cell phenotypes during a viral demyelinating disease in mice. The Journal of Cell Biology. 1989 Nov 1;109(5):2405-16.

75. Carroll WM, Jennings AR. Early recruitment of oligodendrocyte precursors in CNS demyelination. Brain. 1994 Jun 1;117(3):563-78.

76. Fancy SP, Zhao C, Franklin RJ. Increased expression of Nkx2. 2 and Olig2 identifies reactive oligodendrocyte progenitor cells responding to demyelination in the adult CNS. Molecular and Cellular Neuroscience. 2004 Nov 30;27(3):247-54.

77. Chang A, Nishiyama A, Peterson J, Prineas J, Trapp BD. NG2-positive oligodendrocyte progenitor cells in adult human brain and multiple sclerosis lesions. The Journal of Neuroscience. 2000 Sep 1;20(17):6404-12.

78. Carroll WM, Jennings AR, Ironside LJ. Identification of the adult resting progenitor cell by autoradiographic tracking of oligodendrocyte precursors in experimental CNS demyelination. Brain. 1998 Feb 1;121(2):293-302.

79. Nait-Oumesmar B, Picard-Riera N, Kerninon C, Decker L, Seilhean D, Höglinger GU, Hirsch EC, Reynolds R, Baron-Van Evercooren A. Activation of the subventricular zone in multiple sclerosis: evidence for early glial progenitors. Proceedings of the National Academy of Sciences. 2007 Mar 13;104(11):4694-9.

80. Picard-Riera N, Decker L, Delarasse C, Goude K, Nait-Oumesmar B, Liblau R, Pham-Dinh D, Baron-Van Evercooren A. Experimental autoimmune encephalomyelitis mobilizes neural progenitors from the subventricular zone to undergo oligodendrogenesis in adult mice. Proceedings of the National Academy of Sciences. 2002 Oct 1;99(20):13211-6.

81. Wingerchuk DM, Weinshenker BG. Disease modifying therapies for relapsing multiple sclerosis. BMJ. 2016 Aug 22;354:i3518.

82. Havrdova E, Horakova D, Kovarova I. Alemtuzumab in the treatment of multiple sclerosis: key clinical trial results and considerations for use. Therapeutic Advances in Neurological Disorders. 2015 Jan;8(1):31-45.

83. Bomprezzi R. Dimethyl fumarate in the treatment of relapsing – remitting multiple sclerosis: an overview. Therapeutic Advances in Neurological Disorders. 2015 Jan;8(1):20-30.

84. Brinkmann V, Billich A, Baumruker T, Heining P, Schmouder R, Francis G, Aradhye S, Burtin P. Fingolimod (FTY720): discovery and development of an oral drug to treat multiple sclerosis. Nature Reviews Drug discovery. 2010 Nov 1;9(11):883-97.

85. Neuhaus O, Farina C, Wekerle H, Hohlfeld R. Mechanisms of action of glatiramer acetate in multiple sclerosis. Neurology. 2001 Mar 27;56(6):702-8.

86. Dhib-Jalbut S, Marks S. Interferon-β mechanisms of action in multiple sclerosis. Neurology. 2010 Jan 5;74(Supplement 1):S17-24.

87. Neuhaus O, Kieseier BC, Hartung HP. Mechanisms of mitoxantrone in multiple sclerosis – what is known?. Journal of the neurological sciences. 2004 Aug 15;223(1):25-7.

88. Sheremata WA, Minagar A, Alexander JS, Vollmer T. The Role of Alpha-4 Integrin in the Aetiology of Multiple Sclerosis. CNS drugs. 2005 Nov 1;19(11):909-22.

89. Bar-Or A, Pachner A, Menguy-Vacheron F, Kaplan J, Wiendl H. Teriflunomide and its mechanism of action in multiple sclerosis. Drugs. 2014 Apr 1;74(6):659-74.

90. Franklin RJ. Why does remyelination fail in multiple sclerosis?. Nature Reviews Neuroscience. 2002 Sep 1;3(9):705-14.

91. Franklin RJ. Remyelination in the CNS: from biology to therapy. Nature Reviews Neuroscience. 2008 Nov 1;9(11):839-55.

92. Sim FJ, Zhao C, Penderis J, Franklin RJ. The age-related decrease in CNS remyelination efficiency is attributable to an impairment of both oligodendrocyte progenitor recruitment and differentiation. The Journal of Neuroscience. 2002 Apr 1;22(7):2451-9.

93. Ludwin SK. Chronic demyelination inhibits remyelination in the central nervous system. An analysis of contributing factors. Laboratory Investigation; a Journal of Technical Methods and Pathology. 1980 Oct 1;43(4):382-7.

94. Mason JL, Toews A, Hostettler JD, Morell P, Suzuki K, Goldman JE, Matsushima GK. Oligodendrocytes and progenitors become progressively depleted within chronically demyelinated lesions. The American Journal of Pathology. 2004 May 31;164(5):1673-82.

95. Kuhlmann T, Miron V, Cuo Q, Wegner C, Antel J, Brück W. Differentiation block of oligodendroglial progenitor cells as a cause for remyelination failure in chronic multiple sclerosis. Brain. 2008 Jul 1;131(7):1749-58.

96. J van der Star B, YS Vogel D, Kipp M, Puentes F, Baker D, Amor S. In vitro and in vivo models of multiple sclerosis. CNS & Neurological Disorders – Drug Targets. 2012 Aug 1;11(5):570-88.

97. Denic A, Johnson AJ, Bieber AJ, Warrington AE, Rodriguez M, Pirko I. The relevance of animal models in multiple sclerosis research. Pathophysiology. 2011 Feb 28;18(1):21-9.

98. Constantinescu CS, Farooqi N, O'Brien K, Gran B. Experimental autoimmune encephalomyelitis (EAE) as a model for multiple sclerosis (MS). British Journal of Pharmacology. 2011 Oct 1;164(4):1079-106.

99. Rivers TM, Sprunt DH, Berry GP. Observations on attempts to produce acute disseminated encephalomyelitis in monkeys. The Journal of Experimental Medicine. 1933 Jul 1;58(1):39-53.

100. Rivers TM, Schwentker FF. Encephalomyelitis accompanied by myelin destruction experimentally produced in monkeys. The Journal of Experimental Medicine. 1935 May 1;61(5):689-702.

101. Libbey JE, Fujinami RS. Experimental autoimmune encephalomyelitis as a testing paradigm for adjuvants and vaccines. Vaccine. 2011 Apr 12;29(17):3356-62.

102. Procaccini C, De Rosa V, Pucino V, Formisano L, Matarese G. Animal models of multiple sclerosis. European Journal of Pharmacology. 2015 Jul 15;759:182-91.

103. Lafaille JJ, Nagashima K, Katsuki M, Tonegawa S. High incidence of spontaneous autoimmune encephalomyelitis in immunodeficient anti-myelin basic protein T cell receptor transgenic mice. Cell. 1994 Aug 12;78(3):399-408.

104. Anderson AC, Chandwaskar R, Lee DH, Sullivan JM, Solomon A, Rodriguez-Manzanet R, Greve B, Sobel RA, Kuchroo VK. A transgenic model of central nervous system autoimmunity mediated by $CD4^+$ and $CD8^+$ T and B cells. The Journal of Immunology. 2012 Mar 1;188(5):2084-92.

105. Becher B, Bechmann I, Greter M. Antigen presentation in autoimmunity and CNS inflammation: how T lymphocytes recognize the brain. Journal of Molecular Medicine. 2006 Jul 1;84(7):532-43.

106. Lassmann H, Ransohoff RM. The CD4–Th1 model for multiple sclerosis: a crucial re-appraisal. Trends in Immunology. 2004 Mar 31;25(3):132-7.

107. Theiler M. Spontaneous encephalomyelitis of mice – a new virus disease. Science. 1934 Aug 3;80(2066):122.

108. Theiler M. Spontaneous encephalomyelitis of mice, a new virus disease. The Journal of Experimental Medicine. 1937 Apr 30;65(5):705.

109. Dal Canto MC, Melvold RW, Kim BS, Miller SD. Two models of multiple sclerosis: experimental allergic encephalomyelitis (EAE) and Theiler's murine encephalomyelitis virus (TMEV) infection. A pathological and immunological comparison. Microscopy Research and Technique. 1995 Oct 15;32(3):215-29.

110. Rivera-Quinones C, McGavern D, Schmelzer JD, Hunter SF, Low PA, Rodriguez M. Absence of neurological deficits following extensive demyelination in a class I-deficient murine model of multiple sclerosis. Nature Medicine. 1998 Feb 1;4(2):187-93.

111. Blakemore WF, Franklin RJ. Remyelination in experimental models of toxin-induced demyelination. In Advances in multiple Sclerosis and Experimental Demyelinating Diseases 2008 (pp. 193-212). Springer Berlin Heidelberg.

112. Carlton WW. Response of mice to the chelating agents sodium diethyldithiocarbamate, α-benzoinoxime, and biscyclohexanone oxaldihydrazone. Toxicology and Applied Pharmacology. 1966 May 1;8(3):512-21.

113. Praet J, Guglielmetti C, Berneman Z, Van der Linden A, Ponsaerts P. Cellular and molecular neuropathology of the cuprizone mouse model: clinical relevance for multiple sclerosis. Neuroscience & Biobehavioral Reviews. 2014 Nov 30;47:485-505.

114. Rossi L, Lombardo MF, Ciriolo MR, Rotilio G. Mitochondrial dysfunction in neurodegenerative diseases associated with copper imbalance. Neurochemical Research. 2004 Mar 1;29(3):493-504.

115. Kipp M, Clarner T, Dang J, Copray S, Beyer C. The cuprizone animal model: new insights into an old story. Acta Neuropathologica. 2009 Dec 1;118(6):723-36.

116. Blakemore WF. Remyelination by Schwann cells of axons demyelinated by intraspinal injection of 6-aminonicotinamide in the rat. Journal of Neurocytology. 1975 Dec 1;4(6):745-57.

117. Felts PA, Woolston AM, Fernando HB, Asquith S, Gregson NA, Mizzi OJ, Smith KJ. Inflammation and primary demyelination induced by the intraspinal injection of lipopolysaccharide. Brain. 2005 Jul 1;128(7):1649-66.

118. Blakemore WF. Ethidium bromide induced demyelination in the spinal cord of the cat. Neuropathology and Applied Neurobiology. 1982 Sep 1;8(5):365-75.

119. Hall SM, Gregson NA. The in vivo and ultrastructural effects of injection of lysophosphatidyl choline into myelinated peripheral nerve fibres of the adult mouse. Journal of Cell Science. 1971 Nov 1;9(3):769-89.

120. Morrison LR, Zamecnik PC. Experimental demyelination by means of enzymes, especially the alpha toxin of Clostridium welchii. Archives of Neurology & Psychiatry. 1950 Mar 1;63(3):367-81.

121. Hall SM. The effect of injections of lysophosphatidyl choline into white matter of the adult mouse spinal cord. Journal of Cell Science. 1972 Mar 1;10(2):535-46.

122. Degaonkar MN, Jayasundar R, Jagannathan NR. Sequential diffusion-weighted magnetic resonance imaging study of lysophosphatidyl choline-induced experimental demyelinating lesion: An animal model of multiple sclerosis. Journal of Magnetic Resonance Imaging. 2002 Aug 1;16(2):153-9.

123. Ousman SS, David S. Lysophosphatidylcholine induces rapid recruitment and activation of macrophages in the adult mouse spinal cord. Glia. 2000 Mar 1;30(1):92-104.

124. Keough MB, Jensen SK, Yong VW. Experimental demyelination and remyelination of murine spinal cord by focal injection of lysolecithin. Journal of Visualized Experiments. 2015 Mar 26; 97(e52679):1-8

125. Carroll WM, Jennings A, Mastaglia FL. Experimental demyelinating optic neuropathy: a model for combined morphological and electrophysiological studies. Clinical and Experimental Neurology. 1982 Dec;19:17-28.

126. Jeffery ND, Blakemore WF. Remyelination of mouse spinal cord axons demyelinated by local injection of lysolecithin. Journal of Neurocytology. 1995 Oct 1;24(10):775-81.

127. Shields SA, Gilson JM, Blakemore WF, Franklin RJ. Remyelination occurs as extensively but more slowly in old rats compared to young rats following gliotoxin-induced CNS demyelination. Glia. 1999 Oct 1;28(1):77-83.

128. Munder PG, Modolell M, Andreesen R, Weltzien HU, Westphal O. Lysophosphatidylcholine (lysolecithin) and its synthetic analogues. Immunomodulating and other biologic effects. In Immunostimulation 1980 (pp. 177-193). Springer Berlin Heidelberg.

129. Kalyvas A, David S. Cytosolic phospholipase A_2 plays a key role in the pathogenesis of multiple sclerosis-like disease. Neuron. 2004 Feb 5;41(3):323-35.

130. Balsinde J, Winstead MV, Dennis EA. Phospholipase A_2 regulation of arachidonic acid mobilization. FEBS Letters. 2002 Oct 30;531(1):2-6.

131. Allt G, Ghabriel MN, Sikri K. Lysophosphatidyl choline-induced demyelination. Acta Neuropathologica. 1988 Sep 1;75(5):456-64.

132. Ryborg AK, Deleuran B, Thestrup-Pedersen K, Kragballe K. Lysophosphatidylcholine: a chemoattractant to human T lymphocytes. Archives of Dermatological Research. 1994 Oct 1;286(8):462-5.

133. Ryborg AK, Deleuran B, Sogaard H, Kragballe K. Intracutaneous injection of lysophosphatidylcholine induces skin inflammation and accumulation of leukocytes. Acta Dermato-Venereologica. 2000 Jul 1;80(4):242-6.

134. Ousman SS, David S. MIP-1α, MCP-1, GM-CSF, and TNF-α control the immune cell response that mediates rapid phagocytosis of myelin from the adult mouse spinal cord. The Journal of Neuroscience. 2001 Jul 1;21(13):4649-56.

135. Bieber AJ, Kerr S, Rodriguez M. Efficient central nervous system remyelination requires T cells. Annals of Neurology. 2003 May 1;53(5):680-4.

136. Birgbauer E, Rao TS, Webb M. Lysolecithin induces demyelination in vitro in a cerebellar slice culture system. Journal of Neuroscience Research. 2004 Oct 15;78(2):157-66.

137. Huang JK, Jarjour AA, Oumesmar BN, Kerninon C, Williams A, Krezel W, Kagechika H, Bauer J, Zhao C, Baron-Van Evercooren A, Chambon P. Retinoid X receptor gamma signaling accelerates CNS remyelination. Nature Neuroscience. 2011 Jan 1;14(1):45-53.

138. Sheridan GK, Dev KK. S1P1 receptor subtype inhibits demyelination and regulates chemokine release in cerebellar slice cultures. Glia. 2012 Mar 1;60(3):382-92.

139. Barateiro A, Afonso V, Santos G, Cerqueira JJ, Brites D, van Horssen J, Fernandes A. S100B as a potential biomarker and therapeutic target in multiple sclerosis. Molecular Neurobiology. 2016 Aug 1;53(6):3976-91.

140. Cho S, Wood A, Bowlby MR. Brain slices as models for neurodegenerative disease and screening platforms to identify novel therapeutics. Current Neuropharmacology. 2007 Mar 1;5(1):19-33.

141. Sundstrom L, Pringle A, Morrison B, Bradley M. Organotypic cultures as tools for functional screening in the CNS. Drug Discovery Today. 2005 Jul 15;10(14):993-1000.

142. Kipp M, van der Star B, Vogel DY, Puentes F, van der Valk P, Baker D, Amor S. Experimental in vivo and in vitro models of multiple sclerosis: EAE and beyond. Multiple Sclerosis and Related Disorders. 2012 Jan 31;1(1):15-28.

143. Zhang H, Jarjour AA, Boyd A, Williams A. Central nervous system remyelination in culture – a tool for multiple sclerosis research. Experimental Neurology. 2011 Jul 31;230(1):138-48.

144. Raineteau O, Rietschin L, Gradwohl G, Guillemot F, Gähwiler BH. Neurogenesis in hippocampal slice cultures. Molecular and Cellular Neuroscience. 2004 Jun 30;26(2):241-50.

145. Kamada M, Li RY, Hashimoto M, Kakuda M, Okada H, Koyanagi Y, Ishizuka T, Yawo H. Intrinsic and spontaneous neurogenesis in the postnatal slice culture of rat hippocampus. European Journal of Neuroscience. 2004 Nov 1;20(10):2499-508.

146. Chechneva O, Dinkel K, Schrader D, Reymann KG. Identification and characterization of two neurogenic zones in interface organotypic hippocampal slice cultures. Neuroscience. 2005 Dec 31;136(1):343-55.

147. De Marchis S, Fasolo A, Shipley M, Puche A. Unique neuronal tracers show migration and differentiation of SVZ progenitors in organotypic slices. Journal of Neurobiology. 2001 Dec 1;49(4):326-38.

148. Sachdeva S, Gupta M. Adenosine and its receptors as therapeutic targets: an overview. Saudi Pharmaceutical Journal. 2013 Jul 31;21(3):245-53.

149. Sheth S, Brito R, Mukherjea D, Rybak LP, Ramkumar V. Adenosine receptors: expression, function and regulation. International Journal of Molecular Sciences. 2014 Jan 28;15(2):2024-52.

150. Palmer JL, Abeles RH. The mechanism of action of S-adenosylhomocysteinase. Journal of Biological Chemistry. 1979 Feb 25;254(4):1217-26.

151. Patel BT, Tudball N. Localization of S-adenosylhomocysteine hydrolase and adenosine deaminase immunoreactivities in rat brain. Brain Research. 1986 Apr 9;370(2):250-64.

152. Latini S, Pedata F. Adenosine in the central nervous system: release mechanisms and extracellular concentrations. Journal of Neurochemistry. 2001 Nov 1;79(3):463-84.

153. Thorn JA, Jarvis SM. Adenosine transporters. General Pharmacology: The Vascular System. 1996 Jun 1;27(4):613-20.

154. Wall MJ, Dale N. Auto-inhibition of rat parallel fibre-Purkinje cell synapses by activity-dependent adenosine release. The Journal of Physiology. 2007 Jun 1;581(2):553-65.

155. Van Wylen DG, Park TS, Rubio R, Berne RM. Increases in cerebral interstitial fluid adenosine concentration during hypoxia, local potassium infusion, and ischemia. Journal of Cerebral Blood Flow & Metabolism. 1986 Oct 1;6(5):522-8.

156. Doolette DJ. Mechanism of adenosine accumulation in the hippocampal slice during energy deprivation. Neurochemistry International. 1997 Feb 28;30(2):211-23.

157. Zhu PJ, Krnjević K. Adenosine release mediates cyanide-induced suppression of CA1 neuronal activity. The Journal of Neuroscience. 1997 Apr 1;17(7):2355-64.

158. Mitchell JB, Lupica CR, Dunwiddie TV. Activity-dependent release of endogenous adenosine modulates synaptic responses in the rat hippocampus. The Journal of Neuroscience. 1993 Aug 1;13(8):3439-47.

159. Ribeiro JA, Sebastiao AM, De Mendonça A. Adenosine receptors in the nervous system: pathophysiological implications. Progress in Neurobiology. 2002 Dec 31;68(6):377-92.

160. Cunha RA. Adenosine as a neuromodulator and as a homeostatic regulator in the nervous system: different roles, different sources and different receptors. Neurochemistry International. 2001 Feb 28;38(2):107-25.

161. Fredholm BB, Abbracchio MP, Burnstock G, Daly JW, Harden TK, Jacobson KA, Leff P, Williams M. Nomenclature and classification of purinoceptors. Pharmacological Reviews. 1994 Jun 1;46(2):143-56.

162. Jacobson KA, Gao ZG. Adenosine receptors as therapeutic targets. Nature Reviews Drug Discovery. 2006 Mar 1;5(3):247-64.

163. Reppert SM, Weaver DR, Stehle JH, Rivkees SA. Molecular cloning and characterization of a rat A_1-adenosine receptor that is widely expressed in brain and spinal cord. Molecular Endocrinology. 1991 Aug 1;5(8):1037-48.

164. Mahan LC, McVittie LD, Smyk-Randall EM, Nakata HI, Monsma F, Gerfen CR, Sibley DR. Cloning and expression of an A_1 adenosine receptor from rat brain. Molecular Pharmacology. 1991 Jul 1;40(1):1-7.

165. Calker DV, Müller M, Hamprecht B. Adenosine regulates via two different types of receptors, the accumulation of cyclic AMP in cultured brain cells. Journal of Neurochemistry. 1979 Nov 1;33(5):999-1005.

166. Jarvis MF, Williams M. Direct autoradiographic localization of adenosine A_2 receptors in the rat brain using the A_2-selective agonist, [^{3}H]CGS21680. European Journal of Pharmacology. 1989 Sep 13;168(2):243-6.

167. Parkinson FE, Fredholm BB. Autoradiographic evidence for G-protein coupled A_2-receptors in rat neostriatum using [^{3}H]-CGS21680 as a ligand. Naunyn-Schmiedeberg's Archives of Pharmacology. 1990 Jul 1;342(1):85-9.

168. Fink JS, Weaver DR, Rivkees SA, Peterfreund RA, Pollack AE, Adler EM, Reppert SM. Molecular cloning of the rat A_2 adenosine receptor: selective co-expression with D_2 dopamine receptors in rat striatum. Molecular Brain Research. 1992 Jul 31;14(3):186-95.

169. Cunha RA, Johansson B, van der Ploeg I, Sebastiao AM, Ribeiro JA, Fredholm BB. Evidence for functionally important adenosine A_{2A} receptors in the rat hippocampus. Brain Research. 1994 Jun 27;649(1-2):208-16.

170. Kull B, Svenningsson P, Fredholm BB. Adenosine A_{2A} receptors are colocalized with and activate G_{olf} in rat striatum. Molecular Pharmacology. 2000 Oct 1;58(4):771-7.

171. Stehle JH, Rivkees SA, Lee JJ, Weaver DR, Deeds JD, Reppert SM. Molecular cloning and expression of the cDNA for a novel A_2-adenosine receptor subtype. Molecular Endocrinology. 1992 Mar 1;6(3):384-93.

172. Feoktistov I, Biaggioni I. Adenosine A_{2B} receptors. Pharmacological Reviews. 1997 Dec 1;49(4):381-402.

173. Peakman MC, Hill SJ. Adenosine A_{2B}-receptor-mediated cyclic AMP accumulation in primary rat astrocytes. British Journal of Pharmacology. 1994 Jan 1;111(1):191-8.

174. Fredholm BB, Irenius E, Kull B, Schulte G. Comparison of the potency of adenosine as an agonist at human adenosine receptors expressed in Chinese hamster ovary cells. Biochemical Pharmacology. 2001 Feb 15;61(4):443-8.

175. Zhou QY, Li C, Olah ME, Johnson RA, Stiles GL, Civelli O. Molecular cloning and characterization of an adenosine receptor: the A_3 adenosine receptor. Proceedings of the National Academy of Sciences. 1992 Aug 15;89(16):7432-6.

176. Dunwiddie TV, Diao L, Kim HO, Jiang JL, Jacobson KA. Activation of hippocampal adenosine A_3 receptors produces a desensitization of A_1 receptor-mediated responses in rat hippocampus. The Journal of Neuroscience. 1997 Jan 15;17(2):607-14.

177. Abbracchio MP, Brambilla R, Ceruti S, Kim HO, Von Lubitz DK, Jacobson KA, Cattabeni F. G protein-dependent activation of phospholipase C by adenosine A_3 receptors in rat brain. Molecular Pharmacology. 1995 Dec 1;48(6):1038-45.

178. Abbracchio MP, Ceruti S. P1 receptors and cytokine secretion. Purinergic Signalling. 2007 Mar 1;3(1-2):13-25.

179. Koscsó B, Csóka B, Selmeczy Z, Himer L, Pacher P, Virág L, Haskó G. Adenosine augments IL-10 production by microglial cells through an A_{2B} adenosine receptor-mediated process. The Journal of Immunology. 2012 Jan 1;188(1):445-53.

180. Müller CE, Jacobson KA. Recent developments in adenosine receptor ligands and their potential as novel drugs. Biochimica et Biophysica Acta (BBA)-Biomembranes. 2011 May 31;1808(5):1290-308.

181. Corvol JC, Studler JM, Schonn JS, Girault JA, Herve D. $G\alpha_{olf}$ is necessary for coupling D1 and A_{2A} receptors to adenylyl cyclase in the striatum. Journal of Neurochemistry. 2001 Mar 1;76(5):1585-8.

182. Sassone-Corsi P. The cyclic AMP pathway. Cold Spring Harbor Perspectives in Biology. 2012 Dec 1;4(12).

183. Kopperud R, Krakstad C, Selheim F, Døskeland SO. cAMP effector mechanisms. Novel twists for an “old” signaling system. FEBS Letters. 2003 Jul 3;546(1):121-6.

184. Li P, Rial D, Canas PM, Yoo JH, Li W, Zhou X, Wang Y, Van Westen GJ, Payen MP, Augusto E, Gonçalves N. Optogenetic activation of intracellular adenosine A_{2A} receptor signaling in the hippocampus is sufficient to trigger CREB phosphorylation and impair memory. Molecular Psychiatry. 2015 Nov 1;20(11):1339-49.

185. Waltereit R, Weller M. Signaling from cAMP/PKA to MAPK and synaptic plasticity. Molecular Neurobiology. 2003 Feb 1;27(1):99-106.

186. Seidel MG, Klinger M, Freissmuth M, Höller C. Activation of Mitogen-activated Protein Kinase by the A_{2A}-adenosine Receptor via a rap1-dependent and via a $p21^{ras}$-dependent Pathway. Journal of Biological Chemistry. 1999 Sep 3;274(36):25833-41.

187. Torii S, Yamamoto T, Tsuchiya Y, Nishida E. ERK MAP kinase in G_1 cell cycle progression and cancer. Cancer Science. 2006 Aug 1;97(8):697-702.

188. Cargnello M, Roux PP. Activation and function of the MAPKs and their substrates, the MAPK-activated protein kinases. Microbiology and Molecular Biology Reviews. 2011 Mar 1;75(1):50-83.

189. Mori Y, Higuchi M, Masuyama N, Gotoh Y. Adenosine A_{2A} receptor facilitates calcium-dependent protein secretion through the activation of protein kinase A and phosphatidylinositol-3 kinase in PC12 cells. Cell Structure and Function. 2004;29(4):101-10.

190. Martini M, De Santis MC, Braccini L, Gulluni F, Hirsch E. PI3K/AKT signaling pathway and cancer: an updated review. Annals of Medicine. 2014 Sep 1;46(6):372-83.

191. Zhou J, Du T, Li B, Rong Y, Verkhratsky A, Peng L. Crosstalk between MAPK/ERK and PI3K/AKT signal pathways during brain ischemia/reperfusion. ASN Neuro. 2015 Sep 1;7(5).

192. Vanhaesebroeck B, Alessi DR. The PI3K–PDK1 connection: more than just a road to PKB. Biochemical Journal. 2000 Mar 15;346(3):561-76.

193. Parcellier A, Tintignac LA, Zhuravleva E, Hemmings BA. PKB and the mitochondria: AKTing on apoptosis. Cellular Signalling. 2008 Jan 31;20(1):21-30.

194. Duronio V. The life of a cell: apoptosis regulation by the PI3K/PKB pathway. Biochemical Journal. 2008 Nov 1;415(3):333-44.

195. Mayne M, Shepel PN, Jiang Y, Geiger JD, Power C. Dysregulation of adenosine A_1 receptor-mediated cytokine expression in peripheral blood mononuclear cells from multiple sclerosis patients. Annals of Neurology. 1999 May 1;45(5):633-9.

196. Johnston JB, Silva C, Gonzalez G, Holden J, Warren KG, Metz LM, Power C. Diminished adenosine A_1 receptor expression on macrophages in brain and blood of patients with multiple sclerosis. Annals of Neurology. 2001 May 1;49(5):650-8.

197. Tsutsui S, Schnermann J, Noorbakhsh F, Henry S, Yong VW, Winston BW, Warren K, Power C. A_1 adenosine receptor upregulation and activation attenuates neuroinflammation and demyelination in a model of multiple sclerosis. The Journal of Neuroscience. 2004 Feb 11;24(6):1521-9.

198. Chen GQ, Chen YY, Wang XS, Wu SZ, Yang HM, Xu HQ, He JC, Wang XT, Chen JF, Zheng RY. Chronic caffeine treatment attenuates experimental autoimmune encephalomyelitis induced by guinea pig spinal cord homogenates in Wistar rats. Brain Research. 2010 Jan 14;1309:116-25.

199. Hedström AK, Mowry EM, Gianfrancesco MA, Shao X, Schaefer CA, Shen L, Olsson T, Barcellos LF, Alfredsson L. High consumption of coffee is associated with decreased multiple sclerosis risk; results from two independent studies. Journal of Neurology, Neurosurgery & Psychiatry. 2016 Mar 3;0:1-7.

200. Haskó G, Pacher P. A_{2A} receptors in inflammation and injury: lessons learned from transgenic animals. Journal of Leukocyte Biology. 2008 Mar 1;83(3):447-55.

201. Zhang Y, Raud J, Hedqvist P, Fredholm BB. Propentofylline inhibits polymorphonuclear leukocyte recruitment in vivo by a mechanism involving adenosine A_{2A} receptors. European Journal of Pharmacology. 1996 Oct 17;313(3):237-42.

202. Sitkovsky MV, Lukashev D, Apasov S, Kojima H, Koshiba M, Caldwell C, Ohta A, Thiel M. Physiological control of immune response and inflammatory tissue damage by hypoxia-inducible factors and adenosine A_{2A} receptors. Annual Review of Immunology. 2004 Apr 23;22:657-82.

203. Csóka B, Himer L, Selmeczy Z, Vizi ES, Pacher P, Ledent C, Deitch EA, Spolarics Z, Németh ZH, Haskó G. Adenosine A_{2A} receptor activation inhibits T helper 1 and T helper 2 cell development and effector function. The FASEB Journal. 2008 Oct 1;22(10):3491-9.

204. Vincenzi F, Corciulo C, Targa M, Merighi S, Gessi S, Casetta I, Gentile M, Granieri E, Borea PA, Varani K. Multiple sclerosis lymphocytes upregulate A_{2A} adenosine receptors that are antiinflammatory when stimulated. European Journal of Immunology. 2013 Aug 1;43(8):2206-16.

205. Rissanen E, Virta JR, Paavilainen T, Tuisku J, Helin S, Luoto P, Parkkola R, Rinne JO, Airas L. Adenosine A_{2A} receptors in secondary progressive multiple sclerosis: a [^{11}C]TMSX brain PET study. Journal of Cerebral Blood Flow & Metabolism. 2013 Sep 1;33(9):1394-401.

206. Mills JH, Thompson LF, Mueller C, Waickman AT, Jalkanen S, Niemela J, Airas L, Bynoe MS. CD73 is required for efficient entry of lymphocytes into the central nervous system during experimental autoimmune encephalomyelitis. Proceedings of the National Academy of Sciences. 2008 Jul 8;105(27):9325-30.

207. Ingwersen J, Wingerath B, Graf J, Lepka K, Hofrichter M, Schröter F, Wedekind F, Bauer A, Schrader J, Hartung HP, Prozorovski T. Dual roles of the adenosine A_{2A} receptor in autoimmune neuroinflammation. Journal of Neuroinflammation. 2016 Feb 26;13(48):1-11.

208. Wei W, Du C, Lv J, Zhao G, Li Z, Wu Z, Haskó G, Xie X. Blocking A_{2B} adenosine receptor alleviates pathogenesis of experimental autoimmune encephalomyelitis via inhibition of IL-6 production and Th17 differentiation. The Journal of Immunology. 2013 Jan 1;190(1):138-46.

209. Lee JY, Jhun BS, Oh YT, Lee JH, Choe W, Baik HH, Ha J, Yoon KS, Kim SS, Kang I. Activation of adenosine A_3 receptor suppresses lipopolysaccharide-induced TNF-α production through inhibition of PI3-kinase/Akt and NF-κB activation in murine BV2 microglial cells. Neuroscience Letters. 2006 Mar 20;396(1):1-6.

210. Sicotte NL, Voskuhl RR. Onset of multiple sclerosis associated with anti-TNF therapy. Neurology. 2001 Nov 27;57(10):1885-8.

211. Arnason BG, Jacobs G, Hanlon M, Clay BH, Noronha AB, Auty A, Davis B, Nath A, Bouchard JP, Belanger C, Gosselin F. TNF neutralization in MS-results of a randomized, placebo-controlled multicenter study. Neurology. 1999 Aug 11;53(3):457-65.

212. Stevens B, Porta S, Haak LL, Gallo V, Fields RD. Adenosine: a neuron-glial transmitter promoting myelination in the CNS in response to action potentials. Neuron. 2002 Dec 5;36(5):855-68.

213. Othman T, Yan H, Rivkees SA. Oligodendrocytes express functional A_1 adenosine receptors that stimulate cellular migration. Glia. 2003 Nov 1;44(2):166-72.

214. Coppi E, Cellai L, Maraula G, Pugliese AM, Pedata F. Adenosine A_{2A} receptors inhibit delayed rectifier potassium currents and cell differentiation in primary purified oligodendrocyte cultures. Neuropharmacology. 2013 Oct 31;73:301-10.

215. Benito-Muñoz M, Matute C, Cavaliere F. Adenosine A_1 receptor inhibits postnatal neurogenesis and sustains astrogliogenesis from the subventricular zone. Glia. 2016 Sep 1;64(9):1465-78.

216. Sui Y, Horne MK, Stanić D. Reduced proliferation in the adult mouse subventricular zone increases survival of olfactory bulb interneurons. PLoS ONE. 2012 Feb 21;7(2):e31549.

217. Eiriz MF. Migration and differentiation of neuronal precursors in the postnatal brain: insights from the subventricular zone and cerebellum. PhD Dissertation, Faculdade de Ciências e Tecnologia, Universidade Nova de Lisboa, 2013.

218. Schmitz C, Hof PR. Design-based stereology in neuroscience. Neuroscience. 2005 Dec 31;130(4):813-31.

219. Armentano M, Canalia N, Crociara P, Bonfanti L. Culturing conditions remarkably affect viability and organization of mouse subventricular zone in ex vivo cultured forebrain slices. Journal of Neuroscience Methods. 2011 Apr 15;197(1):65-81.

220. Walker AS, Goings GE, Kim Y, Miller RJ, Chenn A, Szele FG. Nestin reporter transgene labels multiple central nervous system precursor cells. Neural Plasticity. 2011 Mar 9;2010.

221. Zhang S, Cui W. Sox2, a key factor in the regulation of pluripotency and neural differentiation. World Journal of Stem Cells. 2014 Jul 26;6(3):305-311.

222. Roelofs RF, Fischer DF, Houtman SH, Sluijs JA, Van Haren W, Van Leeuwen FW, Hol EM. Adult human subventricular, subgranular, and subpial zones contain astrocytes with a specialized intermediate filament cytoskeleton. Glia. 2005 Dec 1;52(4):289-300.

223. Ohsawa K, Imai Y, Sasaki Y, Kohsaka S. Microglia/macrophage-specific protein Iba1 binds to fimbrin and enhances its actin-bundling activity. Journal of Neurochemistry. 2004 Feb 1;88(4):844-56.

224. Brown JP, Couillard-Després S, Cooper-Kuhn CM, Winkler J, Aigner L, Kuhn HG. Transient expression of doublecortin during adult neurogenesis. Journal of Comparative Neurology. 2003 Dec 1;467(1):1-10.

225. Gusel'nikova VV, Korzhevskiy DE. NeuN as a neuronal nuclear antigen and neuron differentiation marker. Acta Naturae. 2015 Apr-Jun;7(2):42-7.

226. Soltani MH, Pichardo R, Song Z, Sangha N, Camacho F, Satyamoorthy K, Sangueza OP, Setaluri V. Microtubule-associated protein 2, a marker of neuronal differentiation, induces mitotic defects, inhibits growth of melanoma cells, and predicts metastatic potential of cutaneous melanoma. The American Journal of Pathology. 2005 Jun 30;166(6):1841-50.

227. Pekny M, Nilsson M. Astrocyte activation and reactive gliosis. Glia. 2005 Jun 1;50(4):427-34.

228. Hol EM, Pekny M. Glial fibrillary acidic protein (GFAP) and the astrocyte intermediate filament system in diseases of the central nervous system. Current Opinion in Cell Biology. 2015 Feb 28;32:121-30.

229. Ito D, Imai Y, Ohsawa K, Nakajima K, Fukuuchi Y, Kohsaka S. Microglia-specific localisation of a novel calcium binding protein, Iba1. Molecular Brain Research. 1998 Jun 1;57(1):1-9.

230. Lalancette-Hébert M, Gowing G, Simard A, Weng YC, Kriz J. Selective ablation of proliferating microglial cells exacerbates ischemic injury in the brain. The Journal of Neuroscience. 2007 Mar 7;27(10):2596-605.

231. Lull ME, Block ML. Microglial activation and chronic neurodegeneration. Neurotherapeutics. 2010 Oct 31;7(4):354-65.

232. Aguirre A, Gallo V. Postnatal neurogenesis and gliogenesis in the olfactory bulb from NG2-expressing progenitors of the subventricular zone. The Journal of Neuroscience. 2004 Nov 17;24(46):10530-41.

233. Miyoshi G, Butt SJ, Takebayashi H, Fishell G. Physiologically distinct temporal cohorts of cortical interneurons arise from telencephalic Olig2-expressing precursors. The Journal of Neuroscience. 2007 Jul 18;27(29):7786-98.

234. Furusho M, Ono K, Takebayashi H, Masahira N, Kagawa T, Ikeda K, Ikenaka K. Involvement of the Olig2 transcription factor in cholinergic neuron development of the basal forebrain. Developmental Biology. 2006 May 15;293(2):348-57.

235. Ono K, Takebayashi H, Ikeda K, Furusho M, Nishizawa T, Watanabe K, Ikenaka K. Regional-and temporal-dependent changes in the differentiation of Olig2 progenitors in the forebrain, and the impact on astrocyte development in the dorsal pallium. Developmental Biology. 2008 Aug 15;320(2):456-68.

236. Cai J, Chen Y, Cai WH, Hurlock EC, Wu H, Kernie SG, Parada LF, Lu QR. A crucial role for Olig2 in white matter astrocyte development. Development. 2007 May 15;134(10):1887-99.

237. Marshall CA, Novitch BG, Goldman JE. Olig2 directs astrocyte and oligodendrocyte formation in postnatal subventricular zone cells. The Journal of Neuroscience. 2005 Aug 10;25(32):7289-98.

238. Kuhn HG, Cooper-Kuhn C, Eriksson P, Nilsson M. Signals regulating neurogenesis in the adult olfactory bulb. Chemical Senses. 2005 Jan 1;30(S1):i109-10.

239. Notterpek LM, Bullock PN, Malek-Hedayat S, Fisher R, Rome LH. Myelination in cerebellar slice cultures: development of a system amenable to biochemical analysis. Journal of Neuroscience Research. 1993 Dec 15;36(6):621-34.

240. Hamano K, Iwasaki N, Takeya T, Takita H. A quantitative analysis of rat central nervous system myelination using the immunohistochemical method for MBP. Developmental Brain Research. 1996 May 31;93(1):18-22.

241. Gerlach J, Donkels C, Münzner G, Haas CA. Persistent Gliosis Interferes with Neurogenesis in Organotypic Hippocampal Slice Cultures. Frontiers in Cellular Neuroscience. 2016 May 18;10(131):1-17.

242. Bolteus AJ, Bordey A. GABA release and uptake regulate neuronal precursor migration in the postnatal subventricular zone. The Journal of Neuroscience. 2004 Sep 1;24(35):7623-31.

243. Nam SC, Kim Y, Dryanovski D, Walker A, Goings G, Woolfrey K, Kang SS, Chu C, Chenn A, Erdelyi F, Szabo G. Dynamic features of postnatal subventricular zone cell motility: A two-photon time-lapse study. Journal of Comparative Neurology. 2007 Nov 10;505(2):190-208.

244. Platel JC, Gordon V, Heintz T, Bordey A. GFAP-GFP neural progenitors are antigenically homogeneous and anchored in their enclosed mosaic niche. Glia. 2009 Jan 1;57(1):66-78.

245. Cavaliere F, Dinkel K, Reymann K. Microglia response and P2 receptor participation in oxygen/glucose deprivation-induced cortical damage. Neuroscience. 2005 Dec 31;136(3):615-23.

246. Cavaliere F, Dinkel K, Reymann K. The subventricular zone releases factors which can be protective in oxygen/glucose deprivation-induced cortical damage: an organotypic study. Experimental Neurology. 2006 Sep 30;201(1):66-74.

247. Tanvig M, Blaabjerg M, Andersen RK, Villa A, Rosager AM, Poulsen FR, Martinez-Serrano A, Zimmer J, Meyer M. A brain slice culture model for studies of endogenous and exogenous precursor cell migration in the rostral migratory stream. Brain Research. 2009 Oct 27;1295:1-12.

248. Vergni D, Castiglione F, Briani M, Middei S, Alberdi E, Reymann KG, Natalini R, Volonté C, Matute C, Cavaliere F. A model of ischemia-induced neuroblast activation in the adult subventricular zone. PLoS ONE. 2009 Apr 23;4(4):e5278.

249. Guy Y, Rupert AE, Sandberg M, Weber SG. A simple method for measuring organotypic tissue slice culture thickness. Journal of Neuroscience Methods. 2011 Jul 15;199(1):78-81.

250. Savelyev SA, Larsson KC, Johansson AS, Lundkvist GB. Slice preparation, organotypic tissue culturing and luciferase recording of clock gene activity in the suprachiasmatic nucleus. Journal of Visualized Experiments. 2011 Feb 15;48(e2439):1-8.

251. Dean JM, Riddle A, Maire J, Hansen KD, Preston M, Barnes AP, Sherman LS, Back SA. An organotypic slice culture model of chronic white matter injury with maturation arrest of oligodendrocyte progenitors. Molecular Neurodegeneration. 2011 Jul 5;6(46):1-10.

252. Haskó G, Pacher P, Vizi ES, Illes P. Adenosine receptor signaling in the brain immune system. Trends in Pharmacological Sciences. 2005 Oct 31;26(10):511-6.

253. Mathew A, Pakan JM, Collin EC, Wang W, McDermott KW, Fitzgerald U, Reynolds R, Pandit AS. An ex-vivo multiple sclerosis model of inflammatory demyelination using hyperbranched polymer. Biomaterials. 2013 Jul 31;34(23):5872-82.